

2016

# Material Transfer Buildup on PVD Coated Work Rolls during Hot Rolling of an Al Alloy

Boya Li

*University of Windsor*

Follow this and additional works at: <http://scholar.uwindsor.ca/etd>

---

## Recommended Citation

Li, Boya, "Material Transfer Buildup on PVD Coated Work Rolls during Hot Rolling of an Al Alloy" (2016). *Electronic Theses and Dissertations*. Paper 5881.

This online database contains the full-text of PhD dissertations and Masters' theses of University of Windsor students from 1954 forward. These documents are made available for personal study and research purposes only, in accordance with the Canadian Copyright Act and the Creative Commons license—CC BY-NC-ND (Attribution, Non-Commercial, No Derivative Works). Under this license, works must always be attributed to the copyright holder (original author), cannot be used for any commercial purposes, and may not be altered. Any other use would require the permission of the copyright holder. Students may inquire about withdrawing their dissertation and/or thesis from this database. For additional inquiries, please contact the repository administrator via email ([scholarship@uwindsor.ca](mailto:scholarship@uwindsor.ca)) or by telephone at 519-253-3000ext. 3208.

# Material Transfer Buildup on PVD Coated Work Rolls during Hot Rolling of an Al Alloy

By

Boya Li

A Thesis  
Submitted to the Faculty of Graduate Studies  
through the Department of Mechanical, Automotive, and Materials Engineering  
in Partial Fulfillment of the Requirements for  
the Degree of Master of Applied Science  
at the University of Windsor

Windsor, Ontario, Canada

2016

© 2016 Boya Li

# **Material Transfer Buildup on PVD Coated Work Rolls during Hot Rolling of an Al Alloy**

by

**Boya Li**

APPROVED BY:

---

Dr. R. Rashidzadeh, Outside Program Reader  
Department of Electrical and Computer Engineering

---

Dr. H. Hu, Program Reader  
Department of Mechanical, Automotive, and Materials Engineering

---

Dr. M. Shafiei, Co-Advisor  
Novelis Global Research & Technology Center

---

Dr. A. R. Riahi, Advisor  
Department of Mechanical, Automotive, and Materials Engineering

September 20, 2016

## **DECLARARION OF CO-AUTHORSHIP/PREVIOUS PUBLICATION**

### **I. Co-Authorship Declaration**

I hereby declare that this thesis incorporates material that is a result of joint research, as follows:

This thesis incorporates the outcome of a joint research performed by the author under the supervision of Dr. A.R. Riahi and Dr. M. Shafiei. The collaboration is covered in Chapter 4 and 5 of the thesis. The collection of electron images, energy dispersive spectroscopy and experimental designs were performed jointly by Mr. O.A. Gali (University of Windsor) and the author. The primary contributions and interpretations of the data and their analyses were carried out by the author. Dr. J.A. Hunter (Novelis Global Research & Technology Center) assisted with the provision of samples and brought an industrial perspective during discussions of the results analyzed by the author.

I am aware of the University of Windsor Senate Policy on Authorship and I certify that I have properly acknowledged the contribution of other researchers to my thesis, and have obtained written permission from each of the co-author(s) to include the above material(s) in my thesis.

I certify that, with the above qualification, this thesis, and the research to which it refers, is the product of my own work.

## II. Declaration of Previous Publication

This thesis includes one original paper that have been previously published/submitted for publication in peer reviewed journals, as follows:

Thesis Chapter	Publication title/full citation	Publication status*
<i>Chapter 4,5</i>	B. Li, O. A. Gali, M. Shafiei, J.A. Hunter, A.R. Riahi. "Aluminum transfer buildup on PVD coated work rolls during thermomechanical processing" <i>Surface &amp; Coating Technology</i> (2016).	In Press

I certify that I have obtained a written permission from the copyright owner(s) to include the above published material(s) in my thesis. I certify that the above material describes work completed during my registration as graduate student at the University of Windsor.

I declare that, to the best of my knowledge, my thesis does not infringe upon anyone's copyright nor violate any proprietary rights and that any ideas,

techniques, quotations, or any other material from the work of other people included in my thesis, published or otherwise, are fully acknowledged in accordance with the standard referencing practices. Furthermore, to the extent that I have included copyrighted material that surpasses the bounds of fair dealing within the meaning of the Canada Copyright Act, I certify that I have obtained a written permission from the copyright owner(s) to include such material(s) in my thesis.

I declare that this is a true copy of my thesis, including any final revisions, as approved by my thesis committee and the Graduate Studies office, and that this thesis has not been submitted for a higher degree to any other University or Institution.

## **ABSTRACT**

This study examines material transfer and adhesion from Al-Mg alloy samples to various PVD coatings deposited on AISI M2 steel rolls during hot rolling. It explores to examine if these PVD coatings can aid in extending the work roll life by either mitigating against material transfer or aiding in the early development of the roll coatings.

Scanning electron microscopy (SEM) and focus ion beam (FIB) microscopy were used to investigate material transfer and adhesion to the surfaces of the work rolls. Aluminum and magnesium transfers were observed on all work rolls' surfaces from the 1st hot rolling pass. A two-way material transfer mechanism between the work roll and the rolled aluminum alloy surfaces was confirmed to determine the amount of material transfer on the work roll surfaces.

The lubrication flow rate was reduced to examine the lubrication's influence on the Al/Mg adhesion mitigation behavior of Cr and TiCN PVD coatings during hot rolling. The emulsion was identified as playing a significant role in the Al/Mg transfer and buildup of roll coatings on the work roll surfaces. Under both high and low lubrication conditions during hot rolling no damage was observed on the work roll surfaces which indicated that the PVD coatings were effective at extending the work roll life, although they were not able to totally mitigate against Al/Mg transfer and buildup on the work roll surfaces.

## **DEDICATION**

To my parents;

Thank you for your unconditional love and support.

I dedicate my thesis work to my advisor Dr. A.R. Riahi. He is the guide for my graduate study and research.

I also dedicate my colleague Mr. O.A. Gali, thank you for everything.



## **ACKNOWLEDGEMENTS**

My sincerest gratitude to Dr. A.R. Riahi for his supervision and valuable suggestions that guided me in this research for my M.A.Sc. at University of Windsor, to Dr. A. Edrisy for her help and encouragement of my study.

My thanks to Dr. M. Shafiei and Dr. J.A. Hunter from Novelis Global Research and Technology Center, as well for their valuable comments, support and suggestions during this work.

My special thanks to Mr. O.A. Gali for training me on the experiments, for valuable suggestions and inspiring ideas in my research. I would also like to thank the all the members of the whole tribology group. They were always kind to provide equipment and guidance during my research.

Sincere thanks to my committee members, Dr. H. Hu and Dr. R. Rashidzadeh, for their helpful comments and suggestions. Technical support from senior technician Mr. A. Jenner is greatly acknowledged.

## TABLE OF CONTENTS

DECLARARION OF CO-AUTHORSHIP/PREVIOUS PUBLICATION .....	III
ABSTRACT .....	VI
DEDICATION .....	VII
ACKNOWLEDGEMENTS .....	VIII
LIST OF TABLES .....	XI
LIST OF FIGURES .....	XII
CHAPTER 1 INTRODUCTION .....	1
1.1 Background .....	1
1.1.1 Al and alloys .....	1
1.1.2 Rolling .....	4
1.1.3 Dynamic Recovery .....	8
1.1.4 Hot rolling .....	9
1.1.5 Cold Rolling .....	10
1.1.6 Warm forming .....	11
1.1.7 Rolling Parameters .....	11
1.1.8 Work roll .....	14
1.1.9 Steel roll alloys .....	18
1.1.10 Coatings .....	19
1.1.11 PVD .....	22
1.2 Thesis objective .....	28
1.3 Organization of thesis .....	29
CHAPTER 2 LITERATURE REVIEW .....	31
2.1 Friction and tribology .....	31
2.2 Lubricant .....	36
2.3 Cr and Cr oxide coatings .....	38
2.4 Ti coatings .....	42
2.5 Surface Defects .....	46
2.6 Near-surface layers .....	47

2.7 Aluminum oxide layer.....	52
2.8 Mg diffusion.....	54
2.9 Roll coating.....	55
2.10 Summary of literature survey.....	58
CHAPTER 3 EXPERIMENTAL PROCEDURE.....	60
3.1 The work piece.....	60
3.2 The work rolls.....	60
3.3 PVD coatings.....	60
3.4 Laboratory simulation.....	60
CHAPTER 4 EXPERIMENTAL RESULTS.....	64
4.1. Material transfer to work roll surface after 1 rolling pass.....	64
4.2. Material transfer buildup on work roll surface after 10 rolling passes.....	65
4.3. Material transfer buildup on work roll surface after 20 rolling passes.....	67
4.4. Microstructural analysis of material transfer buildup on work roll surface after 20 rolling passes.....	69
4.5. Al-Mg alloy surface examination after 20 rolling passes.....	70
4.6 Material transfer buildup on the work roll surfaces after 1 rolling pass at low lubrication flow rate.....	71
4.7 Material transfer buildup on the work roll surfaces after 10 rolling passes at low lubrication flow rate.....	72
CHAPTER 5 DISCUSSION.....	74
CHAPTER 6 CONCLUSIONS.....	82
FIGURES.....	84
REFERENCES.....	127
VITA AUCTORIS.....	132

## LIST OF TABLES

Table 1. Aluminum alloy designation.....	2
Table 2. Chemical composition of Al-Mg alloy.....	2
Table 3. Chemical composition of M2 molybdenum high speed tool steels.....	19
Table 4. Rolling schedule of the experiments.....	62

## LIST OF FIGURES

Figure 1. General view of experimental setup of hot rolling simulation.....	84
Figure 2. SEM images displaying material transfer to the (a) uncoated (b) Cr-coated (c) TiN-coated and (d) TiCN-coated work rolls after 1 hot rolling pass against an Al-Mg alloy.....	85
Figure 3. EDS maps displaying Al/Mg transfer, oxygen and carbon on the (a) uncoated, (b) Cr-coated, (c) TiN-coated and (d) TiCN-coated work rolls after 1 pass against an Al-Mg alloy. Aluminum, magnesium, oxygen, carbon, titanium, iron and chromium are represented by blue, red, green, purple, cyan, yellow and magenta, respectively. (For interpretation of the references to colour in this figure legend, the reader is referred to the web version of this article.).....	86-89
Figure 4. Material transfer area fractions on the work roll surfaces plotted for each coated work roll after 1 rolling pass.....	90
Figure 5. SEM images displaying material transfer to the (a) uncoated (b) Cr-coated (c) TiN-coated and (d) TiCN-coated work rolls after 10 hot rolling passes against an Al-Mg alloy.....	91
Figure 6. EDS maps displaying Al/Mg transfer, oxygen and carbon on the (a) uncoated (b) Cr-coated (c) TiN-coated and (d) TiCN-coated work rolls after 10 passes against Al-Mg Alloy with blue representing aluminum, red representing magnesium, green representing oxygen, purple representing carbon, cyan representing titanium, yellow representing iron and magenta representing chromium.....	92-95

Figure 7. Material transfer area fraction on the work roll surfaces plotted for each coated work roll after 10 rolling passes.....	96
Figure 8. SEM images displaying material transfer to the (a) uncoated, (b) Cr-coated, (c) TiN-coated and (d) TiCN-coated work rolls after 20 hot rolling passes against an Al-Mg alloy.....	97
Figure 9. EDS maps displaying Al/Mg transfer, oxygen and carbon on the (a) uncoated, (b) Cr-coated, (c) TiN-coated and (d) TiCN-coated work rolls after 20 passes against the an Al-Mg alloy. Aluminum, magnesium, oxygen, carbon, titanium, iron and chromium are represented by blue, red, green, purple, cyan, yellow and magenta, respectively. (For interpretation of the references to colour in this figure legend, the reader is referred to the web version of this article.).....	98-101
Figure 10. Material transfer area fractions on the work roll surfaces plotted for each coated work roll after 20 rolling passes.....	102
Figure 11. Al/Mg transfer area fractions on the work roll surfaces after 1, 10 and 20 passes.....	103
Figure 12. Cross-sectional FIB/SEM images displaying Al/Mg transfer to the (a) uncoated, (b) Cr-coated, (c) TiN-coated and (d) TiCN-coated work rolls after 20 hot rolling passes.....	104
Figure 13. SEM images displaying pickup defects on the Al-Mg alloy surfaces rolled against the (a) uncoated (b) Cr-coated (c) TiN-coated and (d) TiCN-coated work rolls after 20 hot rolling passes.....	105

Figure 14. EDS maps of the SEM images displayed in Fig. 14, displaying the rich aluminum content of the pickup defects on the Al-Mg alloy surfaces rolled against the (a) uncoated, (b) Cr-coated, (c) TiN-coated and (d) TiCN-coated work rolls after 20 hot rolling passes.....	106
Figure 15. SEM images displaying material transfer to the (a) Cr-coated work roll at lower magnification (b) Cr-coated work roll at higher magnification after 1 hot rolling pass against an Al-Mg alloy under low lubrication flow rate.....	107
Figure 16. SEM images displaying material transfer to the (a) TiCN-coated work roll at lower magnification (b) TiCN-coated work roll at higher magnification after 1 hot rolling pass against an Al-Mg alloy under low lubrication flow rate.....	108
Figure 17. EDS maps displaying Al, Mg, oxygen and the main elements of the coatings on the (a) Cr-coated, (b) TiCN-coated work rolls after 1 pass against an Al-Mg alloy under low lubrication flow rate.....	109,110
Figure 18. Material transfer area fractions on the work roll surfaces plotted for Cr and TiCN-coated work roll after 1 rolling pass under low lubrication flow rate.....	111
Figure 19. SEM images displaying material transfer to the (a) Cr-coated work roll at lower magnification (b) Cr-coated work roll at higher magnification after 10 hot rolling passes against an Al-Mg alloy under low lubrication flow rate.....	112

Figure 20. SEM images displaying material transfer to the (a) TiCN-coated work roll at lower magnification (b) TiCN-coated work roll at higher magnification after 10 hot rolling passes against an Al-Mg alloy under low lubrication flow rate.....	113
Figure 21. EDS maps displaying Al, Mg, oxygen and the main elements of the coatings on the (a) Cr-coated, (b) TiCN-coated work rolls after 10 passes against an Al-Mg alloy under low lubrication flow rate.....	114,115
Figure 22. Material transfer area fractions on the work roll surfaces plotted for Cr and TiCN-coated work roll after 10 rolling passes under low lubrication flow rate.....	116
Figure 23. (a) SEM image displaying cracks in Al/Mg transfer layer to the uncoated work roll surface and (b) cross-sectional SEM image displaying delamination of a fractured Al/Mg transfer layer on the uncoated work roll surface.....	117
Figure 24. Al/Mg transfer area fraction on the work roll surfaces plotted against area fraction of the rolled aluminum alloy surface covered with pickup defects for the uncoated and coated work rolls after the 20 pass hot rolling schedule.....	118
Figure 25. Material transfer area fractions on the work roll surfaces plotted for Cr and TiCN-coated work roll after 1 rolling pass under high lubrication flow rate.....	119
Figure 26. Material transfer area fractions on Cr-coated work roll after 1 pass under low and high lubrication flow rate.....	120



Figure 27. Material transfer area fractions on TiCN-coated work roll after 1 pass under low and high lubrication flow rate.....	121
Figure 28. Material transfer area fractions on the work roll surfaces plotted for Cr and TiCN-coated work roll after 10 rolling passes under high lubrication flow rate.....	122
Figure 29. Material transfer area fractions on the work roll surfaces plotted for Cr and TiCN-coated work roll after 10 rolling passes under low lubrication flow rate.....	123
Figure 30. Material transfer area fractions on Cr-coated work roll after 10 passes under low and high lubrication flow rate.....	124
Figure 31. Material transfer area fractions on TiCN-coated work roll after 10 passes under low and high lubrication flow rate.....	125
Figure 32. Material transfer area fractions on the work roll surfaces plotted for Cr and TiCN-coated work roll after 1 and 10 passes under high and low lubrication flow rate.....	126

## CHAPTER 1 INTRODUCTION

### 1.1 Background

#### 1.1.1 Al and alloys

Aluminum is the second-most used metal after steel, due in part to its versatility and efficiency. It is a lightweight and malleable metal which has been in use for centuries. Once the aluminum has been separated from the ore, it can be combined with other elements to create the desired properties for a variety of aluminum alloys. The most commonly used alloying elements for aluminum alloys are magnesium, manganese, copper, silicon, and zinc. Aluminum alloys can be processed with many techniques to fit specific applications. Aluminum is readily processed using several casting methods and a wide variety of forming processes including rolling, forging, drawing and extrusion. The flexibility in processing makes it possible for aluminum to be manufactured to satisfy most geometric or performance requirement [1].

Aluminum has strong corrosion resistance to common atmospheric and marine atmospheres with thin oxide film ( $\text{Al}_2\text{O}_3$ ) forming on its surface. Its corrosion resistance and scratch resistance can be enhanced by anodizing. Aluminum has high reflectivity thus can be used for decorative purpose. Aluminum can provide strong structural support to machined parts and construction material without adding excess weight to the products, which allows for more efficient fuel consumption in vehicles using aluminum parts. Aluminum alloys have been used as basic materials with low density and high strength characteristics. Some aluminum alloys can match or even exceed the strength of common construction steel. Aluminum retains its toughness at very low temperatures, without becoming brittle like carbon steels. Aluminum is a good conductor of heat and electricity.

It is non-toxic and is commonly used in contact with foodstuffs and readily recycled. To promote the application of aluminum alloys, the improvement in workability is one of the key issues.

Aluminum alloys for sheet products are identified by a four-digit numerical system which is administered by the Aluminum Association. The alloys are divided into eight groups based on their principal alloying element. The first digit identifies the alloy group as follows:

Table 1. Aluminum alloy designation [2]

Alloy group	Principal alloying elements	Properties
1xxx	Unalloyed Aluminum	Purity of 99.0% or Greater
2xxx	Copper	Heat Treatable Alloys
3xxx	Manganese	
4xxx	Silicon	Low Melting Point Alloys
5xxx	Magnesium	
6xxx	Magnesium and Silicon	Heat Treatable Alloys
7xxx	Zinc	Heat Treatable Alloys
8xxx	Other Elements	

Al-Mg alloy is a wrought alloy type with good corrosion resistance. Weldability and resistance to corrosion of aluminum magnesium alloy is considered favorable. The following datasheet will provide more details about Al-Mg alloy.

The following table shows the chemical composition of Al-Mg alloy.

Table 2. Chemical composition of Al-Mg alloy [3]

Element	Content (%)
Aluminum, Al	95.2
Magnesium, Mg	4.5
Manganese, Mn	0.35

Non-heat treatable aluminum (NHT) alloys are utilized in all of the major industrial markets for aluminum flat-rolled products. Transportation, packaging, building and

construction sectors have represented the largest usage of NHT sheet. Higher performance non-heat treatable alloys have been developed for new and existing applications ranging from foil to high strength structural products. The development of new or improved aluminum alloys has been based on the requirement for structural performance or exterior in the final products and productivity during manufacturing process. The ability to control microstructure by manipulating the alloy composition and process of the final product, as it goes through solidification, thermal and deformation processing has enabled these products to be manufactured with the good quality, consistency, and low cost required by the marketplace. The aluminum alloys with the highest strength are of strengths similar to many of the heat treatable alloys while the aluminum alloys with the low strength can provide high levels of formability.

There are three major criteria for selecting or developing new NHT aluminum alloy products: structural—based on durability and strength; forming—based on productivity or complexity in making the final part; surface—based on finishing characteristics, reflectivity or surface exterior.

Surface quality has become a key attribute for many types of NHT alloy sheet products. Structural products with bright rolled finishes are commonly used for tanks and tread sheet. These products are manufactured from corrosion resistant 3xxx or 5xxx aluminum alloys and provide an attractive surface finish without hand polishing or other finishing operations. These finishes can be obtained by either cold or hot rolling to the final thickness.

During the last 10 years, the growth of NHT alloys has been most notable in the transportation sector, with the volume of sheet and foil nearly doubling to more than

600,000 tones. This is principally owing to the growth of sheet for automotive applications. Aluminum alloys have drawn major attention in the automotive industry these years as manufacturers seek to design lightweight vehicles with improved fuel efficiency and reduced vehicle emissions [4].

### **1.1.2 Rolling**

Rolling involves passing the material between two revolving rolls at the same peripheral speed but in opposite directions. The gauge between them is less than the height of the metal stock. There are two types of rolling process: flat and profile rolling. In flat rolling, the final shape of the product is either classified as sheet or strip (thickness less than 3 mm) or plate (thickness more than 3 mm). In profile rolling, the final product is either a round rod or other cross-section shaped products such as structural sections (beam, channel, joist, rails, etc.). These rolls can either be flat or grooved (contoured) for the hot rolling of rods or shapes. Under these conditions, the rolls grip the piece of metal and deliver it, reduced in cross-sectional area and increased in length.

The initial breakdown of ingots into blooms and billets is done by hot-rolling. It is possible to reduce a slab of 600 mm thickness down to plate with thicknesses of 6 – 250 mm and further down as low as 2 mm for successive cold rolling to sheet with thicknesses as low as 0.2 mm. Further rolling operation can reduce the foil to a thinnest thickness as low as 0.006 mm, approximately one third of a human hair thickness [5].

Rolling aluminum and its alloys is one of the principle ways of converting cast aluminum slab from the smelters and wrought re-melts into a usable industrial form.

Almost 80 % of metal devices have been exposed to rolling at least one time in their production history. Rolled products, i.e. sheet, plate and foil consist of almost half of all

aluminum products.

The direct chilling (DC) casting ingot after casting is usually cooled to room temperature and then re-heated to around 500 °C before subsequent passes through the hot rolling mill which reduces its thickness to around 4 - 6 mm. A process of homogenization is needed of some alloys at certain pre-heat temperature for the held time of ingot is important, which makes the material in the best condition for rolling and achieve subsequent properties.

In conventional rolling, aluminum slabs are heated to around 525 °C and then passed repeatedly through a hot rolling mill until either the demanded plate thickness is attained or the metal is thin enough (generally about 3 mm thick), to be coiled ready for subsequent cold rolling. The last 3 or 4 hot rolling passes are usually performed consecutively through a 3 or 4 stand tandem mill.

The hot rolling process involves two stages. In the first stage, at the end of the preheating cycle, the ingots are loaded onto the hot rolling line. The ingot is then processed passing the reversing hot roughing mill also known as a breakdown mill. The initial hot rolling process reduces the thickness of the ingot by up to 95% and increases its length by 24 times, through a sequence of precisely controlled reversing rolling passes. The lead and tail ends of the strip are cropped during the process to achieve uniformity along the length. In the second stage, the slab, which is now approximately 140 m in length, is delivered to the run-out table to the hot finishing mill, where rolling parameters including rolling force, speed, tension, emulsion and temperature are precisely controlled, ensures that it is rolled to a tight tolerance intermediate thickness. In this process, the strip is rolled and coiled on a twin coiler after each three passes, afterwards it is removed

from the hot rolling line and cooled to ambient temperature from a temperature of 300-360 °C.

From this stage right down to the thinnest foil thicknesses, the metal is fed in coil form through a sequence of single or multi-stand cold rolling mills which subsequently reduce the metal thickness and recoil it after each rolling pass, until the required thickness is attained. Annealing may be needed between passes depending on the final temper (hardness) required.

Properties such as strength, toughness, formability and corrosion resistance are controlled by the control of alloy, rolling schedule and heat treatments before, during and after rolling. Other requirements such as flatness, surface finish quality and gauge uniformity have been attained by control to the mechanics and chemistry of the rolling process. The surface finish in sheet products is primary where the surface of the sheet affects successive forming operations by influencing lubricant retention and pickup on the rolls.

All plate is produced by the DC casting/hot rolling route and the final product is often surface machined for good quality. Besides, the demanded strength properties such as toughness, machinability, stress corrosion resistance and fatigue strength are achieved by controlling alloying elements and specific heat treatments. In plate the hardness of the product is enough to avoid distortion but very high residual stresses can adversely influence the performance of product in service or cause distortion when machined. Control stretching removes this residual stress but it involves stresses thus adding to production costs [6].

The properties of a hot rolled material depends on the evolved structure, which is a

function of the restoration processes, i.e., recrystallization and recovery occurring during the hot deformation which in turn depends on the structural parameters of the hot rolling process.

Recrystallization may occur during or after deformation (during cooling or following heat treatment). As the rolling process breaks up the grains, they recrystallize maintaining an equiaxed structure and preventing the metal from hardening. The rate of recrystallization is strongly depends on the extent of deformation applied. Heavily deformed materials recrystallize faster than those deformed to a lesser extent and below a certain percentage deformation recrystallization may never occur. In industry, recrystallization is mostly used in the softening of hardened metals which have lost their ductility during previous cold work, and the control of the grain size of the final product [5].

The presence of recrystallized grains is a common defect found in the surface region of hot deformed aluminum alloy products. Whereas most rolled products are composed of hot-deformed and textured grains, the near-surface region very often consists of recrystallized grains which are free of dislocations on a large scale, and hence slightly softer than the underlying bulk material. This results in an inhomogeneous distribution of mechanical properties throughout the product. Besides, these recrystallized grains lead to poor quality of surface finish and a distinction in corrosion resistance. For cases where homogeneous mechanical properties are demanded, consumers of the rolled product will purchase oversized deformed product and then machine away the recrystallized exterior in order to ensure the product has homogeneous mechanical properties [7].



### 1.1.3 Dynamic Recovery

Dynamic recrystallization and dynamic recovery are important scientific and industrial processes in thermomechanical processing responsible for the microstructure evolution during high temperature deformation of high-strength aluminum alloys [8].

The high stacking fault energy (SFE) FCC aluminum alloys and the BCC steels have good workability result from dynamic recovery (DRV) which is characterized by polygonized substructures in deformed grains. The low SFE, FCC alloys (Cu, Ni, austenitic Fe) have good workability attributed to dynamic recrystallization (DRX) which is characterized by repeated formation of equiaxed grains which provide a substructure to nucleation. Generally, the dynamic recrystallization during high temperature deformation of high stacking fault energy (SFE) aluminum alloys is continuously converting subgrain microstructures to high angle grains microstructures.

It is argued that dynamic recovery produces a steady state substructure by remaining the subgrains of constant size, low misorientation and equiaxed in elongating grains as observed in Al alloys and in  $\alpha$ -Fe alloys. Dynamic recovery allows a limited number of discontinuous segments with higher misorientation especially when temperature diminishes. As temperature falls, strain rate increases, or alloying restrains dislocation movement, a warm regime is reached where reduced dynamic recovery does not provide complete realignment of the substructure so that the distribution of misorientations extends to above  $10^\circ$  (still without the appearance of microbands or block walls) [9].

Dynamic recovery and recrystallization play an important role in reducing flow stress and enhancing ductility to improve industrial processing at elevated temperatures [10].

#### **1.1.4 Hot rolling**

Hot rolling process allows large plastic deformations of the metal attained with a small number of rolling cycles which is accompanied by a reduction in the hardness and strength with an increase in the ductility of the material. Hot rolling results in grain refinement, uniform distribution of phases, absence of inhomogenities and proper dispersion of second phase particles [11]. The rolling process on cast aluminum alloys alters its metallic structure and renders the metal with new characteristics and properties. The brittleness of the coarse, as-cast material is substituted by a stronger structure. The extent of strength and ductility is variable factors which are functions of the amount of deformation applied on the metal, alloy composition, rolling temperature and the use of annealing.

Hot rolling uses large pieces of metal heated above the recrystallization temperature. After rolling, its grains reform and left in a stress-free state. The metal stock is subjected to high compressive stresses, deformed between the rolls to reduce its cross section. These cross sections are thinner than those formed by cold rolling. Coefficient of friction between two rolls and the stock is high, which may even result in shearing of the metal in contact with rolls. Large deformation can be successively repeated, as the metal remains soft and ductile, thus heavy reduction in area of the work piece can be achieved. Hot rolling also reduces the average grain size of metal but remains an equiaxed microstructure. Hot rolled surface has metal oxide on it, leading to poor surface finish. Typically, hot rolled material does not need subsequent annealing process and the high temperature during hot rolling prevents residual stress from accumulating in the material.

During hot rolling, the major reduction is done to enable the sheet to its desired

gauge. Hot rolling permits large quantities of reduction because the deformation is done at elevated temperatures where the flow stress is lowered, thus the level of stored energy is lowered compared to cold rolled material under similar conditions. The effect of stored energy accumulated during hot rolling can be relieved in later processes of recovery and recrystallization.

### **1.1.5 Cold Rolling**

Cold rolling is performed below the metal's recrystallization temperatures. It increases the hardness and yield strength of the metal by introducing quantities of defects into the crystal structure of the metal to harden the microstructure which prevents further slip. Compared to hot rolling, it is less malleable than metal rolled above its recrystallization temperature, therefore, heavy reduction is not possible, which makes cold rolling a more labor intensive and less cost efficient than hot rolling. Coefficient of friction between two rolls and the stock is comparatively lower. Cold rolling can also reduce the grain size of the metal leading to Hall-Petch hardening. Its grains remain elongated and flattened, leaving the metal in an anisotropic state and full of cold work. The surface after cold rolling is more smooth, imperfections and oxide free.

Cold rolling is mostly used as the final step of the rolling process, which is performed around room temperature. Annealing treatments are applied to the work piece after cold rolling which relieves some of the strain hardening and stored energy generated during cold rolling which may limit its formability [1, 12].

Hot rolling, due to recrystallization, reduces the average grain size of a metal while maintaining an equiaxed microstructure whereas cold rolling will produce a hardened microstructure with unidirectional grains. This difference between hot and cold rolling

generates distinctions in the amount of overall deformation the rolled material will experience and the surface finish.

### **1.1.6 Warm forming**

Warm forming is a metal forming process carried out above the temperature range of cold working, but below the recrystallization temperature of the metal. Warm forming may be preferred over cold forming because it will reduce the force and the amount of annealing of the metal required to perform the operation.

Al-Mg alloys are desirable for the automotive industry due to their superior high-strength to weight ratio, weldability and corrosion resistance. However, the formability and the surface quality of the final product of these alloys are not good enough if it is processed at room temperature. If these alloys can be formed in a soft condition and heat treated, better formability enables it attractive for manufacturing various aircraft and missile parts. Recent studies show that the formability of these alloys is increased at temperatures range from 200 to 300 °C and better surface quality of the final product has been obtained [13].

The warm forming method improves the formability, deep drawability and shape fixability of the aluminum alloys, which is principal at the elevated temperatures due to the increased strain rate hardening [14, 15].

### **1.1.7 Rolling Parameters**

Parameters of the rolling process can be utilized for designing and optimizing pass schedules and providing setup data to the mills to achieve the requirement of product development.

When stock is compressed between two rolls, it moves in the direction of least

resistance. The rolls are subjected to elastic deformation due to this stress generated by the work piece. The contour of the roll gap controls the geometry of the product. The stock under vertical compression meets some longitudinal resistance to free elongation which facilitates in causing sideways spread. Therefore, the rolls apply a reduction (vertically), this reduction generates an elongation (horizontally) and spread (sideways). The higher the coefficient of friction, the higher is the resistance to lengthwise flow and the more is the spread.

The main variables in rolling are: the work roll diameter, i.e., the higher diameter of the work rolls, the greater drafting is possible; the contact length, i.e., the biting angle is reduced by reducing the roll radius, lesser the biting angle, lesser is the reduction; the deformation resistance of the metal is influenced by temperature, metallurgy and strain rate.

Rolls change temperature all the time, varying in the surface temperature. A too high thermal gradient increases the risk of roll breakage due to thermal stress. Therefore, heat should not penetrate the roll and the roll surface should be cooled as soon as possible at the exit side of the rolling gap.

While the finished product is of good quality, the surfaces of rolls are covered with oxide mill scale which forms at high temperatures. It is usually removed by pickling, which reveals a smooth surface.

To achieve the best possible surface quality of rolled products it is necessary to maintain the rolling process and all parameters as constant as possible. The rolled material varies in temperature and cross-section from pass to pass. Heat is transferred to the rolls. The surface structure of the rolls changes due to wear and other factors during

each pass. Quality aspects mainly depend on surface temperatures and temperature gradients. It takes some time to reach stable conditions in rolling schedules [5, 16].

Deformation resistance indicates how much a given metal offers resistance to deformation from external load. Higher the deformation resistance higher is the difficulty to deform. Higher the dislocation density higher is the deformation resistance. Higher the working temperature lesser is the deformation resistance. Coarser grains in the metal offer less resistance for deformation.

The temperature of the work piece during deformation has an impact on the level of stored energy. Processing aluminum at elevated temperatures permits the occurrence of dynamic recovery which is linked to aluminum's high SFE, which makes it easier for dislocation to climb and cross slip with lowered stored energy generated during deformation. By increasing deformation temperature, a slower rate of recrystallization can be expected because of lower levels of stored energy due to potential recovery mechanisms. Friction between the rolls and the work piece will facilitate increasing the temperature at the surface of rolled sheet. Also the inhomogeneous deformation will induce thermal gradients from the surface to the center of the material due to the heat generated during deformation. This contribution of heat from deformation will increase as the total reduction increases, which facilitates compensating the heat lost by contact between the heated sheet and the cooler rolls.

Generally, tribology in the rolling process controls the friction forces between the roll and the strip. By controlling the interfacial forces, the production of high quality rolled surfaces can be achieved easily, and makes it possible of reducing the loads on the mill, contributing to energy savings and reducing roll wear. In hot rolling process, the

temperature, rolling speed, reduction and the lubricating conditions are of concern.

The average coefficient of friction and the forward slip increase with temperature and reduction. The coefficient of friction was found to decrease with increasing rolling speeds and apparently increase as the reduction was increased.

The rolling speed, the reduction and the emulsion concentration are considered as independent variables. The surfaces of the rolled strip and the effects of the process parameters such as roll separating forces, roll torques, forward slip, interfacial roll pressure and shear stress during the hot rolling on their quality are also of concern.

The roll separating forces and the roll torques depended on the reduction and emulsion concentration but were only slightly influenced by the rolling speed [17].

### **1.1.8 Work roll**

Work rolls are important parts in the operating costs of a modern hot rolling mill. Work rolls have to be changed frequently according to downtime, and must be ground to required profile crown, before being replaced into the mill. In many cases rolls have been substituted because their surfaces have deteriorated, such as wear and the surface roughening, rather than changes in shape or crown owing to thermal expansion or wear [18]. Therefore, the durability of the roll is significant in rolling industry. The mechanism of the surface deterioration varies depending on the roll material and the rolling conditions. The roll surface induces severe and complicated friction conditions which are the temperature, stresses, materials and the atmosphere etc., so a great number of tribological phenomena can occur.

A roll must experience heating and stressing during about 1000 to 10000 cycles in its lifetime. The heating factor is the temperature of the roll surface which increases by

conduction and friction, the stressing factor is the normal and tangential stresses from the rolled strip between about 100 MPa and 1 GPa. The other factor is the Hertzian stress between the work roll and the back-up roll. Other factors are the materials of the rolled strip and the roll, and the atmosphere, which is influenced by the cooling liquid. These factors vary based on the rolling conditions.

One of the main mechanisms of surface roughening is probably the rolling contact fatigue of roll material which has previously induced perpendicular cracks by thermal fatigue [19].

The damages that work rolls may experience are thermal fatigue and abrasive wear of the finishing train. The wear and damage resistance of a roll material is restrained by its mechanical and physical properties. The mechanical properties are important where abrasive wear is predominant, which are defined by the roll material's microstructure. Indeed, the abrasive wear resistance is determined by carbide hardness, their homogeneous distribution, and matrix capacity to hold these carbides.

During rolling process, work rolls are exposed to thermal fatigue, mechanical fatigue and wear impacts so that good thermal, mechanical and tribological properties are required. High hot wear resistance is the most important property of rolls in the finishing stands, since their yield is determined in terms of tons strip rolled per millimeter of roll consumption. However, the gradual deterioration of the roll finishing, which is often related with the high coefficient of friction between roll and strip materials, negatively influences the surface quality of the rolled strip so that rolls are periodically dismantled to be ground and renew their initial surface roughness. The real yield of the rolls is, thus, lower than the theoretical one, because a certain amount of material is removed out of



service. It can be deduced that the wear resistance of these materials must be evaluated on the theoretical yield and the ability to worn homogeneously.

Abrasion is probably one of the major wear mechanisms in rolls, based on the area increased of scratches in a matrix by every rubbing. The wear mechanism of rolls is mainly due to the abrasion exerted by the oxide scale of the strip. The formation of a thin oxide layer on the roll surface seems to positively affect the roll performance, although contradictory effects have been reported on this argument.

The formation of a hard oxide layer produced in the high contact temperature, positively affects the wear rate and lowers the surface irregularities. Oxidation which is lower than in real rolls owing to the lower test temperature preferentially occurs on the matrix, while carbides becomes oxidized in the later stage of the test.

The surface finishing of work roll materials are mainly dependent on their abrasion resistance. The mean surface roughness  $R_a$  is related to the difference in hardness between matrix and carbides. Generally, the higher microhardness of the martensite, the softer phase which is preferentially worn out, corresponds to a lower final  $R_a$ . A substantial and uniform surface oxidation also contributes in reducing the final  $R_a$ , because of the preferential oxidation of the matrix which decreases surface irregularities. The positive influence of high microhardness, particularly at elevated temperatures, seems mostly related to the high load bearing capability backing the protective oxide layer [20].

Further, the substrate hardness has a strong impact on the wear of the PVD coatings onto it and consequently on the frictional characteristics and galling tendency of the coating/substrate composite. Low substrate hardness, leading to a low load bearing

capacity, increases the tendency to cracking and subsequently chipping of the brittle coating.

Work roll wear is influenced by load, friction, sliding length, abrasive and corrosive particles in the lubricant. It is important to note that although high friction can induce deterioration to the work roll topography, to the extent that rolls need to be reground to restore the initial finish, low friction can also be detrimental, as this may cause slippage and excessive roll wear. Roll wear can occur on the contact surface or locally in deep wear bands, which is result from the interactions between oxidation, friction and thermal fatigue, with damage mechanisms attributed to abrasion (exerted by the oxide scale of the work piece), adhesion, thermal fatigue and oxidation. Uniform wear has been attributed to abrasion and thermal fatigue causing micro-chipping and crack formation perpendicular to the roll surface. Thermal fatigue caused cracks occur during the early rolling stages and can induce other wear mechanisms. Therefore, it can be said that the work roll life is shortened by high temperature and high pressure during contact with the work piece, thus materials used in work roll manufacturing demand good mechanical, thermal and tribological properties.

Many wear mechanisms have been identified including adhesion, mechanical interaction of surface asperities, ploughing of one surface by asperities on the other, and deformation and fracture of surface oxide layer. These mechanisms mostly act simultaneously but may occur in different proportions under different conditions. The behavior of the forming tool/aluminum (or magnesium) interfaces during high temperature is critical to achieve the desired shape and surface finish [21].

Generally, the averaged coefficient of friction depends critically on a large number

of variables [22].

### **1.1.9 Steel roll alloys**

Molybdenum high speed steels are designated as M group steels based on the AISI classification system. Over 95% of the high-speed steels fabricated in the US are M group steels. Tungsten is present in all types of M group steels from M1 to M10, except M6, and cobalt is not present in any these steels. Molybdenum high speed steels have similar performance compared to tungsten high speed steels. However, the initial cost of molybdenum tool steels is lower.

M2 is the most widely used industrial high-speed steel (HSS). It has fine and evenly distributed carbides giving high wear resistance. It is mostly used in manufacturing a variety of tools, such as taps, reamers, drill bits and cutting tools.

M2 is suitable for cold work applications, such as tools for forming, punching and pressing. M2 has a good combination of toughness, compressive strength and wear resistance. This combination of properties makes it superior to many high alloyed cold worked steels.

M2 tool steels can be deformed using grinding methods. However, they have poor grinding performance, therefore are regarded as medium machinability tool steel under annealed conditions. The machinability of these steels is only 50% of that of the easily machinable W group steels. M2 steels are hardened by heat treatment and quenching.

The life of high-speed steel can be extended by coating the tool. TiN, TiCN, Cr and several other coatings can be used on the steel tools by physical vapor deposition method to improve the performance of the tool. Generally, a tool's hardness and lubricity can be increased by coatings. For example, coatings allow the cutting edge of a tool to cleanly

pass through the material without having the material gall or stick to it. The coating also helps to decrease the temperature during the rolling process and increase the life of the tool.

Table 3 shows the chemical composition of M2 molybdenum high speed tool steels.

Table 3. Chemical composition of M2 molybdenum high speed tool steels [23]

Element	Content (%)
C	0.78-1.05
Mn	0.15-0.40
Si	0.20-0.45
Cr	0.20-0.45
Ni	0.3
Mo	4.50-5.50
W	5.50-6.75
V	1.75-2.20
Cu	0.25
P	0.03
S	0.03

### 1.1.10 Coatings

Coating may be defined as a coverage which is applied over the surface of metal substrate tools. The purpose of applying coatings is to improve surface properties of a bulk material which is usually referred to as a substrate.

The most important mechanical and physical properties of a coating for tooling applications are the coating porosity, (hot) hardness, wear, adhesion, corrosion, scratch and oxidation resistance, etc.

Coating a tool improves wear resistance and prolongs tool life. Coating performance is strongly dependent on the chemical and mechanical properties of the coating material. In a machining process, the selection of coating depends on the working conditions. In addition, many factors, such as coating thickness, composition ratio, sequences of layers

in multilayer coatings, and the deposition method all influence the performance of a coating.

Tool wear affects the operation of the machining process and consequently the surface quality of products. Vital requirements for hard metal machining tools include tool performance, profitability, and cost effectiveness, which allow tools to achieve high-dimension accuracy, high-quality machined surface, and high productivity at low costs.

A thin layer of wear-resistant material is deposited onto the surfaces of carbide tools to improve the surface properties and wear resistance. Hardness, wear resistance, and coefficient of friction of tools strongly depend on the surface properties of the tools. Physical vapor deposition (PVD) and chemical vapor deposition (CVD) are the most commonly used methods to produce coatings on carbide substrates.

In industry, the following coating defects are observed: coating peeled off, coating chipped off, uneven distributed coating thickness, insufficient coating thickness, absence of coating, rough coating deposition, dual color coating, marks/scratches in coating, dent, pitting, etc. [24]. The lack of chemical affinity between different coatings and work pieces results in reduction of material pickup which is the leading cause of cutting edge breakdown.

Surface engineering has attracted major interest in applications throughout a wide variety of industrial applications these days. Engineering surface treatments and coatings can provide specialized properties of wear and corrosion resistance, without compromising the desirable characteristics of the substrate metal. Many new processes are arising: vapor deposition, implantation, thermal spray coatings and many others methods, all attempting to attain the ultimate hard, tough, wear resistant, low friction and

anti-corrosion surface.

The rising use of high strength steels in a variety of mechanical engineering sectors has raised problems associated with galling in sheet metal forming processes. Galling is a tribological phenomenon evolved material transfer from the aluminum sheet to the work roll surface during rolling process, which results in seizure of the tool/aluminum sheet interface and extensive scratching the surface of the aluminum product. The material transfer between the contacting surfaces is frequently a problem since it will strongly influence the contact conditions and thus the behavior of the tribosystem. In sheet metal forming processes, adhesion buildup of sheet metal fragments on the tool surface, ultimately resulting in galling, is one of the most important parameters controlling the surface quality of the formed products and the tool life. As a result, many concepts have been developed in order to decrease the tendency of galling in sheet metal forming, evolving the development of new dry lubricants, new forming tool steel grades and thin surface coatings deposited on the forming tool.

Depending on the sheet metal, many of these coatings can reduce the friction forces and wear under both lubricated and unlubricated contact conditions by minimizing the adhesive interaction between the mating surfaces and the plastic deformation of the substrate. The material transfer is a direct consequence of either abrasive or adhesive wear mechanisms being active at the rolling interface. Besides the intrinsic frictional properties of the coatings, the size and density of surface irregularities/defects will influence the pickup tendency since both macro particles and shallow craters will increase the interaction tendency with the counter surface.

### **1.1.11 PVD**

Deposition can be done in different ways: plasma spraying, flame (TSC), chemical deposition (CVD, PA CVD), electroplating deposition and physical deposition (PVD). However, the most progressive technology among these is the PVD technology. PVD technology enables deposition of thin films with unique features at very low temperatures (as opposed to CVD, PA CVD, TSC).

PVD is a family of coating processes which comprises a group of surface coating technologies used for decorative, tool, and other equipment coating applications. It is basically a vaporization coating process in which the fundamental mechanism is an atom by atom transfer of material from the solid phase to the vapor phase and back to the solid phase, gradually building a film on the surface to be coated. PVD produces metal-based hard coatings by means of generation of partially ionized metal vapor, reaction with certain gases and forming a thin film with a specified composition on the substrate. The process is similar to chemical vapor deposition (CVD) except that the material to be deposited starts out in solid form, whereas in CVD, the counterpart is introduced to the reaction chamber in the gaseous state. PVD processes include arc evaporation, sputtering, ion plating, enhanced sputtering, electron beam and pulsed laser deposition. The most commonly used methods are sputtering and cathodic arc. In sputtering, the vapor is formed by a metal target being bombarded with energetic gas ions. Cathodic arc method uses repetitive vacuum arc discharges to strike the metal target to evaporate the material. Each of the PVD technologies generates and deposits material in a little bit different way, requiring equipment unique to each process. All PVD processes are carried out under high vacuum conditions.

In the case of reactive deposition, the depositing material reacts with reactive gases such as nitrogen, oxygen or acetylene to create a film of a variety of compound coating compositions, such as oxides, nitrides, carbides and carbonitrides of Ti, Cr, Zr and alloys like AlCr, AlTi, TiSi on a wide range of tools and components. Common industrial coatings applied by PVD are TiN, ZrN, CrN and TiAlN.

The result is a very strong bond between the coating and the substrate and precisely controlled structural, physical and tribological properties of the film. Materials can be deposited with modified properties compared with the substrate material. The resulting coatings have homogeneous thickness over the entire surface and excellent reproducibility of the results.

Good coating adhesion is required for wear and corrosion resistance. Many reasons can lead to premature failure including coating delamination, cracking and plastic deformation. Besides, thin ceramic PVD coatings usually have columnar grain structure with micro cracks, pinholes, transient grain boundaries and often high through coating porosity, which all result in accelerated pitting corrosion and failure at the coating/substrate interface, especially in adverse environments. Coating adhesion, wear and mechanical properties are strongly influenced by its microstructure.

Coating thickness plays a significant part in enhancing both PVD-coated tool cutting performance and resistance to abrasive and erosive wear. It appears that thicker coatings will improve corrosion resistance in aqueous environments by eliminating through-thickness pin-hole defects.

Substrate surface conditions before deposition, characterized by surface stress, roughness and oxidation state, are of importance in controlling coating properties [25].



Coating properties, such as structure, adhesion, hardness, chemical and temperature resistance can be precisely controlled. A homogeneous coating thickness is obtained by spinning the part at a constant speed around several axes. The typical processing temperature for PVD coatings is between 250 and 450 °C, in some cases, can be deposited at temperatures below 70 °C or up to 600 °C, depending on substrate materials and expected behavior in the application.

The thickness of coating ranges from 2 to 5 µm, but can be as thin as a few hundred nanometers or as thick as 15 or more µm.

The coatings can be deposited as mono-, multi- and graded layers. The latest generation films are nano-structured and superlattice variations of multi-layered coatings providing enhanced properties.

Substrate materials include steels, tungsten carbides, non-ferrous metals and pre-plated plastics. The suitability of the substrate material for PVD coating is only constrained by its stability at the depositing temperature and electrical conductivity. Besides, after completion of deposition, the properties and microstructure of main materials are not influenced [26].

PVD is environmentally friendly. The application of PVD surface coating technology at large scale, high volume operations will lead to the decline of hazardous waste generated compared to electroplating and other metal finishing processes which use a great number of hazardous and toxic materials. PVD is a desirable alternative to electroplating and some painting applications because it generates less hazardous waste and utilizes less hazardous materials (i.e., no plating baths). In addition, PVD coatings are sometimes harder and more corrosion resistant than coatings applied by the electroplating

process.

PVD processes involve four steps: evaporation, transportation, reaction and deposition.

During the evaporation stage, a target, consisting of the material to be deposited is bombarded by a high energy source such as a beam of electrons or ions. This dislodges atoms from the surface of the target in order to vaporize them.

Transportation process comprises of the movement of vaporized atoms from the target to the substrate to be coated and will generally be a straight line affair.

In some cases coatings will be composed of metal oxides, carbides, nitrides and other such materials. In these cases, the targets consist of the metals. The atoms of metal will then react with the appropriate gas during the transport stage. For the examples above, the reactive gases may be oxygen, methane or nitrogen. Depending on the actual process, some reactions between target materials and the reactive gases may also take place at the substrate surface simultaneously with the deposition process. In cases where the coating consists of the target material alone, this step would not be involved.

The deposition process involves coating buildup on the substrate surface.

The final result of the coating/substrate composite is a function of each material's individual property, the interaction of the materials and any process constraints that may exist.

The selection criteria for determining the best method of PVD is dependent on several factors: the type of material to be deposited, the rate of deposition, limitations imposed by the substrate such as the maximum deposition temperature, shape and size, adhesion of the deposition to the substrate, throwing power (rate and thickness

distribution of the deposition process), purity of coating materials, equipment requirements and their availability, cost and ecological considerations.

PVD is used in the manufacture where thin films are required for mechanical, optical, chemical or electronic functions, etc. PVD coatings are generally used to improve hardness, wear and oxidation resistance. Thus, such coatings are used in a wide range of applications such as aerospace, automotive, surgical/medical devices, dies, molds for all manner of material processing, cutting and forming tools, mechanical components, fire arms, optics, architectural elements and much more. The use of PVD coatings is aimed at improving efficiency through advanced performance and longer component life. They may also allow coated components to operate in environments which the uncoated component would not be able to perform. The coating structure can be modified to produce the desired properties. Besides PVD tools for manufacturing, special smaller tools (mainly for scientific purposes) have been developed. The final coating choice is determined by the demands of the application. The application of PVD coatings for metal cutting, punching and forming is one of the biggest advances in recent metalworking industry technology.

PVD coatings on cutting tools are highly profitable to extend tool life and improve productivity and reduce costs, consequently enhance the surface quality of the final product significantly. They operate more efficiently, thereby shorten cycle times and increase production volume. They are resistant to wear, including crater, built-up edges, and depth-of-cut notching. This technology has been widely used in applications where a very sharp and hard cutting edge is required for optimum performance, such as threading, drilling and end-milling. PVD coatings reduce the quantities of cutting fluids or coolants,

thereby decreasing the total budget production costs by up to 15%. High-speed, dry machining involves extremely high temperatures. PVD coatings such as TiAlN possess good thermal stability, hot hardness and oxidation resistance, and are able to operate dry or with minimum quantities of coolants. It can cut extremely hard materials or be re-sharpened and re-coated.

PVD and Plasma-Assisted Physical Vapor Deposition (PAPVD) coatings applied in the plastic tooling industry such as die and mold casting, can extend product life, facilitate easier demolding, reduce residue and polishing requirements, increase fluidity and performance of forming material, lessen abrasion and wear resistance, diminish mold adhesion, shorten cycle time, improve injection pressure, melt flow and mold filling, and enable dry or lubricant-free operation.

In automotive industry, PVD, PAPVD and Plasma-Assisted Chemical Vapor Deposition (PACVD) coatings are used for engine, gear drives and hydraulic components to reduce friction, thereby reducing both wear and energy loss. High friction causes excessive heating, deformation of plastics, abrasive and adhesive wear (galling), and eventually seizure of tribological components. To solve these problems, light alloy parts are coated with a high performance coating.

In addition to hardness and adhesion, PVD coatings have many benefits in medical devices, including improved biocompatibility, decorative colors and greater aesthetic exterior, and chemical barrier against saline solutions and other oxidants.

PVD coatings enable to produce a broad spectrum of decorative and aesthetic color options. Titanium, chromium and zirconium are the most commonly used materials for decorative coatings. Most coatings have high temperature and good impact strength, and

are so durable that protective topcoats are almost not necessary.

A variety of thin film characterization techniques can be used to measure the physical properties of PVD coatings. Coating thickness test can be measured by calco tester, hardness test for thin-film coatings by nanoindentation, wear and friction coefficient test by pin on disc tester and coating adhesion test on scratch tester, the investigation of structural features and heterogeneity of elemental composition for the growth surfaces can be carried out by X-ray micro-analyzer.

## **1.2 Thesis objective**

The productivity of the hot rolling of aluminum has been linked to the development of a stable roll coating on the work roll surface in the aluminum rolling industry. It is believed that these roll coatings are essential in mitigating against refusals and further aluminum adhesion. Yet uncontrolled aluminum adhesion to the work roll can lead to galling which results in the damage of the work roll. Material transfer to the work roll surface during the hot rolling of aluminum is therefore a major tribological issue. However there is still limited research available in the area of roll coating buildup and material transfer during the hot rolling process. PVD coatings have long been applied in various high temperature forming processes to mitigate against aluminum adhesion to the die surfaces. Their use has yet to be applied to the rolling industry.

The objective of this study is to investigate the possible application of several PVD coatings in the hot rolling of aluminum. Primarily to investigate their tribological properties, aluminum mitigation behavior and their possible use in extending the life of the work rolls. The influence of the PVD coatings on the development of the roll coatings is also of concern. The research also extends into the examination of the possibility of

these PVD coatings replacing or reducing the reliance on emulsions for the rolling industry, reducing the expenditure and environment hazards of the emulsions.

### **1.3 Organization of thesis**

This thesis is arranged into six different chapters, each of which is briefly described below.

Chapter 1 introduces the background information related to this thesis and the research objectives and organization of the thesis.

Chapter 2 provides a literature survey related to this thesis and includes information on previous research which has been done so far. It focuses on the friction, tribology and lubrication conditions, the PVD coatings, the aluminum alloys and the surface defects and near-surface layers of the rolled aluminum and the development of roll coating during hot rolling process.

Chapter 3 introduces the experimental procedures. It includes descriptions of the experimental setup and sample preparation as well as the aluminum alloy and steel roll alloy elemental composition details and the surface condition of PVD coatings. It describes the working principles of the hot rolling process used in this study as well as the analytical techniques used to examine the material transfer on the work roll surfaces.

Chapter 4 describes the results obtained by SEM, EDS and FIB. This chapter is divided into two parts. One is the results related to the high lubrication flow rate, the other is the results related to low lubrication flow rate.

Chapter 5 discusses the results obtained. It first discusses the influence of the PVD coatings compared with an uncoated steel work roll on the buildup of adhesion. It then moves to the effect of low lubrication condition on the mitigation behavior of Cr and

TiCN coatings during hot rolling simulation.

Chapter 6 summarizes the conclusions of this research. It presents a summary of the results acquired from the research and the conclusions drawn from discussions.

## CHAPTER 2 LITERATURE REVIEW

### 2.1 Friction and tribology

Frictional force is needed to draw the metal into the roll, where large fraction of rolling load comes from. Friction varies from point to point along the arc of the contact of the roll, it will be acting from entry to neutral point and to exit point along the direction of roll rotation. It will be opposing the direction of roll rotation.

High friction leads to high rolling load and a steep friction hill.

Since it is very difficult to measure the variation in coefficient of friction  $\mu$ , it is assumed that  $\mu$  is a constant. For cold rolling it is taken as 0.05-0.1 and for hot rolling it is taken as  $\geq 0.2$ . Coefficient of friction is inversely proportional to the rolling speed. As  $\mu$  reduces, rolling speed increases, from  $F = \mu/N$ ,  $\mu = F/N$

Thinner gage sheet can be produced in cold rolling for coefficient of friction is smaller.

Sublayer plastic deformation, mechanical interaction of surface asperities and ploughing of sample surfaces contribute to the friction force. They act simultaneously, but appear in different measure under different normal pressures [27].

The tribological mechanisms during interaction of aluminum sheets and steel tools at high temperature are very complex and involve deformation, wear, friction and transfer of material simultaneously.

The tribological system involves many parameters, including the lubrication and work roll surface conditions, work piece material and specifications, rolling parameters and the tribological conditions at the roll/work piece interface. The tribological interactions that occur between the work roll and the work piece, both covered by their



oxides individually, are affected by the thermo-physical and mechanical properties of the roll and work piece, such as hardness, shear modulus, yield strength and density. These properties influence the stresses and heat transfer at the roll/work piece interface, which come into play in determining the surface quality of the final product,

Asperity contact between the surfaces of the roll and the work piece under lubricated conditions results from the high shear stresses during hot rolling. Consequently, it is generally accepted that the measurement of the coefficient of friction and the effects of the tribological factors influencing the rolling process are critical in the evaluation of the tribological behavior at the interface. The friction in rolling involves several material and processing parameters, including the roll speed, normal load, temperature, forward speed and reduction. In addition, friction has been reported to be influenced by the oxide layer on aluminum piece surface and to increase along the length of roll contact and with larger reduction of the work piece. However, friction is one of the main compressive forces responsible for the motion and thickness reduction of the work piece between the rolls. Friction largely impacts the rolling load, roll wear, and strip shape. Roll speed control is important during rolling on a hot strip mill.

The PVD coatings improve the thermal stability, enhancing the oxidation resistance of the die. However, the deposition of coatings on a die surface does not guarantee improved friction and wear resistance; the coating topography or morphology has a strong impact on this. A high surface quality of the coating is required to modify the tribological interactions between the coating and the work piece. The measurements of rolling parameters are affected by rolling conditions, which are constantly changing with each pass. Temperature also varies during a rolling pass due to the plastic deformation

which increases the temperature and contact with the roll and emulsion which reduce temperature. Friction measurements involve calculations using parameters such as torque and forward slip, as friction reduces with roll speed increases. Friction has also been estimated from the reduction or spread, the angle of contact and matching measured and calculated roll forces (Hill's formula). This statement is from Dieter.

The presence of scale on the surface of the pieces influences not only the quality of the finished product, but also the interface between the rolls and the pieces, which causes changes in the friction conditions.

The problem caused by the effects of rolling parameters on the frictional conditions is easiest handled by controlled laboratory experiments where one parameter is varied at one time. The coefficient of friction is then calculated from experimentally measured roll separating forces, roll torques, etc. The relevant process parameters are sample temperature, reduction, and roll velocity.

Scale thickness influences the frictional conditions and may be regarded as either a process or a material parameter, which is a function of the steel's chemical composition, temperature, environment, and oxidation time.

Wear in hot rolling is hard to measure or monitor on the spot because the various mechanisms result in different effects: abrasive wear results in material removal, mechanical and thermal fatigue in cracks, adhesion in material pickup or removal, and corrosion in oxidation. The two types of fatigue lead to changes in the coefficient of friction as surface conditions alter, which makes the coefficient of friction suitable for detection of changes in wear conditions. Forward slip is defined as the relative increase in speed the strip experiences upon exiting the roll gap, which is a measurement of the

slippage in the roll gap. A high forward slip indicates a high coefficient of friction and a high wear rate.

Friction in hot rolling can be classified into sliding friction and sticking friction. Sliding friction is the result of sliding of the work piece relative to the roll surface, indicating low friction. Sticking friction can occur either partially over a zone near the neutral plane, or over the whole roll gap, as for a high friction. It is necessary for the development of work rolls and lubricants with the increase in demand for better quality along with the increase of geometrical accuracy.

Generally, coefficient of friction increases with reduction increases and as temperature reduces for rolling without lubrication. With oil as lubricant, the influence of temperature on the coefficient of friction is insignificant. For all temperatures, coefficient of friction reduces as rolling speed increases. Examination on the effect of emulsion lubricant on coefficient of friction indicates the effectiveness of oil-lubrication at reduction less than 35%. At a higher reduction, the 1:100 oil/water mixed emulsion proves to be more effective.

The initial sample surface roughness also plays an important effect on coefficient of friction. It seems that the rougher the initial sample surface is the more sensitive the coefficient of friction is on reduction. It has been found that the oxide scale layer thickness does not seem to have a significant effect on coefficient of friction [28]. In most cases, a high coefficient of friction is not desirable due to the consequent high load and high-energy input required.

Furthermore, high friction usually increases the rate at which material is transferred from the soft work piece to the roll surface thus leads to deterioration in the roll surface

finish and a rough surface of the product which is unacceptable for aesthetic reasons and as well as due to poor mechanical properties.

Many forming processes are operated by close asperity-to-asperity contacts between roll and work piece and grooves of pressurized lubricant between the asperities. Friction is determined by the ratio of the real asperity-to-asperity contact area to the nominal area, as well as by the boundary friction factor on these real contact areas under lubricated condition.

Measurements of friction in strip drawing and cold rolling with lubrication show that the boundary friction factor depends on the reduction in strip thickness, and is correlated with some hydrodynamic actions. It is found that the development of the material transfer on the roll surface can substantially change the frictional stress in metal forming processes. A slurry-like transfer film reduces the coefficient of friction while strongly adhered material to the tool degrades the roll surface and leads to the increase in friction. Recent measurements of friction for plane strain compression tests (PCST) on aluminum strip show that the coefficient of friction may reduce with the development of a transfer film with a reactive boundary additive. Time-of-Flight Secondary Ion Mass Spectroscopy (ToF-SIMS) analyses of tool and strip surface on PSCTs confirm that the transfer film consists of organo-metallic compounds, which has been previously reported in cutting or rolling processes.

Comparing the transfer film formed under dry condition or with base oil is usually a strongly adhered material, and no reduction in friction is observed. Typically, in dry conditions the coefficient of friction is of sticking contact and increases during the process owing to the development of a strongly adhered transfer film and scoring on the

work-piece.

The coefficient of friction under lubricated conditions increases with the initial surface roughness due to more severe asperity-to-asperity contact [29].

The level of friction controls the material flow and the strain distribution during forming and these in turn impact the contact loads, sheet thinning, and forming time. The use of tool coatings and lubricants may have an important influence on the surface quality of formed products [21].

## **2.2 Lubrication**

One of the most important parameters in the forming of aluminum sheets is lubrication condition.

In the 1970s, lubricants were used in hot sheet rolling of steel so as to reduce the rolling force and roll wear. Mase (1979) reviewed that the rolling force with lubricant was 10–30% lower than those without lubricant in industrial mill [30].

Lubricant is used during the forming process to achieve better surface quality and to reduce the friction of die surfaces, which contributes to increasing the die lifetime by reducing wear. Results indicate that reducing the interfacial friction by using a lubricant altered the metal flow after the deformed sheet had contacted with the die surface. The changes of the metal flow during forming process not only developed a better thickness distribution of the formed part, but also improved cavitations distribution. The effects of dry film lubricants on aluminum sheet metal forming were investigated and compared the results with other type lubricants. It was observed that dry film lubricants showed advantages over conventional oil lubricants due to their high deep drawing performance, especially on complex shaped body panels. The formability is increased resulting from

reduced friction and it is possible to obtain more homogeneous sheet thickness distributions. [14].

Control of friction is critical in the success of cold metal forming processes such as rolling. High friction probably results in excessive load and damage to the surface on the work piece. Therefore, oil (either neat or in the form of an emulsion) is usually applied in cold rolling to act as a lubricant, reducing the friction level and protecting the surfaces. An oil film between the roll and strip is hence generated because of the wedge entraining action at the entry to the roll bite. Three regimes of lubrication can be identified, depending on the ratio of the thickness of oil film to the combined surface roughness. In the full-film lubrication regime, the contacting surfaces are separated by a continuous oil film so that friction is low. However, the surfaces tend to roughen, being unconstrained by contacting with the hard smooth roll, which is unacceptable for most products because of poor reflectivity or fatigue strength. In the boundary lubrication regime, the surface of the work piece conforms fully to the smoother roll surface, but friction is usually too high. Therefore, most cold metal rolling processes are conducted in the mixed lubrication regime where there is some asperity contact between the roll and work piece surfaces and trapped oil in the valleys, which provides a compromise between reasonable friction levels and good surface finish. Reactive molecules can chemically adsorb aluminum, particularly on the surface where, as in metal rolling, there is considerable fresh metal surface formed in the roll bite. The used rolling lubricants were examined and confirmed that a number of chemical reactions involving aluminum and boundary additives occurred during aluminum cold rolling. Plane strain compression testing of aluminum proved that the exposure of fresh metal through the oxide layer cracking is essential for

the aluminum to react with the boundary additives. A transfer film is formed on the roll surface which has a significant impact on the friction factor [31].

The droplet size distribution is an independent rolling parameter which affects the loads on the mill of the emulsion with tight emulsions containing oil droplets of small diameter and loose emulsions containing large and widely varying oil droplet sizes.

While the dependence of the rolling loads on oil droplet dimensions was noticed, it was considered less significant. The thermal and mechanical energies transfer at the contact between the work rolls and the rolled metal during rolling. The efficiency of the transfer are dependent on the rolling parameters, the most important of which are the relative velocity between the contacting surfaces and the normal and shear stresses. Material properties as well as surface parameters affect the transfer process, specifically the roughness of the rolls. Lubricant parameters, such as the viscosity and the composition, are critical as well. The characteristics of the oil-in-water emulsion (such as the distributions of oil particle sizes) are expected to contribute to the tribological phenomena in the roll bite in a very important way.

The surfaces of both the roll and the rolled metal have surface topography features, which may attenuate or accentuate lubricant capture and delivery into the contact zone. It is possible that at the rolling speeds used in industry, the droplet dimensions have a more observable influence, owing to speed effect on the amount of oil plating out or on droplet capture.

### **2.3 Cr and Cr oxide coatings**

The properties rolling mills require are anti-adhesion to avoid catastrophic adhesive transfer, and wear resistance. The abrasive wear resistance maintains the strip quality and

process stability at the required level as long as possible, thereby decreasing the frequency of roll changes. Hard Cr coatings provide such properties for aluminum rolling, bringing a variety of desired properties which many engineers require for their components and products. A wide range of parts can be coated, it requires only the proper fixturing, a large enough bath, sufficient lifting capacity, and adequate power sources.

There are many benefits of hard chrome: ultra-hard, superb substrate adhesion, suitability for a wide variety of substrates and geometry, superb abrasion resistance, low deposition temperature, ultra-high metal-to-metal sliding wear resistance, a bright finish, low friction, stable and non-corrodible.

It is difficult to find an appropriate alternative coating technology, which would offer quality and cost-effective production coatings based on the standards. Among numbers of available technologies the most widely viewed as being promising substitutes of chromium plating are the PVD and CVD technologies, which are used to produce decorative thin films or functional hard coatings.

PVD metal or ceramic coatings are equivalent or superior in performance and are a cost-effective alternative to chrome plating in a variety of applications. The plating bath used in chrome plating contains hexavalent chromium ( $\text{Cr}_6$ ), which is adverse to health and environment. There has been a transfer from hexavalent chromium to trivalent chromium ( $\text{Cr}_3$ ) with increasing investments on elemental chromium PVD coatings to maintain the true chromium appearance. The introduction of PVD processes as a replacement for chromium plating represents a development towards an environmentally clean technology [32].

When comparing electroplating and PVD methods, the process steps of applying



chrome and other metal to substrates are different. In electroplating, a number of chemical baths and rinses are needed to deposit 15 to 30  $\mu\text{m}$  of metal for producing a durable chrome appearance. Electroplating processing steps involve cleaning, conditioning, neutralizing, acid etching, catalyzing, accelerating, nickel flash, copper plating, nickel plating, chrome plating and effluent care and disposal.

PVD chrome can be applied with three primary methods: directly to a high quality substrate without a base-coating or clear coating (limited applications due to poor abrasion protection), over a base-coating (will require a thicker metal layer or be under a protective cover), or between a base-coating and clear coating.

PVD coatings method is rapidly progressing as a replacement for electroplated chrome in the aerospace, automotive, appliance and other industry. The ability to fully process the components in a synchronous method from molding to shipping saves much time and cost. The PVD chrome market is substantial, and while new technologies are being developed to provide a cost-effective direct metalized PVD chrome appearance with no base-coat or clear-coat, displaying the same color, brightness, and environmental durability as plated chrome.

PVD chrome is a highly durable process that exceeds the life of chrome plating, unlike traditional chrome plating which pits and peels under normal wear and tear, due to their superior mechanical properties. PVD wheels are 80% lighter than chrome plated wheels which lead to increased fuel economy.

Deposited PVD coatings have a wide color range, for example, titanium nitride (TiN) is gold colored, and titanium carbonitride (TiCN) can vary in color from gold to purple to black depending on the composition. Decorative/wear coatings are used on door

hardware, plumbing fixtures, fashion items, marine hardware, and other such applications.

Chromium oxide shows good mechanical, optical and magnetic properties, which can be used as a selective solar ray collector and for other applications as a protective coating against wear, corrosion, and oxidation.  $\text{Cr}_2\text{O}_3$  is the most chemically stable under ambient conditions among many chromium oxides. The performance and reliability of chromium oxide coatings is often constrained by their mechanical properties.

$\text{Cr}_2\text{O}_3$  coating is quite dense without inclusions or pores appearing, thus good mechanical properties can be expected. Initially, amorphous and random polycrystalline grains grew at the interfaces in deposition. Amorphous layers also allow relieving the growth stress in the coating [33].

$\text{Cr}_2\text{O}_3$  is suitable for wear resistance applications, as it is one of the hardest oxides with 29.5 GPa hardness. Its hardness can range drastically owing to compositional and microstructural variations which depend on the different deposition method.

The high temperature corrosion resistance of chromium alloys is due to the formation of protective layers of  $\text{Cr}_2\text{O}_3$ .  $\text{Cr}_2\text{O}_3$  is the only thermodynamically stable chromium oxide at high temperatures. Below 700°C, the behavior of oxidation reaction changes. In the temperature range from 300°C to 600°C, in the beginning the oxidation experienced an logarithmic stage, with duration decreased with increasing temperature, afterwards parabolic oxidation. The logarithmic rate constant present a positive pressure dependence, while the parabolic rate constant exposed a negative pressure dependence, i.e., this rate constant increased with decreasing oxygen pressure [34].

During the high temperature oxidation of the Cr coating, a thin  $\text{Cr}_2\text{O}_3$  protective oxide scale will form on the surface. Cr would diffuse outwards through the defects

within scales, such as cracks when heated, and reacted with  $O_2$ , in this way, the formed  $Cr_2O_3$  healed the oxide scales [35].

Chromium oxide coatings are also chemically inert, with good optical properties, high mechanical strength and hardness. Therefore, they have been widely used in many applications such as wear resistance, corrosion protection, optics, and electronics [25]

The overall wear resistance may be enhanced by the formation of hard, adhesive, and continuous chromium oxide layers, which form an interface between the rolls and the work piece. These layers take up some of the friction stresses, but they also insulate the rolls thereby reducing the overall risk of spalling of the surface.

## **2.4 Ti coatings**

Ti-based hard coatings enable significant improvement of the surface hardness of tools.

Generally, the harder the material or surface is, the longer the tool will last. Titanium Carbo-Nitride (TiCN) has a higher surface hardness than that of Titanium Nitride (TiN). The addition of carbon makes TiCN have higher hardness and changes its range from about 3,000 to 4,000 Vickers, dependent on the carbon concentration.

A high coefficient of friction causes excessive heat, resulting in a reduction of coating life even coating failure. However, a lower coefficient of friction can highly increase tool life. A smooth surface which lacks coarseness or irregularities can decrease the amount of heat. Higher lubricity of surface enables the chips slide off the surface of the tool and allows for increased speeds when compared to non-coated tools, which generates less heat and further avoids galling of the work material. This property keeps material from adhering onto the tool by weakening chemical reactivity between the tool

and the material. Once the material starts adhering to the tool, it continues to attract more adhesion. A coating with enhanced anti-seizure properties may even be able to aid where poor coolant quality or concentration is a difficulty.

TiN coating has become the standard use on cutting and forming tools, and machine parts for many years, serving as a protective layer for tools due to its wear and corrosion resistance. TiCN is notable for its better oxidation resistance and hot hardness than TiC. The advantages of TiCN-coated carbide insert over TiN-coated inserts include its superior friction behavior contacted with steel and the high thermal transmission coefficient [36].

Titanium Nitride (TiN) is drawing increasing attention and application in tool industries.

TiN is applied primarily to precision metal parts where a cost effective reduction in tool wear is required. It is a first generation thin film hard coating for carbide tools and the most commonly used PVD hard coating.

As the metallic junctions were thought to be responsible for increasing the friction during rolling contact, the coating has low adhesion tendency to molten aluminum combined with moderate resistance to oxidization.

The advantages of TiN coatings of tool steels include a good appearance, excellent adhesion to substrates, high strength, high chemical inertness, tough resistance to wear, corrosion at elevated temperatures, hard surfaces to reduce abrasive wear, a low coefficient of friction with most work piece materials which increases lubricity and results in excellent surface finish and decrease of horsepower requirements, high temperature stability and low maintenance cost and high productivity. In practice, the degree of extended tool life and increased productivity achieved with coated tools

depends primarily on the tool and its application, the work piece material and the operating parameters.

TiN coating has a bright gold metallic color appearance with 1-4  $\mu\text{m}$  thickness. Its hardness is 2300 HV, elastic modulus 600 GPa and melting point at 2800  $^{\circ}\text{C}$ , good electrical conductivity and coefficient of friction of 0.5 depending on application and test conditions. It is chemically inert, resistant to most chemicals, insoluble in all acids except HF and also insoluble in all alkalis.

TiN is a cost effective coating which has a homogeneous thickness over the contour of the part's surface and suitable for many tooling and forming applications. It forms a good molecular bond to substrate metal which will not blister, flake or chip. Thus, the coated tools typically can last two to ten times longer than uncoated tools. TiN coatings are smooth and non-porous combined high density. TiN coatings can be deposited at temperatures below 150  $^{\circ}\text{C}$  while retaining its properties, therefore, it is an environmentally friendly process with less energy consuming.

TiN is applied for many tooling and forming applications, such as drills, punches, dies, mills, reamers, taps, gear cutters insert, cutting tools and injection mold components. It eliminates galling, fretting, microwelding, seizing and adhesive wear. It has been proved success in boosting production and curtailing cost, with decreasing downtime, less frequent tool replacement and cleanup [37].

TiN coating is non-toxic and being used in food processing industry and clinically applied in medical surgical devices such as orthopedic implants for hip, knee, shoulder and ankle replacements as well as dental implants. It is also an efficient coating for aerospace components,

TiCN is an all-purpose coating, which varies a range of colors (from blue-grey to pink) depending on the Ti:C ratio.

The addition of carbon atoms in the TiN lattice substantially increases film hardness and lowers the coefficient of friction. However it is not a direct replacement for TiN in all applications and is only recommended for cutting, punching, and wears applications where moderate temperatures will be generated. TiCN has superior mechanical properties and high chemical stability, such as high hardness, high toughness, high melting point, high electrical conductivity, and good wear resistance.

TiCN is easily stripped from common tool steels which makes it ideal for those applications where maximum tool life is desired, but also the capability to remove the coating when it wears through and needs to be reapplied.

Despite its very high hardness, TiCN has not too high brittleness which is superior in many applications, such as during interrupted cutting in machining. It is also biocompatible, which has been applied on many medical instruments and implantation devices.

TiCN coatings due to the properties of high hardness, abrasive and wear resistance, toughness and elastic modulus, good adhesion, high melting temperature, high level of adhesion to substrate, low coefficient of friction in relation to steel and high wear resistance are widely deposited on cemented carbide cutting tools. TiCN coating is widely used in punching, injection molding, milling, turning, tapping, drilling, drawing, stamping, pressing and forming tools and cutting tool applications for tool steels, high-speed steels, cemented carbides or many other materials [38]. Like TiN, TiCN is also suitable for applications in the decorative sector. Successful applications include end

mills, reamers, drills, taps, hobs, and carbide inserts. It performs well cutting alloy steels and stainless steels and is used to protect punches, trim dies and blanking dies.

## **2.5 Surface Defects**

The problem of surface quality of flat rolling products can cause defect or degradation of quality of final product.

Possible sources of surface defects of hot or cold rolling strips in manufacturing process can be in casting, heating and rolling of material.

The initiators of surface defects include inclusions, blowholes, scars, holes, longitudinal, transverse, edge cracks and lines of oxides aluminum. The condition of heating slabs in pusher furnace, hot rolling and final cold strip rolling process, involve further creation and evolution of defects. During rolling process, the next specific surface defects are shell surface, thermal cracks, hangnails, slivers, scales, squeeze of rolls and scratches. The accumulation of surface defects in material during rolling process caused deterioration in mechanical properties [39].

Hot rolling is one of the key processes which convert cast or semi-finished metal into finished products. Since the rolling operation is often the last process step, the scrap at this stage is very costly thus the quality control of rolling process is of significance. Among all the quality characteristics, the surface integrity is of extremely importance of the hot rolled products. Surface defects remain as the most troubling problems in the hot rolling process as a weakness or stress concentration spot for the bulk material therefore could induce catastrophic failure when the rolled product is in use. Products with severe surface defects have to be scrapped. Hence, it is highly recommended to detect, reduce, and eventually eliminate the surface defects if possible.

The root causes of surface defects in hot rolling processes are very complicated. Surface defects could be originated from different sources. For example, the nonmetallic impurities in the casting during solidification and the mechanical failures in the rolling mills are important potential sources of surface defects [40]. Specifically, during hot rolling process, localized strain cause a deleterious surface microstructure evolution producing surface imperfections such as rolling ridging or roping which would lead to scrapping of the material.

A common defect found in the surface region of hot deformed aluminum alloy products is recrystallized grains. Although most rolled products consist of textured, hot-deformed grains, the near-surface region normally consists of recrystallized grains which are largely free of dislocations, thus slightly softer than the underlying deformed structure, which produces an inhomogeneous distribution of mechanical properties throughout the product. In addition, these recrystallized grains also lead to poor surface finishes as well as a difference in corrosion resistance [7].

## **2.6 Near-surface layers**

The surface composition of an aluminum alloy determines important parameters such as corrosion resistance, adhesion, joining and welding behavior. Rolling, and especially hot rolling has been shown to alter the surface properties of aluminum alloys and to introduce deformed subsurface layers with different metallurgical, chemical, electrochemical and optical properties and potentially mechanical properties of the alloys such as formability and bendability than the underlying bulk material

In conventional manufacturing and finishing processes, for example rolling, the aluminum alloy surface and near-surface regions experience a higher level of



compressive and shear deformation than the underlying bulk material resulting from the friction between the rolls and the metal, which results in significant microstructure refinement, leading to formation of near-surface deformed layers with composition and microstructures different from that of the underlying bulk alloy. Each pass through a rolling mill will contribute to some extent to the formation of the near-surface deformed layer. These subsurface layers are characterized by a nano-sized refined grain structure with rolled-in oxide particles and contain a fine distribution of second phase and intermetallic particles, dispersoids, various voids and cracks. The layers are inhomogeneous in thickness and composition. Furthermore, these rolled-in layers are not continuously present over the whole (sub)surface, but are distributed over the sheet surface [41, 42, 43].

There are two types of near-surface deformed layers observed. Type A is characterized by fine grains with grain boundaries decorated by oxide particles; type B is characterized also by fine grains but with the grain boundaries without oxide particles. The high levels of shear deformation result in dynamic recrystallization, together with mechanical alloying, which are responsible for the formation of the near-surface deformed layer.

Typically, the outermost deformed layer is characterized by ultrafine, equiaxed grains. Between the outermost deformed layer and the bulk microstructure, a microband transition region of elongated grains arranged parallel to the work piece surface might also be present.

Severe shear strains induced in the surface and near-surface region during rolling are of sufficient magnitude to cause geometric dynamic recrystallization and the formation of

microbands, hence leading to considerable microstructure refinement and the formation of a near-surface deformed layer. Consequently, the microstructure variation at different depths from the surface is a reflection of the strain distributions.

The high population density of grain boundaries and the severe deformation in the near-surface region facilitates precipitation of fine dispersion of intermetallics during subsequent heat treatments.

The relatively stable structure of the near-surface deformed layer is correlated with the presence of a large fraction of high-angle grain boundaries. Moreover, the structure in the near-surface deformed layer can survive the typical annealing process particularly through the Zener pinning of the grain boundaries by oxide particles and precipitates [44]. This observation was tested by comparing the experimentally determined grain size with that obtained from theoretical treatments of the Zener grain growth retardation by oxide particles of the observed size and volume fraction [45].

The thickness, structure and homogeneity of the resulting near-surface deformed layer have been characterized by scanning and transmission electron microscopy with the aim of understanding the evolution of near-surface deformed layer during hot rolling and the influence of processing parameters, such as temperature and roll surface morphology. Surface roughness is the imprinted surface morphology of the work roll.

The deformed microstructure is characterized by fine grains of 100–200 nm diameter and oxide particles, with one or two orders of magnitude smaller than the bulk grains above the coarse intermetallic particles. The thickness of the near-surface deformed layer varies across the alloy surface and is directly related to the distribution of coarse intermetallics.

Within the cracked area, a deformed layer of alloy of approximately 1  $\mu\text{m}$  thickness, characterized by fine grains of 100–200 nm diameters and oxide particles is partially delaminated from the underlying bulk alloy, which suggests the delamination of surface/near-surface regions resulting from interaction between the work roll and the alloy. The thickness of the near-surface deformed layer is directly associated with the surface cracks.

The disturbed surface layer is inherent to the thermo-mechanical processes of rolled aluminum, particularly to the exposure to high shear stress at elevated temperatures. GDOES qualitative depth profiles are able to examine characteristic distributions of alloying and impurity elements within the first few microns of a hot rolled aluminum alloy, before and after annealing. These distributions are related with the presence of the deformed layer generated in rolling. The evolution in depth of carbon and oxygen signals is related with oxide clusters and streaks parallel to the rolling direction. These oxide regions are most likely rolled-in oxide particles and cracks, which are inherent during hot rolling process [46].

A subsurface layer composed of a mixture of small grained metal, microcrystalline as well as amorphous oxides was found in all the hot rolled Al-Mg alloy samples by backscattered and transmission electron imaging, and electron diffraction X-ray maps. The subsurface layer extended up to 5–8  $\mu\text{m}$  under the surface after 1 pass, to 3–5  $\mu\text{m}$  under the surface after 2, 3, 4 and 5 passes, and to 1.5–2  $\mu\text{m}$  after 6 passes. The average thickness of the subsurface layer is maximum after the 1st hot roll pass. Subsequent rolling eliminates the surface segregation of alloying elements in the near-surface region and reduces the average thickness of the subsurface layer. The boundary between the

subsurface layer and the bulk metal was found to be very rough and to have a high density of defects mainly in the form of cracks, voids, and inclusions.

Besides amorphous  $\text{Al}_2\text{O}_3$ , the oxides in the subsurface layer were found to contain a mixture of crystalline oxides, whose grain size was in the range 28–300 Å, with almost half of the particles in the range 28–33 Å. The metal grain size of the subsurface layer after 2, 4, and 6 passes was in the range 0.04–0.2 µm, which was at least 25 times smaller than the 2–5 µm grain size of the bulk.

The surface/subsurface crystalline oxides after 1 and 2 passes contained MgO, g- $\text{Al}_2\text{O}_3$ , and  $\text{MgAl}_2\text{O}_4$  phases. After 3, 4, and 5 passes, the  $\text{MgAl}_2\text{O}_4$  spinel phase was not detected, MgO was still detected, and g- $\text{Al}_2\text{O}_3$  was found only in certain locations. After 6 passes, the only crystalline oxide detected was MgO. The amount of crystalline oxide in the mixed layer reduced with the depth from the surface to the boundary of the mixed layer. The small size (28–33 Å) and the equiaxed shape of the large amount of the subsurface MgO particles indicate that they are likely to be secondary magnesium oxides.

The subsurface mixed layer was covered with continuous surface oxides of 250 Å to 1600 Å thick, mostly consisting of MgO mixed with some  $\text{Al}_2\text{O}_3$ .

A three-step hypothesis of the formation subsurface layer was proposed by the observation of the subsurface structure: first, formation of surface depressions (holes) by plowing, adhesive wear, delamination wear or transverse surface cracking in the process of rolling; second, filling the holes with the wear debris constituted of metal and fine oxide particles mixed with lubricants; third, covering the holes with thin metal layers during the subsequent rolling process, which results in a shingled surface appearance [45].

TEM investigation in the roll bite region has revealed the step-by-step formation of

the subsurface layer. Deformation occurs in the near-surface region just after entry into the roll bite of the 1st hot rolling pass, where rolling incorporates surface oxide film with lubricants. The presence of rolled-in oxide reduces the total reflectance of the near-surface region compared with the bulk alloy. Consequently, the total reflectance profile corresponding to depth provides a good estimate of the thickness of the surface layer, as the surface layer is pinned by rolled-in oxides, which was confirmed by a comparison of the total reflectance results with cross-sectional TEM investigations of the alloys. Therefore, the total reflectance method is an effective technique of characterizing the surface layer and in turn measuring the average layer thickness [47].

In previous studies, (sub)surfaces of most higher alloyed materials have been investigated by various methods, often combined with a study of their electrochemical behavior. These layers have been proved to be electrochemically more reactive and more susceptible to corrosion than the underlying bulk material, leading to rapid propagation of filiform corrosion.

Annealing appears to have a negligible influence on the thickness of the subsurface layer and does not significantly affect the elemental distributions. Cold rolling reduces the thickness of the deformed layers, breaks up and smears out rolled-in oxide islands in the subsurface of rolled aluminum alloys [48].

## **2.7 Aluminum oxide layer**

Aluminum alloys exposed at elevated temperatures in air during thermomechanical processing inevitably results in oxide scales forming on their surfaces. The thickness of the oxide layer varies with the environmental temperature. Early work showed that aluminum oxide breaks up into smaller particles as it is elongated during rolling, although

subsequent experiments indicate that the oxide layer might be more ductile at high pressures during contact. Observations of aluminum surfaces showed that the oxide scale formed on ingots during preheating breaks into arrays during tensile testing or rolling.

Analysis of the surface composition of hot rolled aluminum alloys revealed that the average thickness of the oxide layer is reduced significantly as it passes through a conventional hot rolling line, further reduction occurs on a tandem mill. The oxide film thickness is about 2–3 nm before the subsequent cold rolling schedule. It is found that cracks perpendicular to the rolling direction are formed near the entry of the roll bite. The spacing between adjacent cracks increases with the oxide film thickness. Observations of the surface and cross-sections of rolled samples reveal that metal is extruded through cracks in the oxide layer within the roll bite, the height of the extruded metal increases with the bulk strain. The area of the original oxide layer is not considerably increased during rolling process, which demonstrates that the oxide does not extend significantly within the bite. If the oxide film is below a critical thickness, the oxide fragments further break into even smaller pieces soon after the entry region in the roll bite [31].

The oxide scale which forms on aluminum alloys is tough, which can behave in a brittle or ductile way. The plastic deformation probably results in intermixing of the oxide scale and the surface metal, leading to a complex subsurface layer.

A secondary oxide scale is inevitably formed between consecutive rolling passes during hot rolling, which will affect the interaction between the roll and work piece, and the quality of the surface of the hot rolled product. Aluminum oxide is also a good thermal insulator. As a result, it will affect the heat transfer during hot metal forming operations. Furthermore, these oxide layers in hot rolled aluminum alloys are also of

interest to the aluminum industry because of the influence of the notably fine subsurface layers on product quality, and in particular, on subsequent filiform corrosion resistance.

Transmission electron microscopy (TEM) investigations of hot rolled Al–Mg alloys indicated a surface layer of continuous metal oxides, which is approximately 10–160 nm thick, and a subsurface layer of 1.5–8  $\mu\text{m}$  thick [13, 49].

## **2.8 Mg diffusion**

Magnesium is a commonly used alloying element in aluminum alloy which provides excellent mechanical and physical properties, with a combination of good corrosion resistance [50].

The magnesium enrichment observed after annealing is attributed to the formation of magnesium oxides, which is due to the magnesium diffusion towards the surface, especially on the outer layers, and reaction with aluminum oxide [46].

After reheating, substantial Mg enrichment is discovered in the subsurface layer. This layer and the surface oxide then contribute to the formation of the subsurface layer observed after rolling. The thickness and morphology of the subsurface layer are dependent on several factors, including the tribological conditions in the roll gap and the total deforming history. However, the structure and morphology of the subsurface layer seems to be strongly dependent on the depth of the Mg enrichment formed during reheating.

Magnesium diffusion to the surface during heating formed magnesium-rich layers, which reduced the junction strength and adhesion between the Al-Mg alloy and the steel roll. It is well established that a magnesium-rich oxide surface layer forms when Al-Mg alloys are heat-treated in a temperature range of 200-600 °C in air. It was proposed that

the magnesium diffusion to the surface can occur through the existing surface oxide layer by outward magnesium ion diffusion and magnesium vapor transfer from oxide defects and voids which is due to the vapor pressure of the magnesium is eleven orders of magnitude higher than that of the aluminum at 440 °C.

The influence of surface oxides on the strength of adhesive junctions which form between the surfaces in contact was related to a metallic material's adhesion tendency to the thickness of the surface oxide layer. It was found that the severity of close metallic contact between the surfaces reduced as the surface oxide thickness increased, which reduced the junction strength owing to adhesion.

The reduction in junction strength was attributed to the formation of MgO on the alloys' surfaces. The thickness of the oxide layer increased with the magnesium content. Therefore a correlation was established between the low adhesion tendency of the alloys and the high magnesium content [51].

## **2.9 Roll coating**

One of the limiting aspects of aluminum hot forming process is the interaction between the hot tool and aluminum work piece surfaces, which results in adhesion and accumulation of material on the tool surfaces, leading to a decrease in the surface quality of the finished products.

The adhesion of aluminum to forming tools is important since it directly affects the quality of the formed part. The choice of the tooling material and its surface condition influences tool cost, durability, and maintenance.

Therefore, the development of non-stick die coatings is an alternative in order to mitigate aluminum adhesion [52].



The adhesion of aluminum to tool surfaces during the hot forming of sheet aluminum alloys generates challenging tribological problems.

The hot forming of aluminum sheets provides flexibility when forming parts with complex shapes, achieving high production rates at a low cost. However, the adhesion of aluminum to tool surfaces is a disadvantage. The resulting defects not only induce deterioration of the surface quality of the work piece, but also lower production because the adhesion must be removed from the dies [53].

Generally, the risk of material adhesion and transfer increased with the roughness of the tool surface. The aluminum alloy, whose oxide is much harder than the parent metal, has no critical surface roughness below which adhesive transfer will not occur. The oxide fractures and fragments indent on the tool surface increasing the risk of adhesion. Adhesion of material to the tool commonly causes severe trouble in many metal forming operations. When adhered and transferred to the tool, the material may experience several mechanisms of hardening including work hardening, grain refinement, oxide particle incorporation, etc. Repeated forming cycles may cause continuous buildup of patches of hardened material which can damage the subsequent formed components through formation of indentations and scratches. The tendency of work material adhesion and galling increases with tool roughness, among other factors. Aluminum alloys is known to be more difficult to form without using strongly additives lubricants.

Adhesion and transfer can occur almost instantaneously when rolling initiates. A single pass is enough to transfer a fully covering layer and even larger lumps.

The transferred material may form thin layers related with relatively lower friction, while thicker layers or lumps associated with higher friction.

Aluminum showed adhesion and transfer against all tool surfaces, even for the lowest load.

The critical surface roughness to avoid adhesion and transfer for materials with soft oxides is associated with the oxide thickness.

Hard oxides may imitate a mechanical grip between tool and work piece.

Applying a coating to the tool surface with a higher hardness than that of the metal oxide is recommended when forming aluminum alloys and other metals with hard oxides.

Friction is also influenced by the transfer of aluminum to the work roll surface. This transfer from the work piece induces a roll coating on the work roll surfaces and occurs regardless of the roll topography and the applied load. However, aluminum transfer increases with roll roughness and can hinder high production rates through galling and may degrade the surface quality of the finished products. The increase in rolling force is also known to influence the presence of friction pickup. The thickness of the material transfer coating to the roll is determined by the size of the oxide fragments covering the work piece surfaces. The roll coating could also reduce the coefficient of friction, acting as a barricade for further aluminum transfer by weakening the adhesion tendency of aluminum to roll surfaces during subsequent rolling passes. In this way, the roll coating may positively influence the work roll performance. The roll coating has an important impact on the surface morphology of the roll and the surface evolution of the rolled material.

During forming process, the surface and subsurface regions of metal sheet are subjected to different conditions and treatments from the bulk of the metal and the tool. The interactions between the metal and the tool surface result in material transfer from

the work piece to the tool. The metal transfer can occur through a variety of mechanisms: adhesion, delamination, microcutting etc. The material transfer is then oxidized and can be retransferred back from the work roll to the aluminum work piece surface, which adversely affect the surface properties.

The most direct influence is the surface appearance. Other properties influenced by the surface/subsurface region include formability, weldability, and effect of finishing operations on surface appearance.

The coating or treatment should prevent adhesion of aluminum to the die surface, hence preventing galling and abrasion. Research is required to understand the phenomena of aluminum adhesion to the die and find methods to prevent it [54].

The present work examines the interactions between aluminum magnesium (Al-Mg) alloys and a selection of PVD coatings under lubricated thermomechanical processing conditions to examine the buildup of roll coatings and potential advantages of PVD coatings in extending the work roll life. Aluminum adhesion was monitored through a typical hot rolling schedule, after the 1st, 10th and 20th rolling passes. The reduction of the lubrication flow rate was carried out for 10 passes to confirm if the Al/Mg adhesion mitigation behavior of Cr and TiCN coatings during hot rolling was influenced by the application of emulsions. This work aims at providing a better insight into the buildup of aluminum adhesion on dies during lubricated thermomechanical processes, as well as exploring the impact that PVD coatings would have on roll coating buildup.

## **2.10 Summary of literature survey**

The friction, tribology and lubrication conditions, the aluminum alloys and surface defects as well as near-surface layers of the rolled aluminum all affect the interactions

between the aluminum alloy and work roll during hot rolling process. PVD coatings are known aid in the mitigation of aluminum to die surfaces.

However, there is hardly research works done so far in the buildup of aluminum adhesion on dies during lubricated thermomechanical processes, as well as the impact which PVD coatings would have on roll coating buildup, as a result, study of rolling with different PVD coatings and lubrication conditions is necessary.

## CHAPTER 3 EXPERIMENTAL PROCEDURE

### 3.1 The work piece

The Al-Mg alloy samples with a 4.5 wt% Mg content, were machined to dimensions of 10 mm width, 30 mm thickness and a length of 95 mm (the 10 mm × 95 mm face being the rolled surface) and were polished with a 1 μm diamond paste to eliminate the effect of surface roughness during hot rolling. The samples were then ultrasonically cleaned in acetone for 15 min to remove surface contaminants

### 3.2 The work rolls

Rolls were machined to a diameter of 25.5 mm from M2 steel with hardness of 7.1 GPa and composition of 1.0 wt.% C, 4.15 wt.% Cr, 81.5 wt.% Fe, 5.0 wt.% Mo, 6.4 wt.% W, and 1.95 wt.% V.

### 3.3 PVD coatings

The PVD coatings, including Cr, TiN and TiCN with reported hardness values of 15.26 GPa [55], 13.90GPa [52] and 21.15 GPa [38] respectively, were deposited on the rolls. The surface topography of the work rolls consisted of discontinuous grinding grooves and possessed an average roughness ( $R_a$ ) of 0.17 μm after coating.

### 3.4 Laboratory simulation

The experiments were carried out using a rolling tribo-simulator possessing a roll-on-block configuration and allows for the altering of rolling parameters individually, including temperature, rolling load, lubrication and roll surface conditions, as the roll can easily be removed and replaced. The configuration allows for the measurement of the torque (G) and rolling force (P) during each rolling pass. The coefficient of friction is

then calculated from the torque, rolling force and the radius of the roll (R) as  $\mu = G/PR$ . The tribo-simulator comprised of a CNC machine with a stage built on it to hold an aluminum block sample. The stage fixed on the controlled stage of the machine was controlled to move along both the x and y axes. Two load cells were attached to the stage to measure the normal and shear forces. Two cartridge heaters were fixed in sample holders attached to the stage, and a thermocouple was put into the sample through a 10 mm deep 1 mm diameter hole on one side of the aluminum sample to monitor its surface temperature. The image of the experimental setup is shown in Fig. 1.

During the rolling process, the aluminum alloy block sample was fixed between two holders and heated to the required temperature. After reaching the temperature reached, the emulsion flow and roll spin started and the stage started moving towards the roll simultaneously, allowing the roll to run across the face of the sample, simulating rolling process.

Rolling tests were conducted with coated and uncoated rolls against an Al-Mg alloy. The surfaces of the work rolls were ground and their surface morphology and roughness were evaluated with optical interferometry using a WYKO NT1100 in the vertical scanning interferometry, VSI, mode.

An oil-in-water emulsion was used as the lubricant and was applied to the work roll surface constantly during the rolling process. It was prepared by mixing neat oil in water at 4% (v/v) concentration using a homogenizer at 15,000 rpm for approximately 5 min. A contact pressure of about 128 MPa was applied during the rolling process.

Table 4 shows the variable process parameters considered in the experiments.

Table 4. Rolling schedule of the experiments

No. of rolling passes	Direction	Temperature	Lubrication flow rate	Work rolls
1	F	550	0.4	Uncoated, Cr, TiN, TiCN
10	FR	550-510		
20	FR	550-460		
1	F	550	0.2	Cr, TiCN
10	FR	550-510		

Forward slip is defined as the difference between the speed of the stage and that of the (linear) speed of the roller divided by the speed of the stage multiplied by 100. The rolling schedule involved 20 passes with a 9% forward slip and the rolling direction reversed with each pass. Hot rolling temperatures started at 550 °C for the first pass, and a 10 °C temperature reduction after each two-pass sequence, such that the temperature at the final (20th) rolling pass was 460 °C. Then the tests with the lubrication flow rate was cut in to half (from 0.4 ml/sec to 0.2 ml/sec) were carried out on Cr and TiCN-coated work rolls for 10 passes with all the other rolling conditions experienced in previous experiments remained unchanged.

The specimen surfaces were then examined using an FEI Quanta 200 FEG environmental scanning electron microscope (SEM) and energy dispersive x-ray spectroscopy (EDS) and backscattered electron mapping at a voltage of 12 kV under high vacuum. The microstructure of the material transfer on work roll surfaces was also examined, using a ZEISS NVision 40 Cross Beam workstation focused ion beam (FIB), with a Ga ion beam operated at low beam currents and an operating voltage of 30 kV. The surface was protected by the deposition of a thin layer of carbon. Cross-sectional trenches were ion milled using the FIB H-bar method. The samples prepared by using the lift-out

method were examined using a JEOL 2010F transmission electron microscope/scanning transmission electron microscope (TEM/STEM).



## CHAPTER 4 EXPERIMENTAL RESULTS

### 4.1. Material transfer to work roll surface after 1 rolling pass

The work roll surfaces were examined under a scanning electron microscope (SEM) after the 1st rolling pass and the images are displayed in Fig. 2. Material transfer was observed on all the work roll surfaces. Energy dispersive spectrometry (EDS) analysis was used to confirm that the transferred material was composed of aluminum and magnesium. The aluminum/magnesium (Al/Mg) transfer was discontinuous and randomly dispersed on all the work roll surfaces. The transfer was observed occurring within and outside the grooves on the surface of the uncoated steelwork roll (Fig. 2a). Transfer to the Cr-coated work roll (Fig. 2b) was observed mainly within the grooves of the work roll, while on the TiN (Fig. 2c) and TiCN-coated (Fig. 2d) work rolls, Al/Mg transfer was observed within the work roll grooves and cavities in these coatings.

EDS mapping of the work roll surfaces after the 1st pass was also carried out to determine the distribution of material transfer on all the work roll surfaces. The maps of the main elements of the coatings, carbon, oxygen and an Al/Mg overlay are presented in Fig. 3. EDS analysis exposed oxygen on all work roll surfaces with the highest concentrations observed on the uncoated (Fig. 3a) and the Cr-coated (Fig. 3b) work rolls. The uncoated and the Cr-coated work roll surfaces were both covered with oxygen, indicating the oxidation of both surfaces. In the case of the Cr-coated work roll, the oxide composition was most likely  $\text{Cr}_2\text{O}_3$ . It should be noted that the Cr-coating possessed a much higher concentration of oxygen than the uncoated work roll. The oxygen on the TiN (Fig. 3c) and TiCN-coated (Fig. 3d) work rolls corresponded mostly with the Al/Mg transfer which suggested that the transferred material was oxidized. Carbon was also

observed on all the work roll surfaces, which was likely from the lubricant (Fig. 3). However, carbon on the uncoated work roll (Fig. 3a) could also be ascribed to the existence of carbides on the steel roll surface, while carbon detected on the TiCN-coated work roll (Fig. 3d) should be mostly originating from the coating. Examination of the aluminum and magnesium EDS maps revealed that for all the work roll surfaces these elements did not consistently overlap. On the uncoated (Fig. 3a) and Cr-coated (Fig. 3b) work rolls, the surfaces appeared to be mostly covered with magnesium.

The amount of material transfer was quantified on a 27.1 mm by 10.0 mm area (the area of the work roll in direct contact with the aluminum work piece during each hot rolling pass) using an image analysis program. The area fraction of the surface covered with Al, Mg and Al/Mg for each individual coating was plotted and is displayed in Fig. 4. The results of this analysis confirmed that the area covered with magnesium was larger than that covered with aluminum for both the uncoated and Cr-coated surfaces. For the uncoated work roll, the areas covered with magnesium and aluminum were 1.36% and 1.12% respectively, while for the Cr-coated work roll they were 0.43% and 0.35% respectively. The TiN and TiCN coatings both possessed a higher percentage area covered with aluminum than magnesium. The uncoated work roll displayed the highest area covered with Al/Mg transfer at 1.75%. The TiCN coating followed, with Al/Mg transfer at 1.20% while the TiN and Cr-coated work rolls had the smallest areas covered at 0.76% and 0.62% respectively. The work rolls displayed a similar trend when the areas covered with only aluminum transfer were examined.

#### **4.2. Material transfer buildup on work roll surface after 10 rolling passes**

The SEM images of the work roll surfaces examined after 10 hot rolling passes are

displayed in Fig. 5. The Al/Mg transfer observed on all the work roll surfaces at this stage of rolling still possessed a patchy and discontinuously dispersed morphology. Transfer was observed both on the surface and within the grooves of the uncoated work roll (Fig. 5a), while it occurred mainly within the grooves of Cr-coated work roll (Fig. 5b). However, at higher magnification, a very thin layer of material transfer was detected on the Cr-coated work roll surface. Al/Mg transfer on the TiN (Fig. 5c) and TiCN-coated (Fig. 5d) work rolls was mainly within cavities, grooves and on the work roll surfaces.

Corresponding EDS maps of the work roll surfaces after 10 passes (shown in Fig. 6) display material transfer distributions similar to those observed after the 1st rolling pass. The aluminum and magnesium distributions did not consistently overlap. Carbon, which was identified on the work roll surfaces, was observed to overlap with the aluminum transfer on the uncoated work roll. Quantification of the areas of the work roll surfaces covered in material transfer, displayed in Fig. 7, revealed that the uncoated work roll was covered with a larger area of magnesium (1.77%) than aluminum (1.40%). The percentage area covered in magnesium (0.21%) was smaller than that covered in aluminum (0.32%) on the Cr-coated work roll. The same trend was observed for the TiN and TiCN-coated work rolls. The uncoated work roll still had the highest area covered with Al/Mg transfer (1.98%), followed by the TiN (1.19%), TiCN (1.06%) and the Cr (0.36%) coated work rolls. At this stage of rolling, the aluminum transfer area fractions on the TiN and TiCN-coated work rolls were similar, i.e., 0.96% for the TiN and 0.92% for the TiCN-coated work rolls. The difference in their total material transfer was related to the higher magnesium buildup on the TiCN coated work roll surface at this stage of the rolling schedule.

Al/Mg transfer buildup was observed for the uncoated and TiN coated work rolls, increasing 13.1% and 56.6% respectively between the 1st and 10th passes. In contrast, a reduction in material transfer was observed on the Cr and TiCN-coated work rolls, decreasing by 41.3% and 11.7% respectively. This reduction of Al/Mg transfer to the Cr and TiCN coated work rolls could be ascribed to the loss of magnesium transfer on the work roll surfaces.

#### **4.3. Material transfer buildup on work roll surface after 20 rolling passes**

Fig. 8 displays the surface examination of the work rolls after 20 hot rolling passes. Al/Mg transfer was still patchy and discontinuously, randomly dispersed on all the work roll surfaces. The material transfer on the uncoated work roll occurring mainly within the work roll grooves and on the surface appeared thicker than previously observed (Fig. 8a). The Cr, TiN and TiCN-coated work rolls all exhibited material transfer within their grooves and on their surfaces. The transfer streaked in the rolling direction on the Cr-coated work roll (Fig. 8b) also appeared to be thicker than previously observed. The transferred material occurred at a higher frequency, predominately located within the grooves on the work roll. The TiN (Fig. 8c) and TiCN-coated (Fig. 8d) work rolls still possessed material transfer in the coating cavities but a greater percentage of the transfer was observed within the grooves of the work rolls.

EDS analysis of the work rolls' surfaces revealed the presence of aluminum, magnesium and oxygen at this stage of thermomechanical processing as displayed in Fig. 9. The EDS maps of the Al/Mg overlay still displayed regions with no aluminum and magnesium overlap. The EDS maps of the coatings on the work roll surfaces displayed areas coinciding with the Al/Mg transfer where no coating (Fe, Cr, Ti) was observed. The

plot displaying the area fractions covered with material transfer on the work rolls' surfaces is shown in Fig. 10. As with previous passes, the uncoated M2 steel exhibited the largest area covered with Al/Mg transfer (2.41%), while the Cr-coated work roll displayed the lowest (0.60%). TiN and TiCN-coated work rolls showed similar percentage areas covered with Al/Mg transfer (~1.20%). The area fractions covered in aluminum were similar to those covered in magnesium for the uncoated M2 work roll at 1.95% and 1.93% respectively. The same trend was observed for the Cr-coated work roll with aluminum and magnesium each covering 0.43% of the rolls' surfaces. The quantification of material transfer to the TiN and TiCN-coated work rolls showed the aluminum transfer area fractions on these rolls were 1.11% and 0.97% respectively while the magnesium area fractions were 0.89% and 0.81% respectively.

The Al/Mg transfer behavior from the 1st to the 20th pass has been plotted and displayed in Fig. 11. Material transfer buildup was observed on the uncoated M2 work roll, with Al/Mg transfer area fraction increasing by 13.40% between the 1st and 10th pass and increasing again by 8.40% between the 10th and 20th pass. The uncoated M2 steel work roll also presented constant individual aluminum and magnesium transfer buildup during all the rolling passes monitored. However, for the Cr-coated work roll, Al/Mg transfer decreased by 41.93% between the 1st (0.62%) and 10th (0.36%) pass, while an 8.40% increase in material transfer was observed between the 10th and 20th (0.60%) pass. For the TiCN-coated work roll, the Al/Mg transfer area fraction showed an 11.67% decrease between the 1st (1.20%) and 10th (1.06%) pass, but it increased by 15.09% between the 10th and 20th pass (1.22%). However, the work roll coated with TiN showed an Al/Mg transfer buildup of 56.58% between the 1st pass (0.76%) and 10th pass (1.19%);

no further material transfer buildup was observed after the 20th pass (1.20%). After 20 passes the amount of material transfer observed on the TiN and TiCN coated work rolls was noted to be similar, while after the initial 10 passes the TiCN-coated work roll had less material transfer on its surface and after the 1st pass the TiN coating appeared to have less material transfer.

#### **4.4. Microstructural analysis of material transfer buildup on work roll surface after 20 rolling passes**

Subsurface examinations of the material transfer to work rolls after the 20 pass thermomechanical processing schedule were made using FIB-milled cross-sections made along the rolling direction. The FIB cross-section of the Al/Mg transfer to the uncoated work roll surface (Fig. 12(a)) revealed full contact between the transfer and the steel surface indicating adhesion of the Al/Mg to the steel surface. The Al/Mg transfer was observed to possess dark porous regions which had a higher concentration of magnesium. There were also cracks within this Al/Mg transfer layer. The Al/Mg transfer layer on the Cr coating was also fully adhered to the coating surface (Fig. 12(b)). The Al/Mg transfer was identified, using EDS analysis, to be lying on an oxide rich chromium interface, separating it from direct contact with the Cr coating. This layer was most probably  $\text{Cr}_2\text{O}_3$  and was about 50 nm thick. The cross-sectional analysis of Al/Mg transfer layers on the TiN (Fig. 12(c)) and TiCN (Fig. 12(d)) coatings displayed similar porous structures fully adhered to these coatings' surfaces. Areas with loosely adhered Al/Mg transfer on the TiN and TiCN coating surfaces were also identified, which were mostly observed lying on the smooth surface areas of the coatings. Al/Mg transfer to the work roll grooves were mostly observed to be fully adhered to the coatings' surfaces. There was no observable damage

to any of the PVD coatings in any form.

#### **4.5. Al-Mg alloy surface examination after 20 rolling passes**

The SEM images of the rolled aluminum alloy surfaces are presented in Fig. 13. All the rolled aluminum surfaces possessed rolling marks, grooves and ridges. The surfaces appeared white with black spots covering them. EDS analysis confirmed that the surfaces were rich in magnesium and oxygen. EDS mapping of the rolled aluminum surfaces (Fig. 14), revealed randomly dispersed areas rich in aluminum, but low in oxygen and magnesium concentrations, on an otherwise magnesium-rich surfaces. These areas were identified as aluminum pickup defects, which occurred due to the back transfer of aluminum from the Al/Mg transfer (roll coating) on the work rolls to the rolled aluminum sample surface. The pickup defects either distended from the alloy surface (Fig. 13(b) and (d)), or were compressed into the alloy surface (rolled-in) during the rolling schedule (Fig. 13(a) and (c)). The pickup defects that were rolled-in had likely become part of the aluminum alloy near-surface layer, while distended pickup defects had probably been recently transferred back from the roll coating.

The EDS maps were also used to quantify the frequency and the amount of pickup defects covering the rolled aluminum alloy surfaces. Pickup defects were largely observed on the aluminum samples rolled with the uncoated work roll, occurring at a much higher frequency than the samples rolled with the PVD-coated work rolls. The pickup defects also covered the largest area, at 1.32%, of the sample rolled with the uncoated work roll. The aluminum samples rolled with the nitride coatings were covered with a similar amount of pickup defects, i.e., 0.32% for the TiCN and 0.30% for the TiN coatings. The sample rolled with the Cr-coated work roll possessed the smallest area

fraction covered with pickup defects at 0.21%.

Thus, the performance of the coatings in terms of pickup defects on the rolled aluminum samples appeared to follow a similar trend to the Al/Mg transfer on the corresponding work rolls. This will be discussed in greater detail in Chapter 5.

#### **4.6 Material transfer buildup on the work roll surfaces after 1 rolling pass at low lubrication flow rate**

In this study, these experiments were carried out on the Cr and TiCN-coated work rolls using a reduced lubrication flow rate of 0.2 ml/sec which was half of the flow rate (0.4 ml/sec) used in previous experiments. The lubrication flow rate was the only experimental condition that was changed, all the other rolling conditions experienced in previous experiments remained unchanged.

Fig. 15 and Fig. 16 show the Cr and TiCN-coated work rolls under low lubrication flow rate after the 1st hot rolling pass. Material transfer was observed on both of the work roll surfaces. EDS analysis confirmed that the material transfer was composed of aluminum and magnesium. The Al/Mg transfer was discontinuous and appeared to be randomly dispersed on both of the work roll surfaces. The transfer was observed occurring within and outside the grooves on the surface of the Cr-coated work roll (Fig. 15). For TiCN-coated work roll (Fig. 16), material transfer was observed within the grooves and cavities and also on the work roll surface. Material transfer occurring on both of the work roll surfaces was visually observed to be thick and pronounced (Fig. 15(b) and Fig. 16(b)).

EDS mapping of the work roll surfaces after the 1st pass was carried out and the main elements of the coatings, oxygen and an Al/Mg overlay are presented in Fig 17. The



morphology of the material transfer on both work roll surfaces was similar to that observed under high lubrication flow rate (Fig. 3(b), Fig. 3(d)).

The area fraction of the surface covered with Al, Mg and Al/Mg for each coating at low flow was individually plotted and is displayed in Fig. 18. The results revealed that the area covered with material transfer on TiCN coating was larger than that covered with Cr. TiCN had higher area covered with Al/Mg (1.28%) than that of Cr (0.65). The area covered with Mg (0.55%) was noted to be higher than that covered with Al (0.51%) on the Cr-coated work roll, while the area covered with Al (1.16%) was higher than Mg (1.00%) on TiCN.

#### **4.7 Material transfer buildup on the work roll surfaces after 10 rolling passes at low lubrication flow rate**

The SEM images of the work roll surfaces examined after 10 hot rolling passes under the reduced lubrication flow rate are displayed in Fig. 19 and Fig. 20. The material transfer observed on both of the work roll surfaces at this stage of rolling was still patchy and discontinuously dispersed. For the Cr-coated work roll (Fig. 19), material transfer occurred both on the surface and within the grooves. For TiCN-coated work roll (Fig. 20), transfer was observed within grooves, cavities and on the surface of work roll. There was thicker material transfer which could be visually observed covering a wider surface area (Fig. 19 and Fig. 20).

Corresponding EDS maps of the work roll surfaces after 10 passes (Fig. 21) display material transfer distributions similar to those observed after the 1st rolling pass. Quantification of the areas of the work roll surfaces covered in material transfer, displayed in Fig. 22, revealed that the areas covered in Al, Mg and Al/Mg were all higher

on TiCN (5.42%, 5.60%, 6.68%) than on Cr (3.03%, 3.07% and 3.65% respectively). And the area covered in Al is similar to Mg for both coatings.

## CHAPTER 5 DISCUSSION

After a thermomechanical processing schedule consisting of 20 passes, a stable and continuous roll coating was not observed on any of the coated or uncoated work roll surfaces. Material transfer to the work roll surface was detected as individual isolated patches after the 1st (Fig. 2), 10th (Fig. 5) and 20th (Fig. 8) passes. The morphology of the material transfer observed is similar to that described by Smith et al. [56]. The distribution of material transfer has been reported to be reduced by lubrication, commonly reported as patchy and discontinuous during lubricated tests, as the mechanical interactions between the work roll/aluminum alloy surfaces determine the amount of transfer [57]. Material transfer to the work roll surfaces was constantly composed of aluminum, magnesium and oxygen (Figs. 3, 6 and 9). Al/Mg transfer was predominantly observed within the grooves and cavities and, at higher number of passes, on the surfaces of the work rolls. Tripathi [58] has reported that aluminum entrapment is predominantly associated with the rougher features of the work roll surface, i.e., the rough areas of holes and grinding grooves. He related the roll coating development to the surface roughness of the work roll. The low surface roughness of the work rolls used in this study would therefore contribute to the material transfer distribution observed [58].

Al/Mg buildup was observed on most of the work roll surfaces as is evident from the increase in area fractions covered with Al/Mg transfer observed after 20 passes for the uncoated and TiCN coated work rolls (Fig. 11). Analysis of the TiN and Cr-coated work roll surfaces showed Al/Mg buildup after 20 passes in the form of thicker patches of material transfers observed on their surfaces, despite not displaying an increase in Al/Mg transfer area coverage. The reduction of the area covered in Al/Mg on the Cr and TiCN-

coated work roll' surfaces observed between the 1st and 10th pass indicated the back transfer of Al/Mg from the work roll surface to the rolled aluminum sample. Back transfer in the form of pickup defects was observed on all the rolled samples. Pickup defects occurred at a high frequency and area coverage on the aluminum sample rolled against the uncoated work roll, which displayed no Al/Mg transfer loss from its surface (Fig. 11). Al/Mg transfer (evident from roll coating buildup) and back transfer (evident from pickup defects) could therefore be thought of as two competing mechanisms that occur simultaneously during lubricated thermomechanical processes, like hot rolling. Smith et al. [56] have described these competing mechanisms as a continuous two-way material transfer mechanism occurring between the rolled metal surface and the roll coating due to the transfer of aluminum to and from (back transfer) the work roll surface. The rate of occurrence of this two-way transfer mechanism would determine the development of the roll coating on the work roll surface at each stage of the rolling process. Higher magnification analysis of the uncoated M2 steel work roll surface (Fig. 23(a)) was used to confirm the back transfer of roll coating from the work roll surface. This examination of the Al/Mg adhered to the uncoated work roll surface after 20 passes revealed a stable thin Al/Mg transfer layer at the outskirts of a thicker Al/Mg transfer layer buildup on the work roll surface. The more pronounced Al/Mg transfer layer displayed non-uniformed thickness and possessed fractures within the heavier transfer regions. Cross-sectional examination of the fractured regions of the Al/Mg transfer layer (Fig. 23 (b)) showed that the Al/Mg layer was partially delaminated. The delaminating portion could easily be detached and transferred back to the alloy surface (as described by Smith et al. [56]) during the subsequent passes, thereby forming a pickup defect. Loosely

adhered Al/Mg transfer layers were also observed on the smoother surfaces of the TiN and TiCN-coated work rolls. Thus, loosely adhered and fractured Al/Mg transfer could be considered as unstable areas of the roll coating that would easily form pickup defects on aluminum alloys during thermomechanical processes. In that light, while it might be expected that a stable roll coating would be achieved on the uncoated work roll surface by simply increasing the number of rolling passes, based on industrial observations, similar extrapolation for PVD coatings might not be a reasonable assumption, in part due to these competing mechanisms.

The two-way material transfer would explain the fluctuating difference in the amount of Al/Mg transfer observed on the TiN and TiCN coated work rolls' surfaces at each pass. The difference in material transfer on these coatings during the hot rolling stages could also be related to their oxidation temperature. TiCN is known to possess a lower oxidation temperature (500 °C) than TiN (600 °C) and could therefore experience the initiation of oxidation during the first rolling pass which occurs at 550 °C [59-62]. The TiCN-coated work roll might therefore have more material transfer to its surface than back transfer due to the initial formation of a small amount of TiO<sub>2</sub> on its surface, which is known to induce the degradation of Ti-based coatings [60, 62]. The reduction of temperature during subsequent rolling passes to levels well below the oxidation temperature of TiCN, would result in its improved material transfer mitigation properties. While TiCN has been shown to possess a temperature dependent tribological behavior, TiN has been observed to retain its tribological properties at elevated temperatures [61, 63]. TiCN has been reported to display improved Al/Mg mitigating performance at lower

temperatures as observed by Konca et al. [64], who reported lower aluminum transfer to TiCN coatings in comparison to TiN at low temperatures during sliding contact.

Previous work performed with PVD-coated work rolls carried on commercial purity aluminum revealed that the Cr-coated work roll had one of the worst mitigation behaviors during dry cold rolling and lubricated hot rolling tests. However, the previous hot rolling tests were carried out at a lower temperature (450 °C), and Cr as a coating exhibits a temperature dependent behavior, as its adhesion mitigating properties is highly reliant on the formation of a passive, self-healing Cr<sub>2</sub>O<sub>3</sub> layer [65, 25, 34]. The thickness of this oxide layer is an essential factor in enhancing the coatings' tribological performance [25]. The oxidation behavior of Cr has been reported as parabolic above 700 °C while at lower temperatures a logarithmic to parabolic oxidation behavior has been observed [34]. In contrast, the present study reports work with Cr coatings against Al-Mg alloys with rolling occurring at higher temperatures (550 °C – 460 °C). The EDS maps of the Cr coating (Figs. 3(b), 6(b) and 9(b)) showed that the coating surface was covered with oxygen after each examined pass, suggesting that the coating was oxidized. Previous work also revealed the Cr coating surface covered with oxygen after 1 pass at 450 °C [66]. However, cross-sectional analysis, in this study revealed a 50 nm thick Cr<sub>2</sub>O<sub>3</sub> layer between the Al/Mg transfer layer and the Cr coating (Fig. 12(b)) which was not observed in the previous work [66]. It should also be noted that MgO formed on Al-Mg alloy surfaces during heating, as observed from the rolled aluminum surfaces (Fig. 14), has been reported to act as a solid lubricant [51].

Past assessment of coating behavior, coated work rolls in particular, evaluate the coatings after either 1 pass [66] or after a typical rolling schedule [67, 68]. The present

study was focused on the behavior of PVD coatings during the hot rolling schedule, primarily the buildup of aluminum transfer to the work roll surfaces. The coating performance in this study is presented as a graph in Fig. 24, which plots the Al/Mg transfer area fraction on the work rolls against the area fraction of the aluminum sample covered with pickup defects after the 20 pass rolling schedule. It shows the Cr-coating possesses one of the lowest amounts of Al/Mg transfer to its surface and back transfer from its surface. The uncoated M2 steel work roll displayed a steady Al/Mg transfer buildup with the largest Al/Mg transfer area fraction on its surface. Therefore, assuming that the development of a stable roll coating is desired during an industrial hot rolling process, the uncoated work roll would be preferred for roll coating development, as it displayed constant Al/Mg buildup. On the other hand, the Cr coating appeared to efficiently mitigate against Al/Mg transfer to its surface, and as such, it would be preferred when a roll coating is not desired. The large area fraction of the rolled aluminum alloy surface covered with pickup defects accompanying the large amount of Al/Mg buildup on the uncoated work roll, suggests that the buildup of this coating came at the cost of the surface quality of the rolled aluminum sample. The graph in Fig. 24 shows that the increase in the area fraction covered with Al/Mg transfer on the work roll surface correlates to the increase of the area fraction on the aluminum alloy surface covered with pickup defects. This observation highlights the highly unstable nature of roll coatings during their initial buildup on a fresh work roll surface during thermomechanical processing.

There appears to be an increase in the instability of the coating with increase in its area coverage, probably until a continuous coating is achieved on the work roll surface.

Therefore, it is plausible to suggest that an ideal rolling situation would involve either a fully developed roll coating on the work roll surface or a PVD coating that fully mitigates aluminum transfer to its surface.

The Al/Mg transfer on Cr (Fig. 15 and Fig. 19) and TiCN-coated (Fig. 16 and Fig. 20) work rolls was observed within and outside the grooves on the surface during lubrication at low flow rate, while it was observed mainly within the grooves and cavities with previous experiments at high flow (Fig. 2 (b), Fig. 2(d), Fig. 5(b) and Fig. 5(d)). Material transfer was also visually observed to be thicker and to cover a wider surface area for both the Cr and TiCN coatings with the reduction of the lubrication flow rate. The reduction of the lubrication flow rate was carried out to confirm if the Al/Mg adhesion mitigation behavior of these PVD coatings during hot rolling was influenced by the application of emulsions. These results confirm that these coatings are indeed influenced by the emulsion during the hot rolling process. Therefore, the elimination of the application of emulsions during hot rolling even with the application of these PVD coatings to work roll surface might not be practical due to increased adhesion to the work roll surface.

Fig. 25 and Fig. 18 reveal that the area covered with material transfer on TiCN coating was larger than that covered on the Cr coating under both high and low lubrication flow conditions. The Cr coating, thus can be said to better mitigate against the buildup of aluminum adhesion to the work roll surface regardless of the lubrication flow rate in comparison to the TiCN coating. Therefore, it might prove difficult to buildup a roll coating on the Cr coating, if a stable and continuous roll coating is required.



In this study, the material transfer increased with the reduction of the lubrication flow rate on the tested PVD coatings. The ability to reduce the adhesion to the work roll surface of these PVD coatings appeared to be influenced by the emulsion used in these hot rolling experiments. This could be due to the influence of the reduction in the emulsion has on the two-way material transfer mechanism which as stated earlier would determine the amount of material transfer. Reducing the emulsion flow rate might facilitate the transfer from the work piece to the work roll, inducing this to become the dominant mechanism, therefore, the rate of roll coating buildup would increase as observed. The increase indicated the emulsion appeared to be essential in mitigating against adhesion.

Comparing the area covered with material transfer during the 1st hot rolling pass at high flow and low flow rate (Fig. 26) for the Cr-coated work roll, Al transfer was observed to be higher by 33.33%, Mg transfer by 21.82%, and Al/Mg transfer by 4.62% with the reduction of flow rate. Although the Al/Mg transfer area fraction did not show much increase (4.62%), the thickness of the material transfer could visually be observed to be thicker (Fig. 15 and Fig. 2 (b)) than that at high flow. While for the TiCN-coated work roll (Fig. 27), Al transfer was higher by 12.07%, Mg transfer by 14.68%, and Al/Mg transfer by 6.25% when the lubrication flow rate was reduced. The difference in Al/Mg transfer with reduction of flow rate was slightly higher for TiCN (6.25%) compared with Cr (4.62%). Fig. 28 and Fig. 29 show the area fraction covered with material transfer on TiCN coating was larger than that covered with Cr individually at both high and low flow. Fig. 28 reveals that under high flow, area covered in Al was higher than Mg for both coatings. Fig. 29 reveals the area covered with Al and Mg was

similar under low flow rate. Fig 30 plots the area covered with material transfer under high and low flow rate for the Cr coating after 10 passes. A comparison of the area covered with Al transfer under low lubrication flow rate with the high flow rate at this stage of rolling showed it was higher by 84.47%, Mg transfer was higher by 90.55% and the Al/Mg transfer by 85.74%. For TiCN (Fig. 31), Al transfer was higher with the reduction of the lubrication flow rate by 83.0%, Mg by 87.32% increase and Al/Mg transfer by 84.12% at low flow rate compared with high flow. Material transfer was also visually observed to appear thicker with reduction of lubricant flow rate for both coated rolls. The high difference in material transfer covering the coated work roll surfaces after 10 hot rolling passes indicated that roll coating thus appeared to buildup faster with lubrication reduction.

Fig. 32 shows the comparison of the area covered with material transfer Al/Mg at low flow and high flow after 1 pass and 10 passes of both coatings individually. After the initial pass, the area covered with Al/Mg was similar for both coatings under both high and low flow, which indicated the lubrication condition did not influence the transfer in a more dominant way than surface condition. The area covered with Al/Mg transfer did not decrease much from the 1st pass to the 10th passes under high flow rate for both coatings, while it increased dramatically from the 1st pass to the 10th passes under low flow. Therefore, as the number of rolling passes increases, the lubrication condition seems to play a more dominant role in influencing the buildup of roll coating than roll surface conditions, the behavior of the coatings cannot be judged by that of the initial passes.

After 10 passes hot rolling schedule under low flow, there was no damage observed on the tested PVD coatings.

## CHAPTER 6 CONCLUSIONS

The behavior of PVD-coated work rolls during a 20 pass hot rolling schedule of an Al-Mg alloy was examined. Work rolls were coated with Cr, TiN and TiCN, and material transfer buildup on the coated rolls was monitored and compared with the buildup on an uncoated work roll surface. Analysis of the work roll surfaces after the 1st, 10th and 20th passes led to the following observations:

1. The Cr-coated work roll displayed the least Al/Mg transfer to its surface at each stage of the hot rolling schedule, due to the formation of a stable  $\text{Cr}_2\text{O}_3$  layer formed on its surface. Although a reduction of Al/ Mg transfer was observed during the rolling schedule, buildup was observed in the form of an increase in the thickness of Al/Mg transfer after the 20th pass. The aluminum sample rolled with this coating also showed the smallest area fraction covered with pickup defects.

2. The uncoated M2 steelwork roll possessed the largest Al/Mg transfer area fraction on its surface after the 1st, 10th and 20th passes. A continuous buildup of Al/Mg transfer through the 20 pass rolling schedule was observed in terms of area fraction and thickness increase. The aluminum sample surface rolled with the uncoated M2 steel also had a large area fraction covered with pickup defects.

3. A difference in the performance of TiN and TiCN was observed after the 1st and 10th rolling pass, with the TiN coating displaying the better performance after the 1st pass, while the TiCN displayed the better performance after the 10th pass. This was attributed to a two-way material transfer mechanism between the work roll and the rolled aluminum alloy surfaces.

4. The TiN and TiCN-coated work rolls displayed similar performance after 20 passes, with similar amount of Al/Mg transfer observed on both surfaces. This indicates that the material transfer buildup on these coatings during the rolling schedule could not be extrapolated from the early hot rolling passes due to the two-way material transfer mechanism.

5. The reduction of the lubrication flow rate resulted in the increase in material transfer to the PVD work roll surfaces. The Cr-coated work roll experienced a surface area increase in material transfer on its surface of a 4.62% after the 1st pass and an 85.74% after the 10th pass while the TiCN-coated work roll displayed a 6.25% and 84.12% increase after the 1st and 10th pass respectively.

6. The emulsions used during hot rolling of aluminum alloy plays an important role in Al/Mg transfer and the buildup of roll coatings regardless of the work roll surface condition during the aluminum hot rolling processes.

7. The Cr-coated work roll displayed less material transfer on its surface than the TiCN-coated work roll under both high and low lubrication flow rate.

8. As the number of rolling passes increased, the lubrication condition seems to play a more dominant role in influencing the buildup of roll coating under reduced lubrication flow rates. Therefore, the performance of the PVD coatings under this condition cannot be judged by their performance at the initial rolling pass.

9. After all the experiments carried, all the PVD coatings tested showed no damage onto their surfaces visually.

## FIGURES

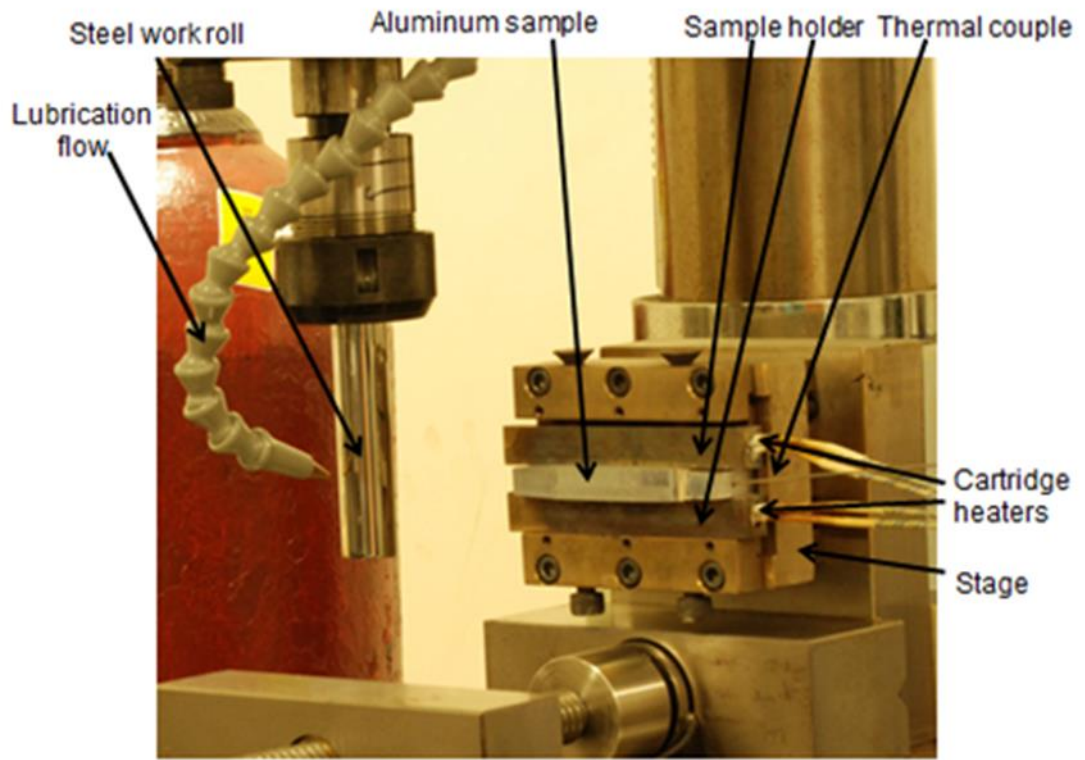


Figure 1. General view of experimental setup of hot rolling simulation.

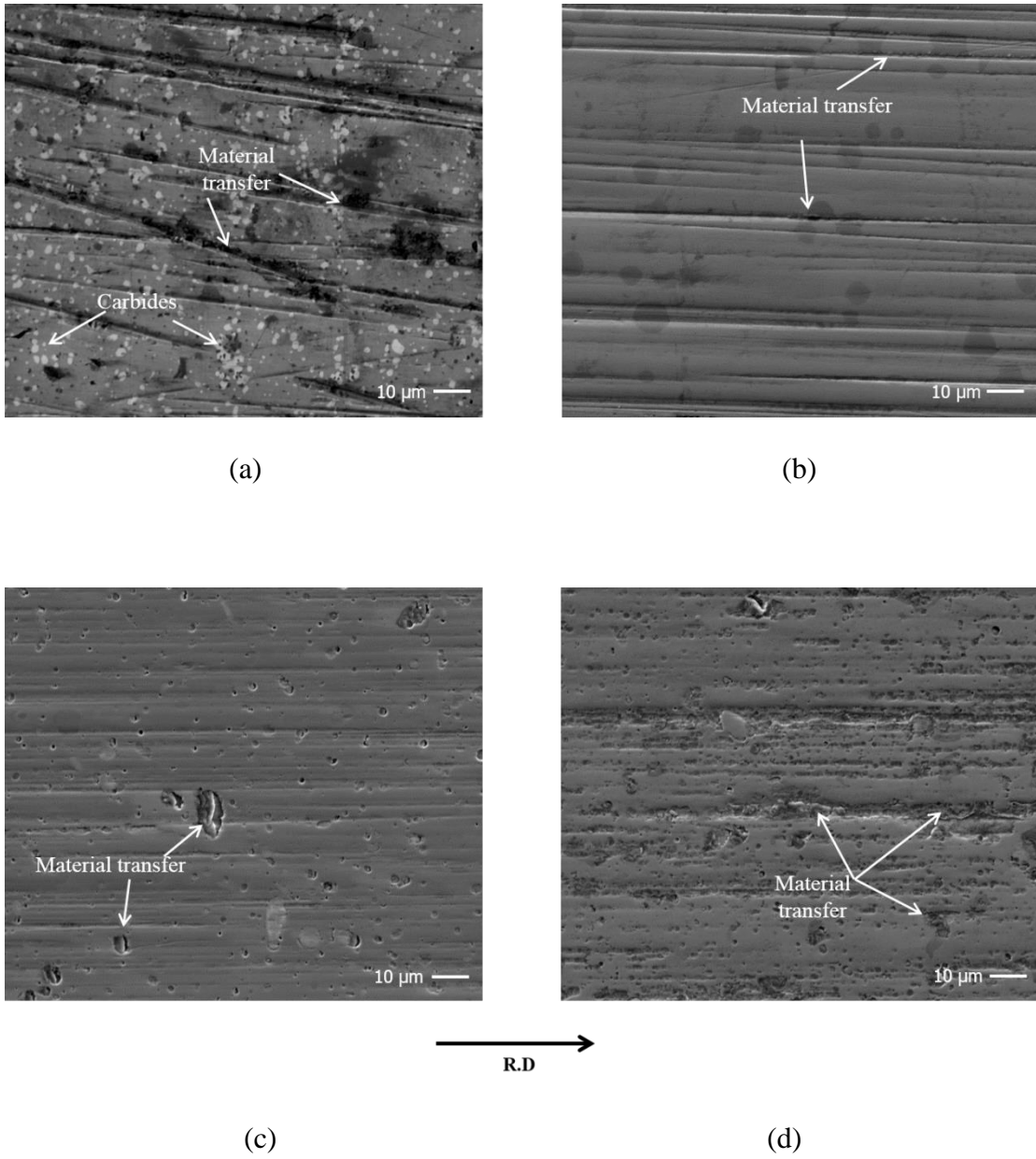
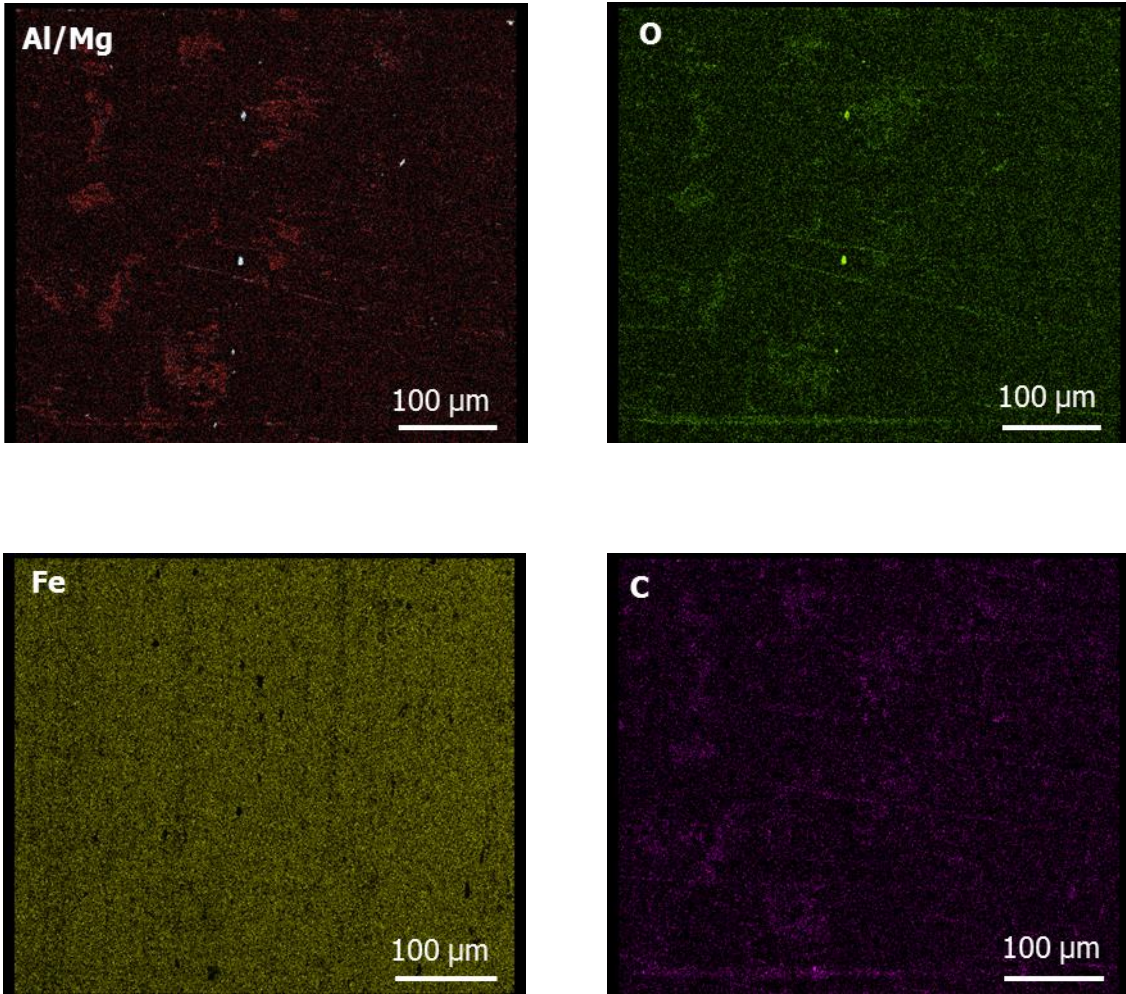
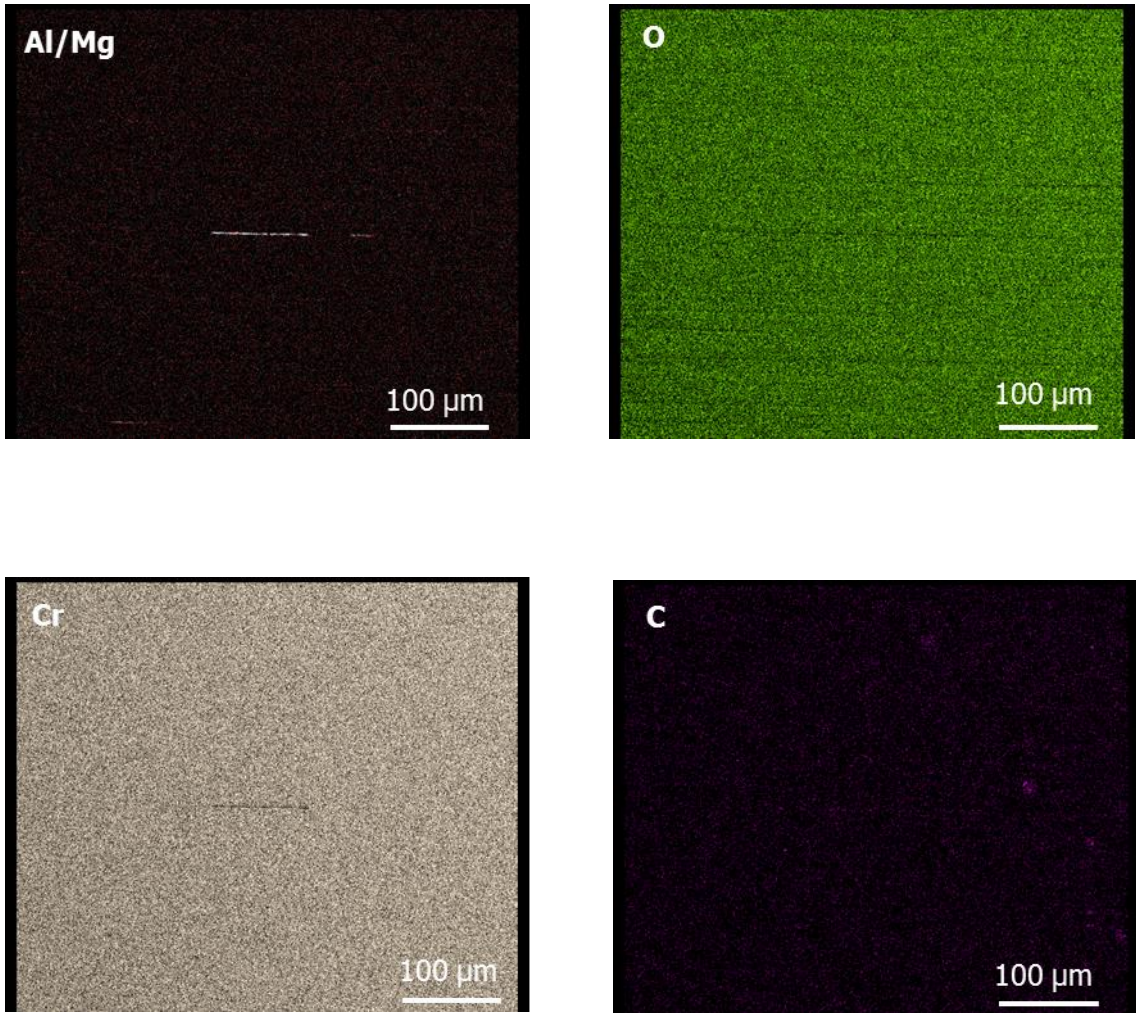


Figure 2. SEM images displaying material transfer to the (a) uncoated (b) Cr-coated (c) TiN-coated and (d) TiCN-coated work rolls after 1 hot rolling pass against an Al-Mg alloy.



(a)

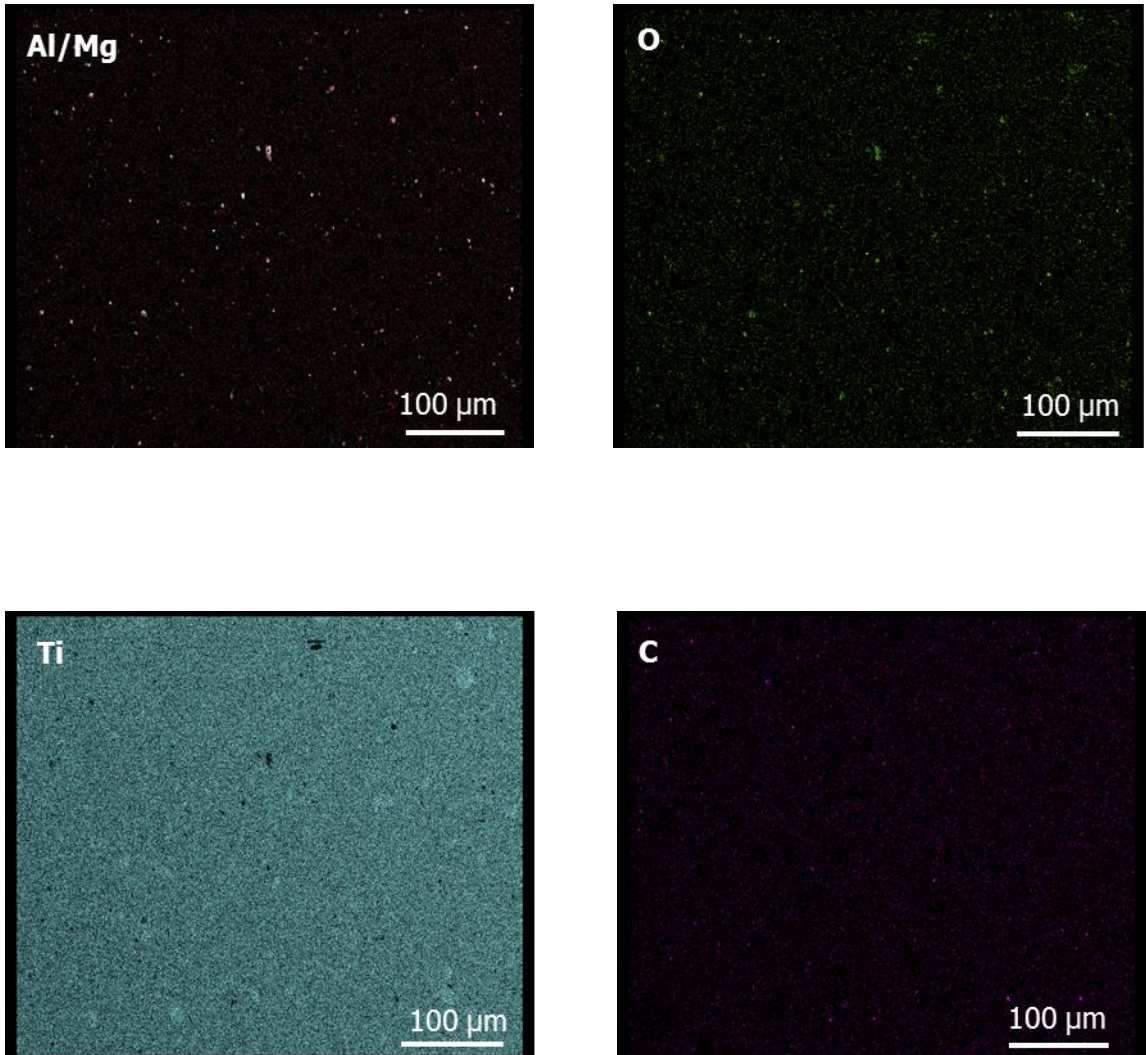
Figure 3. EDS maps displaying Al/Mg transfer, oxygen and carbon on the (a) uncoated work roll after 1 pass against an Al-Mg alloy. Aluminum, magnesium, oxygen, carbon, titanium, iron and chromium are represented by blue, red, green, purple, cyan, yellow and magenta, respectively.



(b)

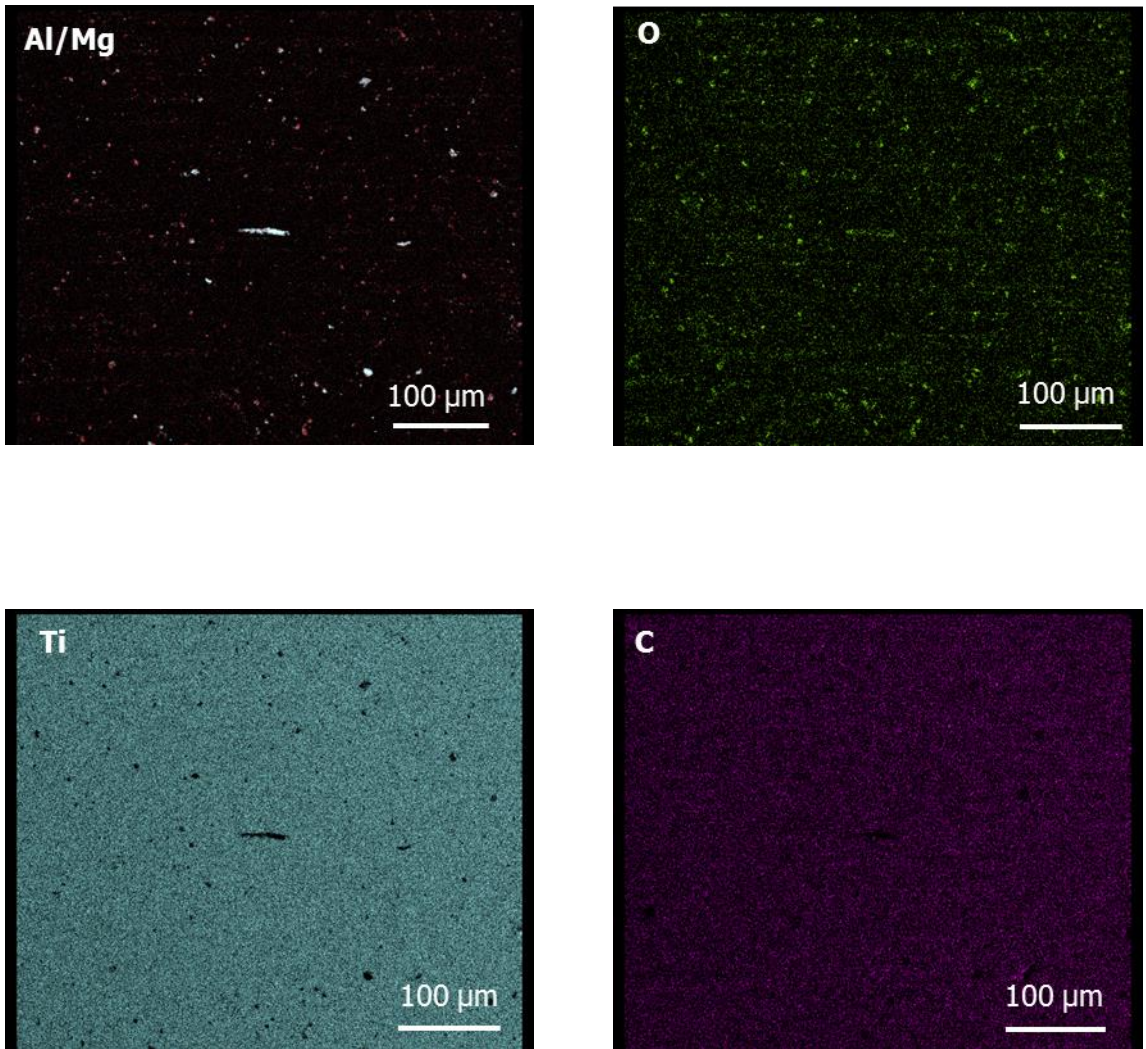
Figure 3. EDS maps displaying Al/Mg transfer, oxygen and carbon on the (b) Cr-coated work roll after 1 pass against an Al-Mg alloy.





(c)

Figure 3. EDS maps displaying Al/Mg transfer, oxygen and carbon on the (c) TiN-coated work roll after 1 pass against an Al-Mg alloy.



(d)

Figure 3. EDS maps displaying Al/Mg transfer, oxygen and carbon on the (d) TiCN-coated work roll after 1 pass against an Al-Mg alloy.

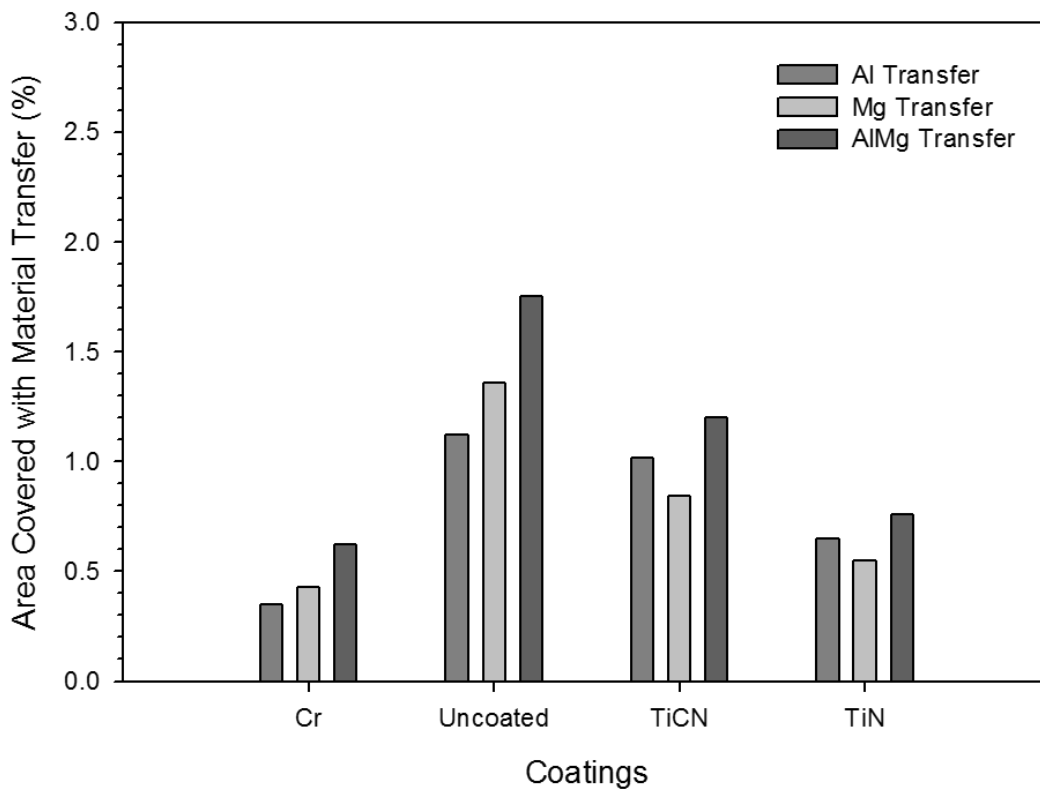


Figure 4. Material transfer area fractions on the work roll surfaces plotted for each coated work roll after 1 rolling pass.

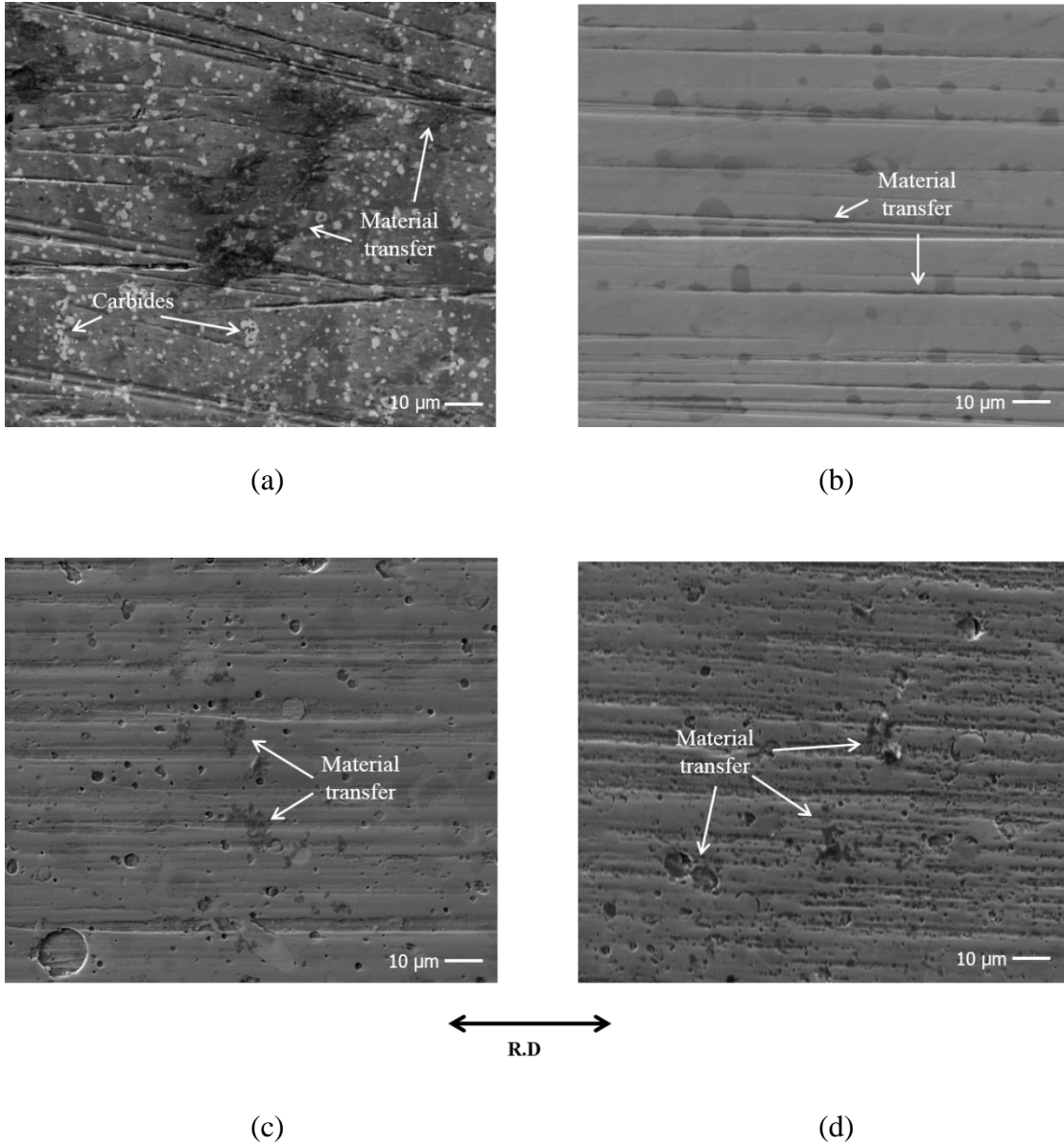
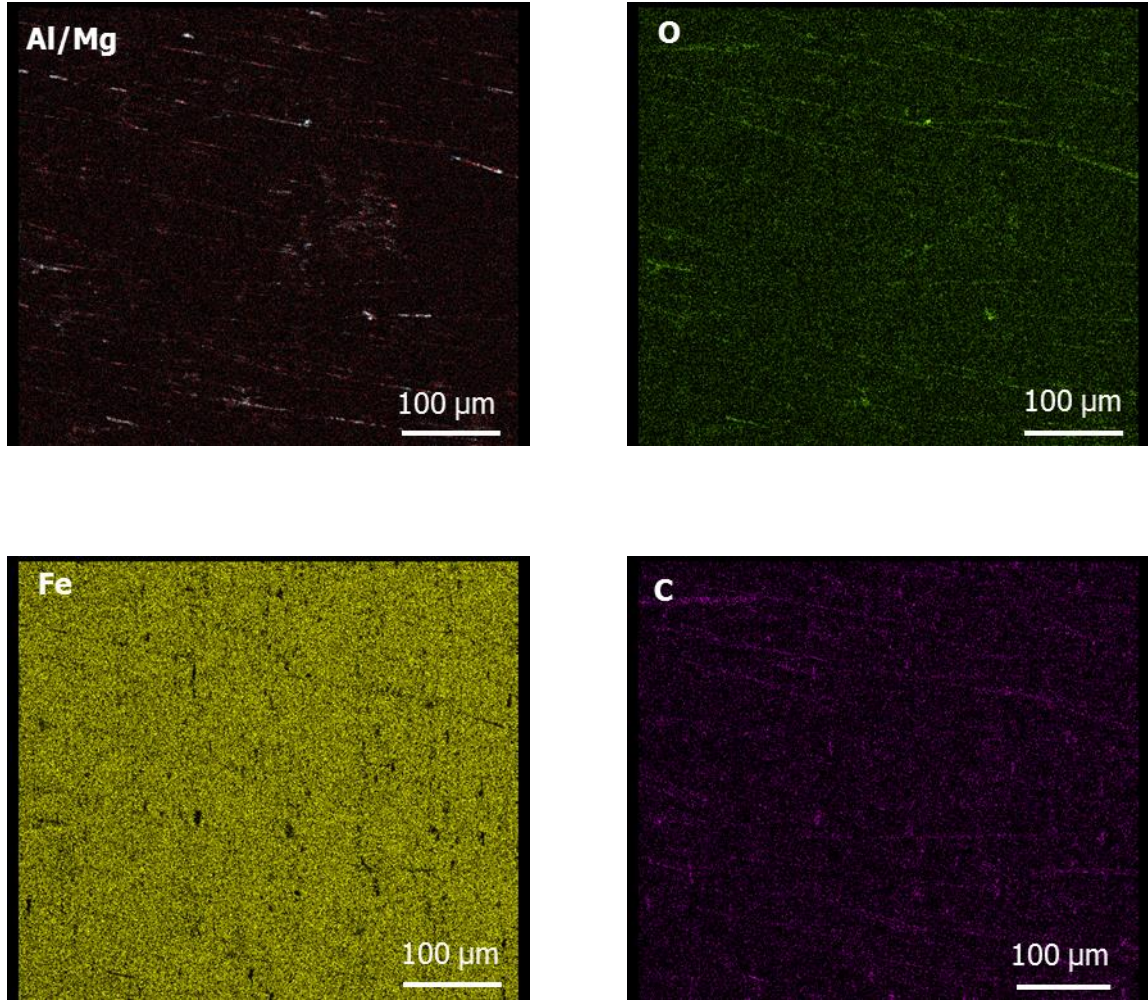
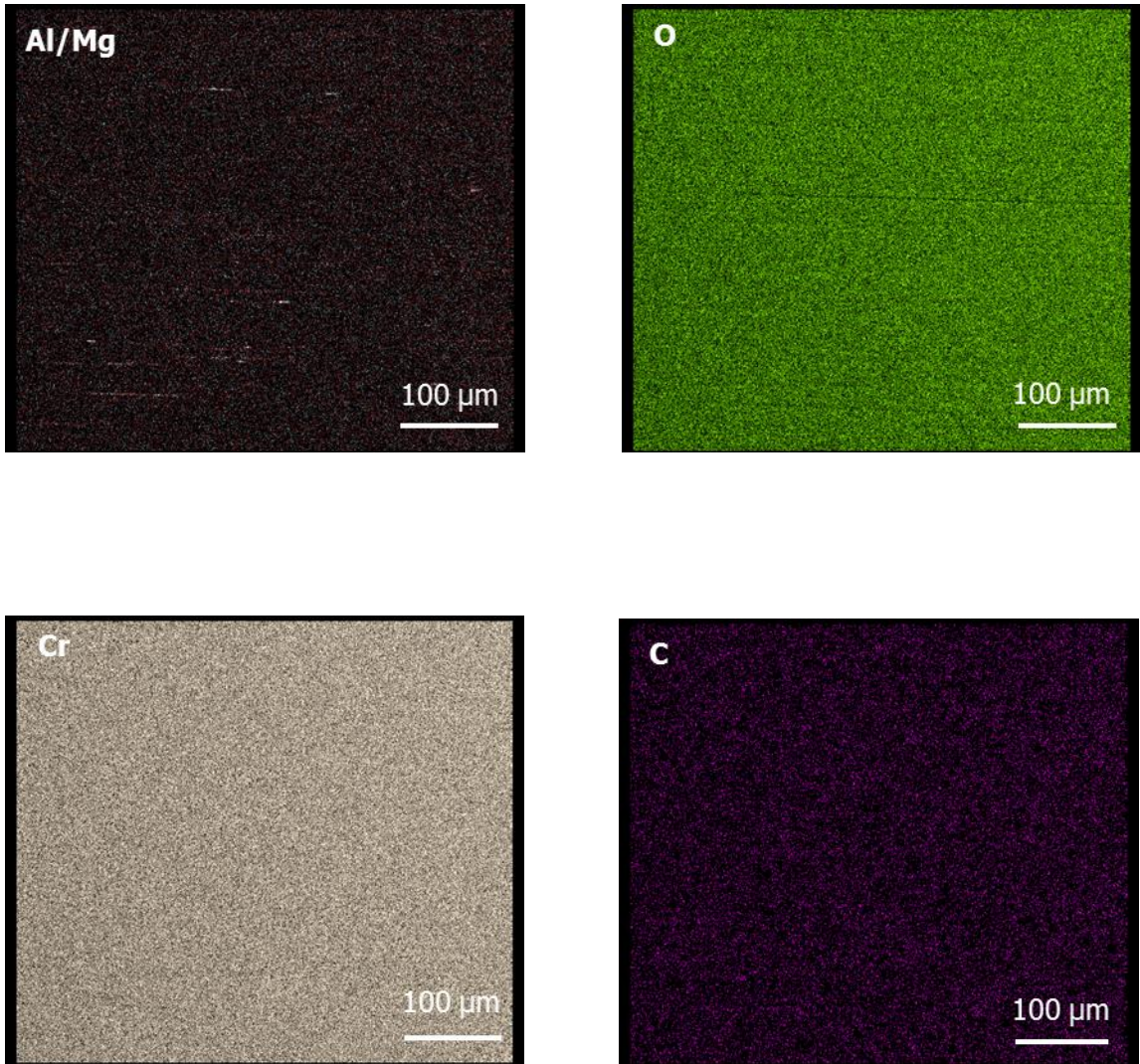


Figure 5 SEM images displaying material transfer to the (a) uncoated (b) Cr-coated (c) TiN-coated and (d) TiCN-coated work rolls after 10 hot rolling passes against an Al-Mg alloy.



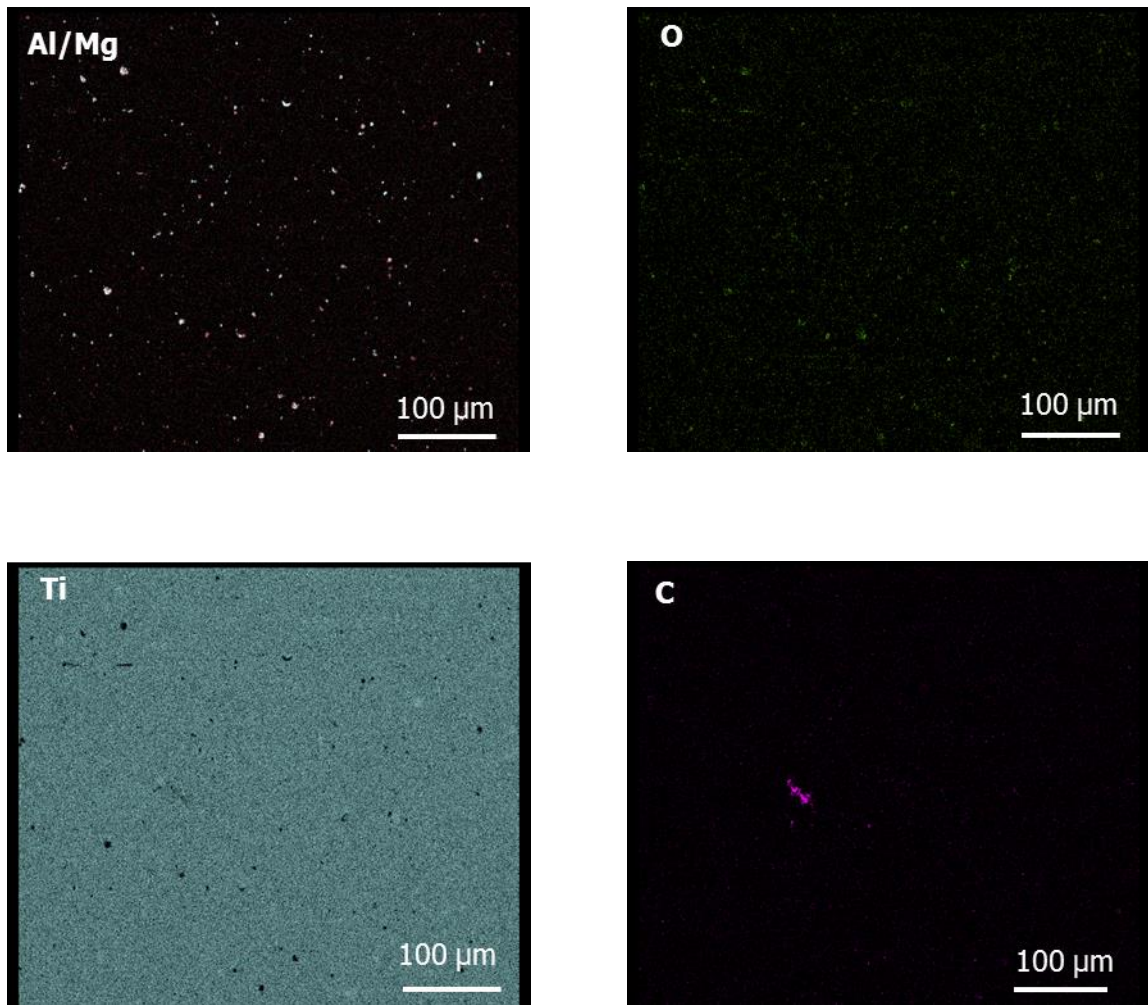
(a)

Figure 6 EDS maps displaying Al/Mg transfer, oxygen and carbon on the (a) uncoated work roll after 10 passes against Al-Mg Alloy with blue representing aluminum, red representing magnesium, green representing oxygen, purple representing carbon, cyan representing titanium, yellow representing iron and magenta representing chromium.



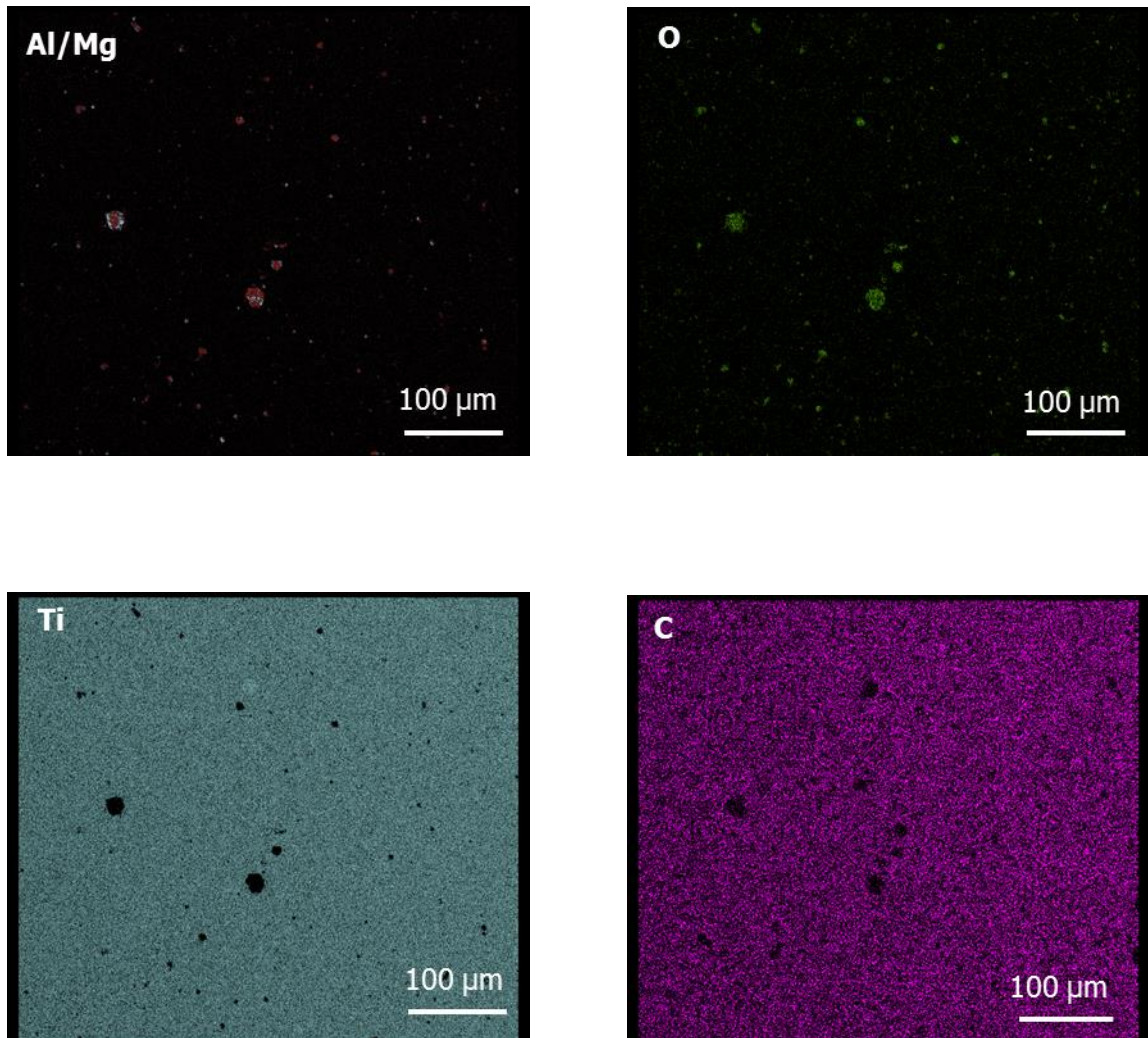
(b)

Figure 6 EDS maps displaying Al/Mg transfer, oxygen and carbon on the (b) Cr-coated work roll after 10 passes against Al-Mg Alloy.



(c)

Figure 6 EDS maps displaying Al/Mg transfer, oxygen and carbon on the (c) TiN-coated work roll after 10 passes against Al-Mg Alloy.



(d)

Figure 6 EDS maps displaying Al/Mg transfer, oxygen and carbon on the (d) TiCN-coated work roll after 10 passes against Al-Mg Alloy.



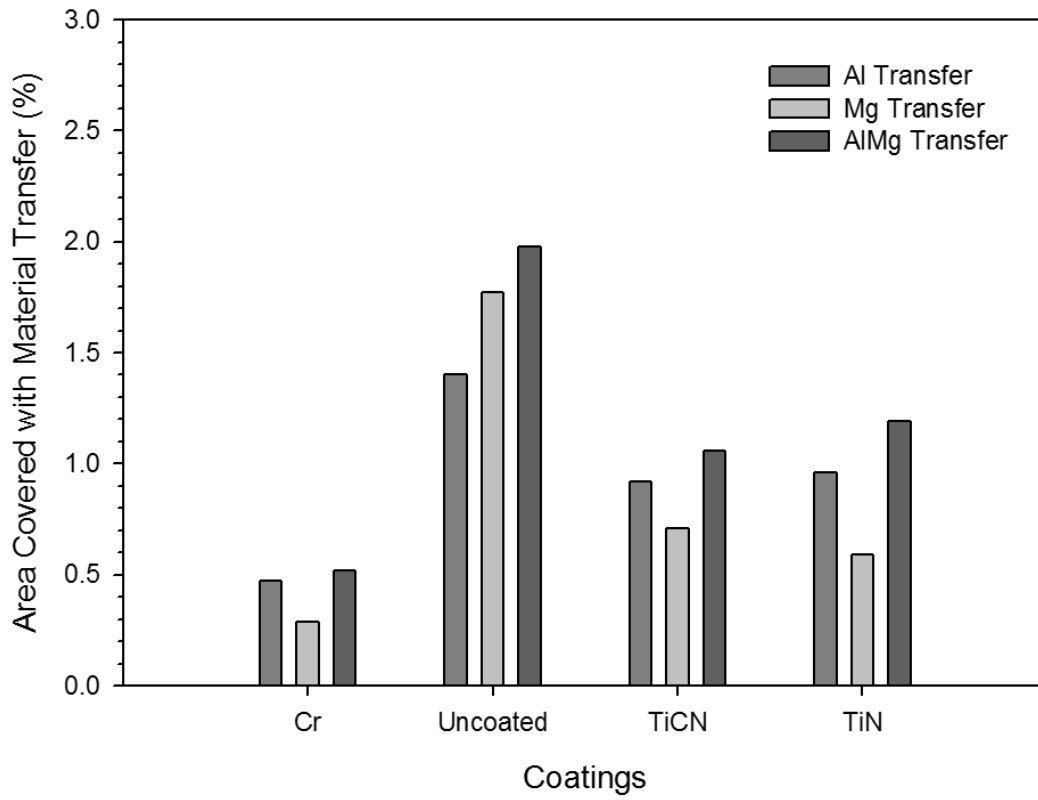


Figure 7 Material transfer area fraction on the work roll surfaces plotted for each coated work roll after 10 rolling passes.

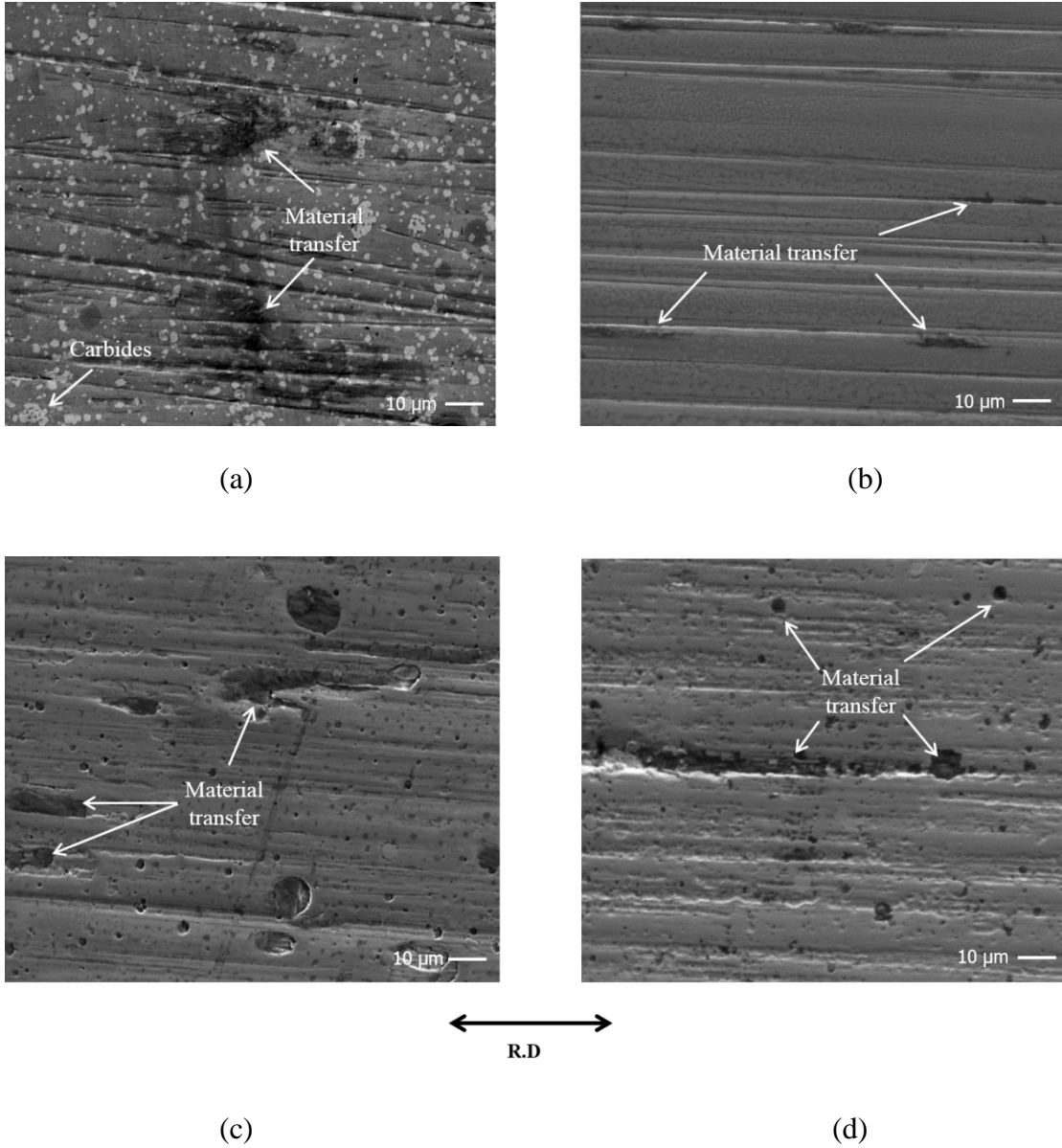
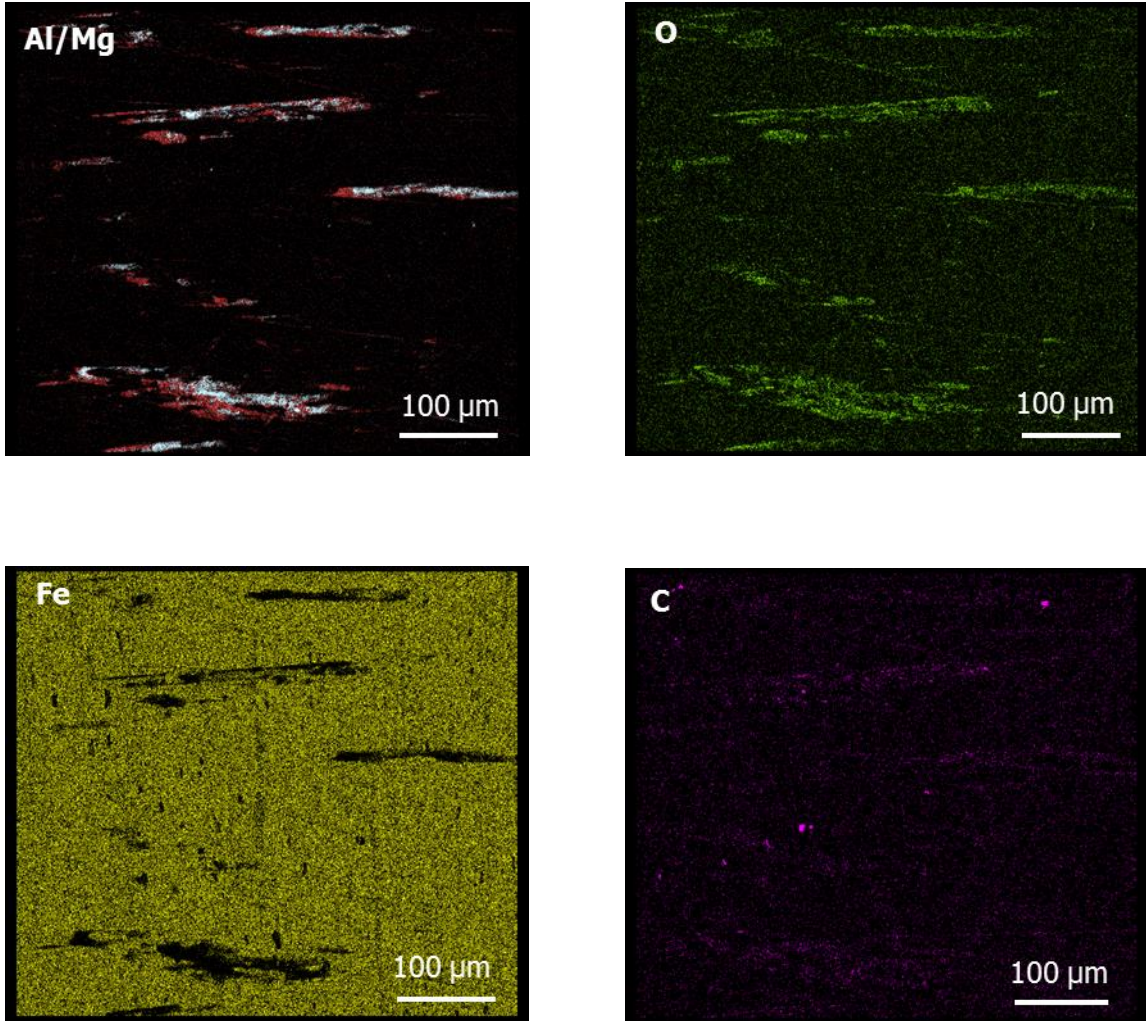
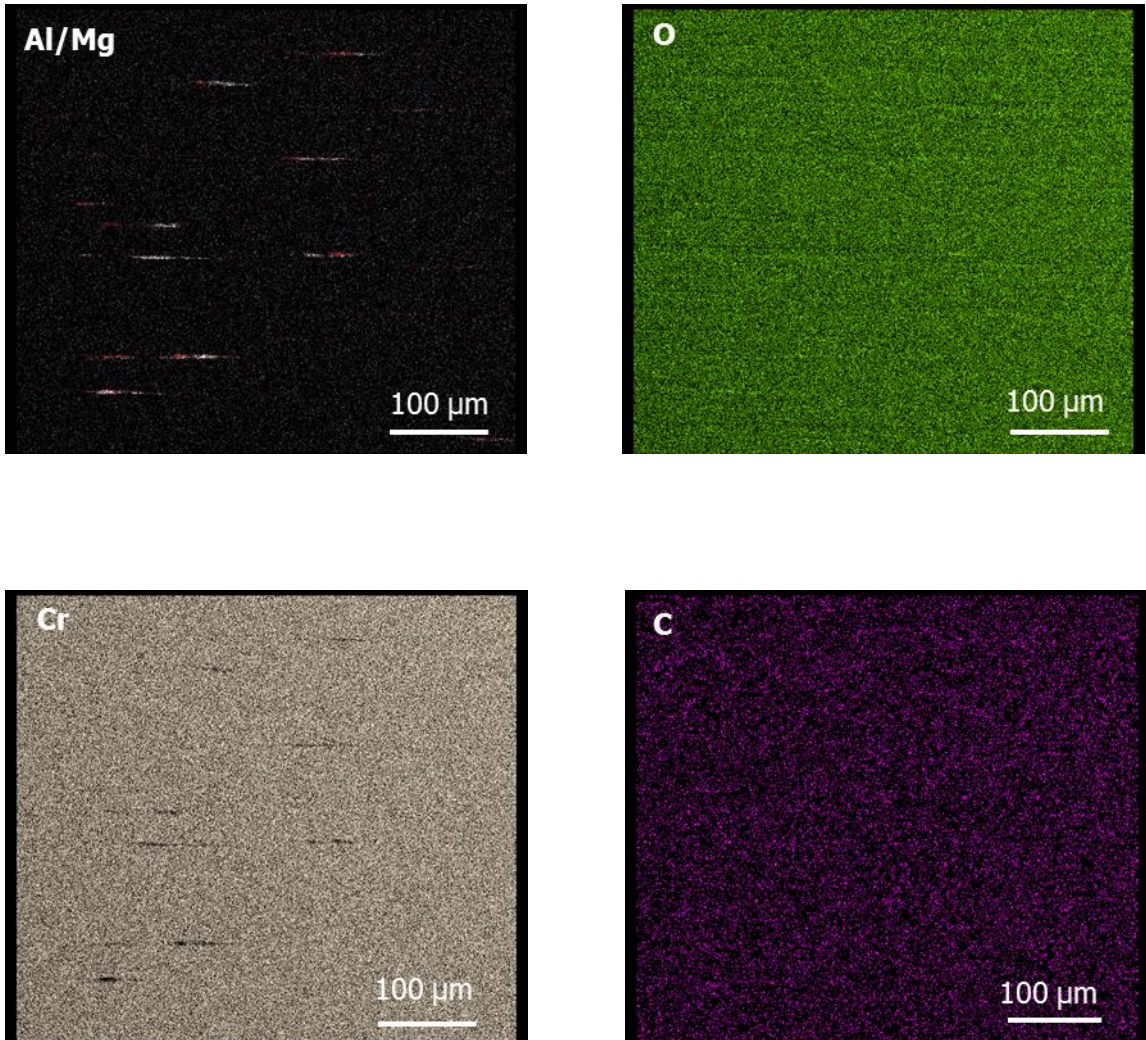


Figure 8 SEM images displaying material transfer to the (a) uncoated, (b) Cr-coated, (c) TiN-coated and (d) TiCN-coated work rolls after 20 hot rolling passes against an Al-Mg alloy.



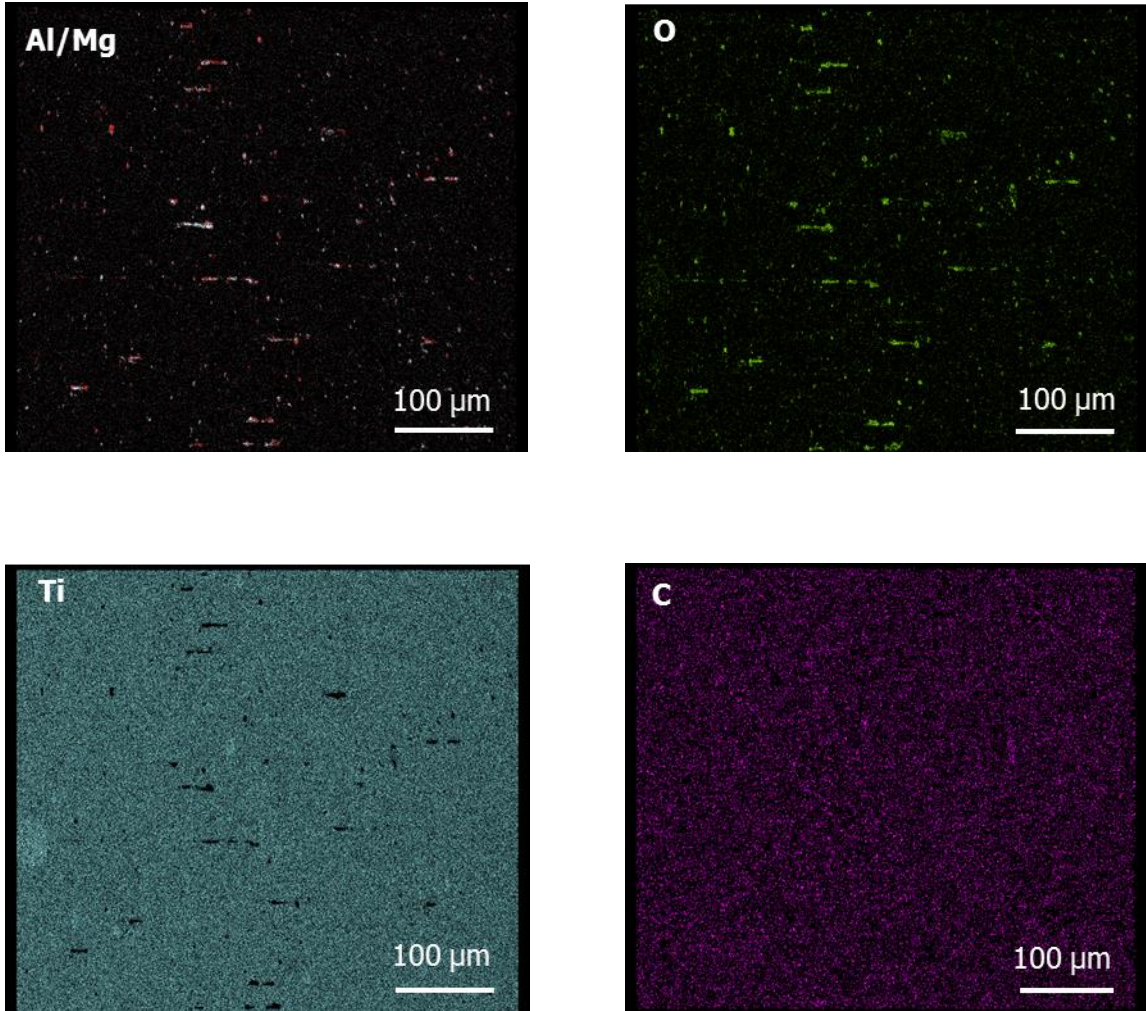
(a)

Figure 9 EDS maps displaying Al/Mg transfer, oxygen and carbon on the (a) uncoated work roll after 20 passes against the an Al-Mg alloy. Aluminum, magnesium, oxygen, carbon, titanium, iron and chromium are represented by blue, red, green, purple, cyan, yellow and magenta, respectively.



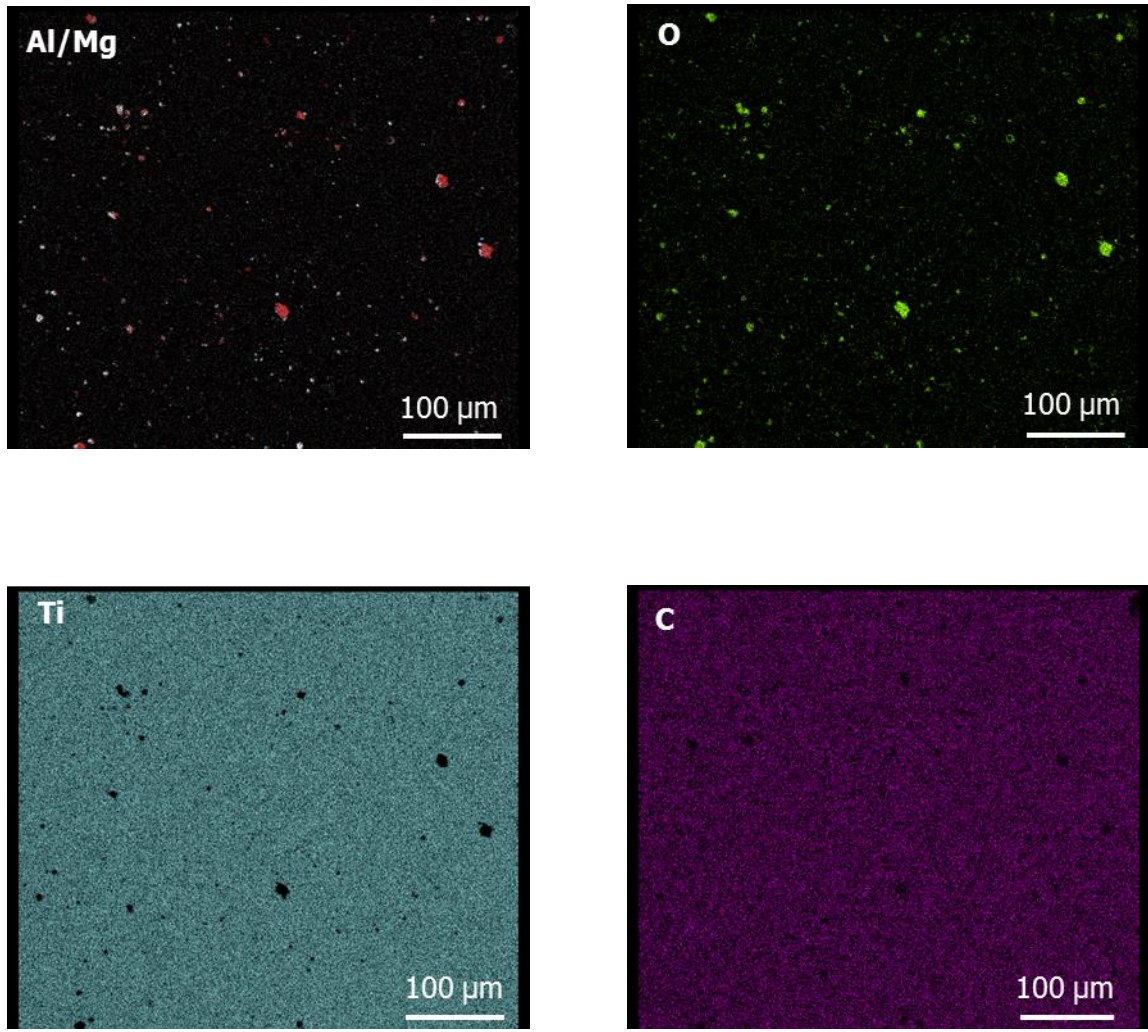
(b)

Figure 9 EDS maps displaying Al/Mg transfer, oxygen and carbon on the (b) Cr-coated work roll after 20 passes against the an Al-Mg alloy.



(c)

Figure 9 EDS maps displaying Al/Mg transfer, oxygen and carbon on the (c) TiN-coated work roll after 20 passes against the an Al-Mg alloy.



(d)

Figure 9 EDS maps displaying Al/Mg transfer, oxygen and carbon on the (d) TiCN-coated work roll after 20 passes against the an Al-Mg alloy.

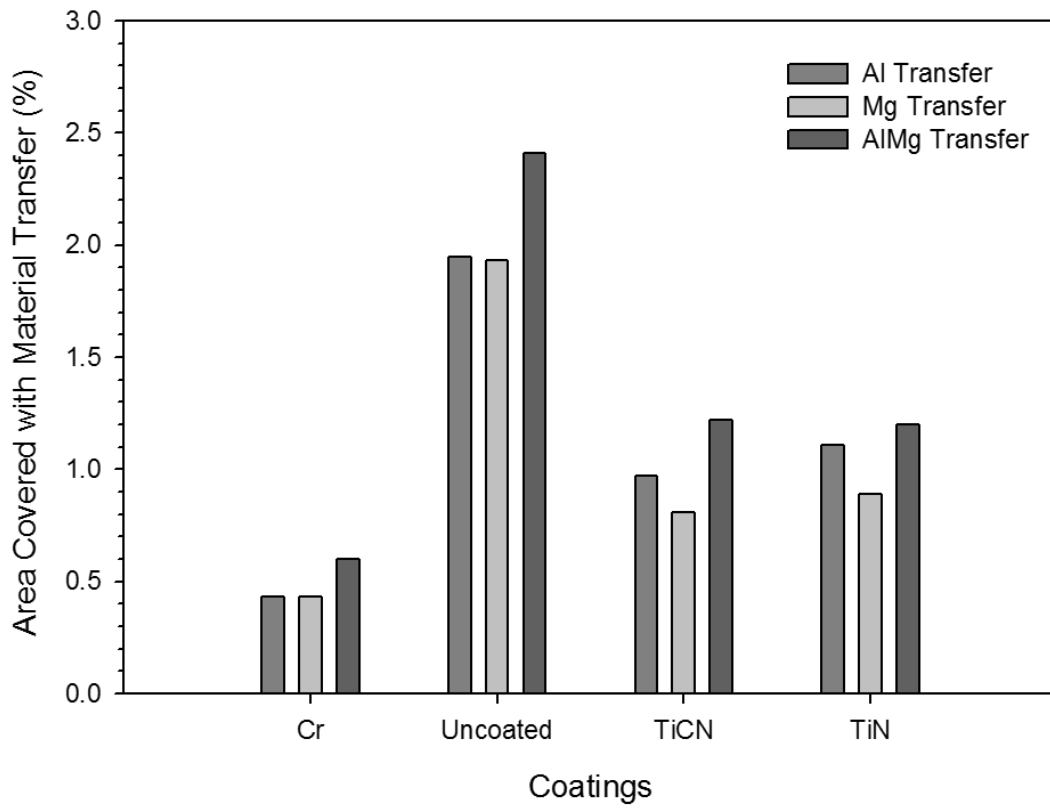


Figure 10 Material transfer area fractions on the work roll surfaces plotted for each coated work roll after 20 rolling passes.

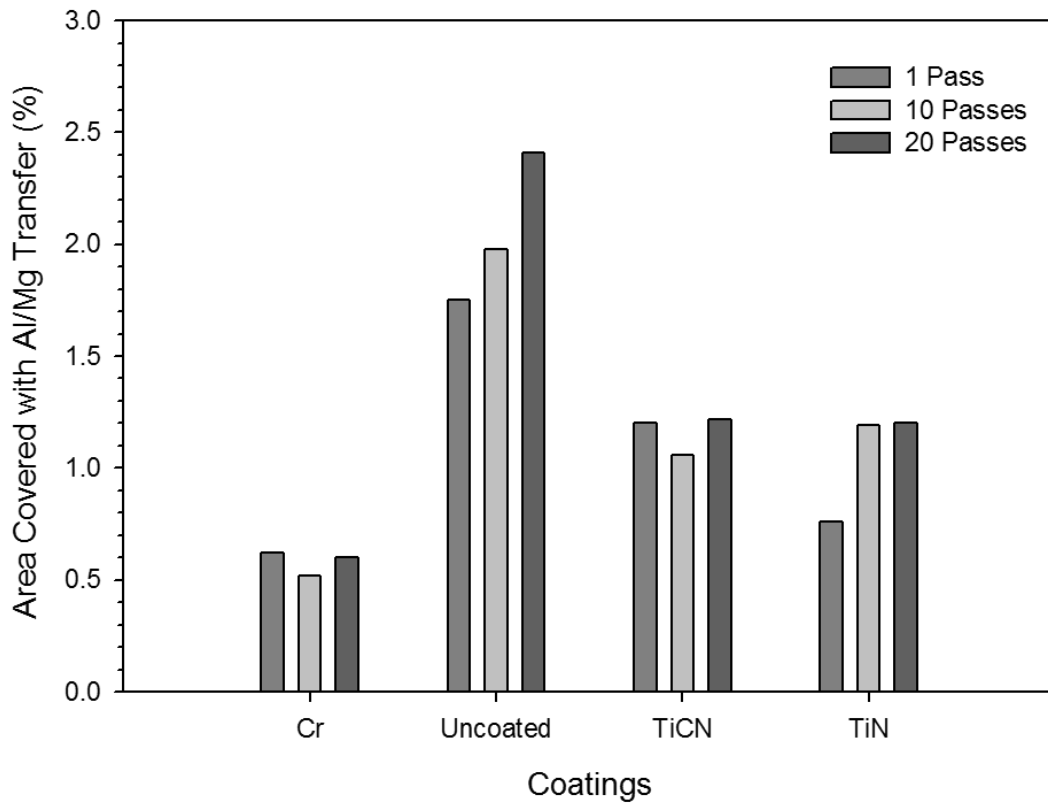
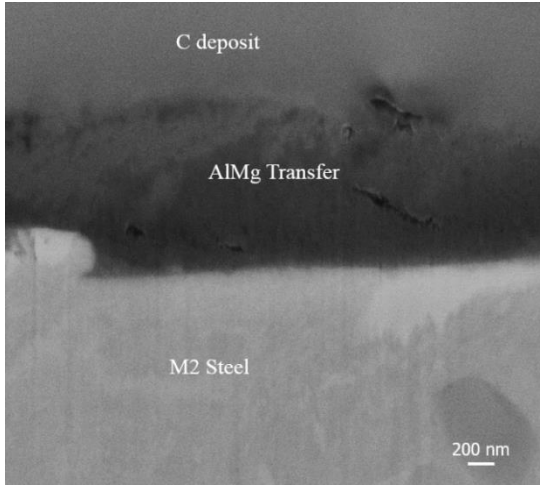
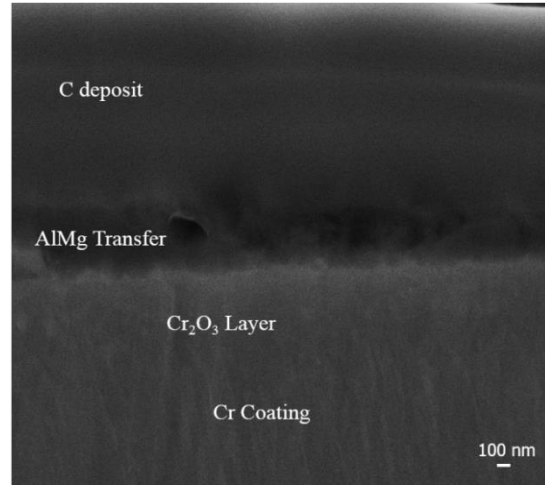


Figure 11 Al/Mg transfer area fractions on the work roll surfaces after 1, 10 and 20 passes.

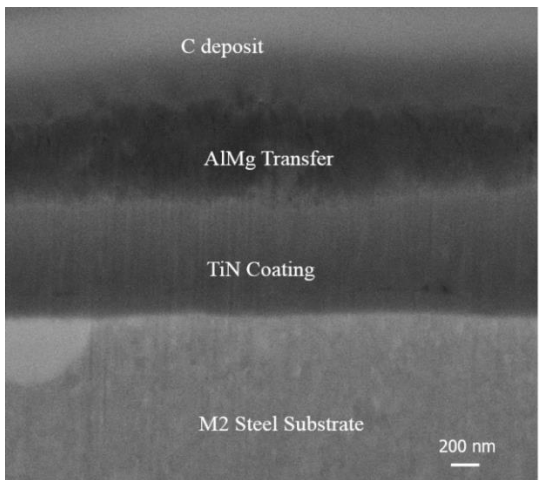




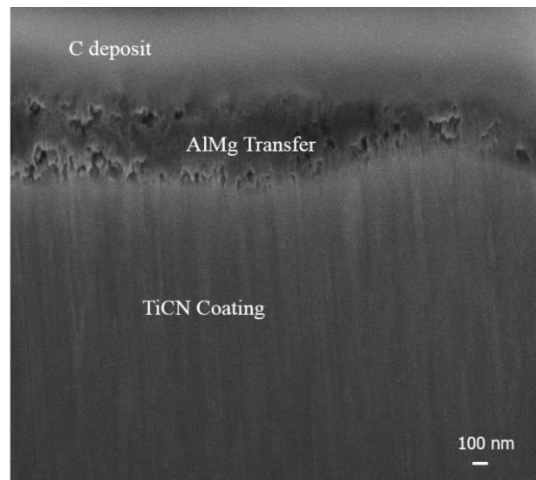
(a)



(b)



(c)



(d)

Figure 12 Cross-sectional FIB/SEM images displaying Al/Mg transfer to the (a) uncoated, (b) Cr-coated, (c) TiN-coated and (d) TiCN-coated work rolls after 20 hot rolling passes.

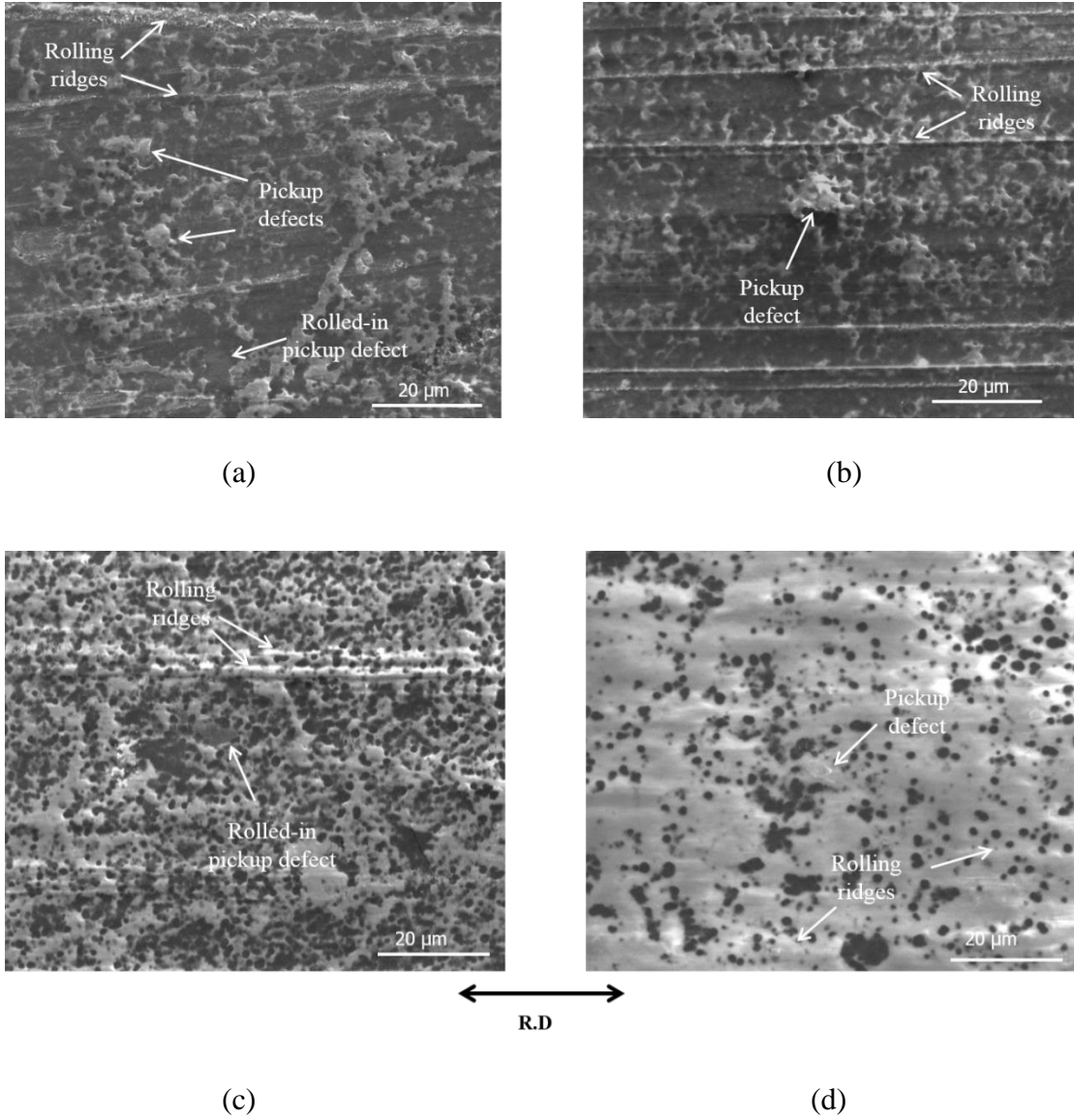
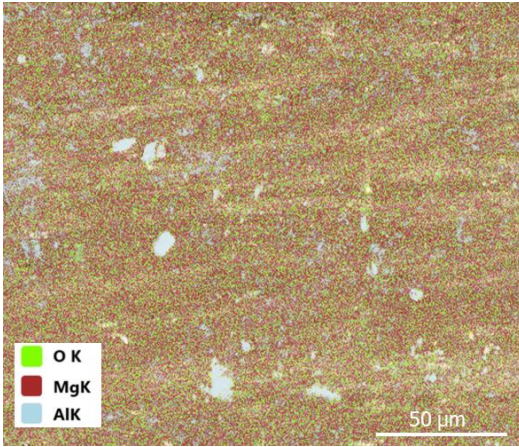
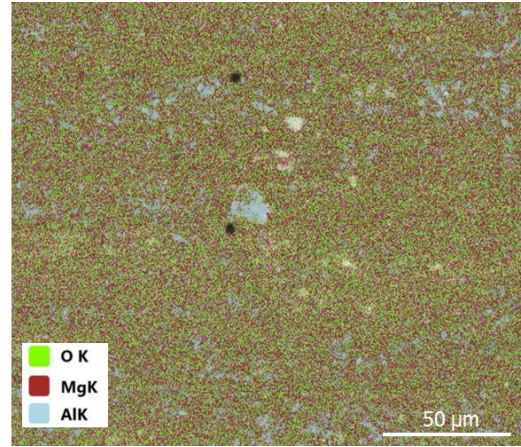


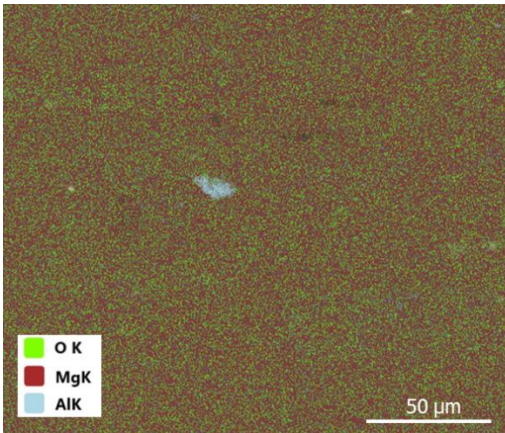
Figure 13 SEM images displaying pickup defects on the Al-Mg alloy surfaces rolled against the (a) uncoated (b) Cr-coated (c) TiN-coated and (d) TiCN-coated work rolls after 20 hot rolling passes.



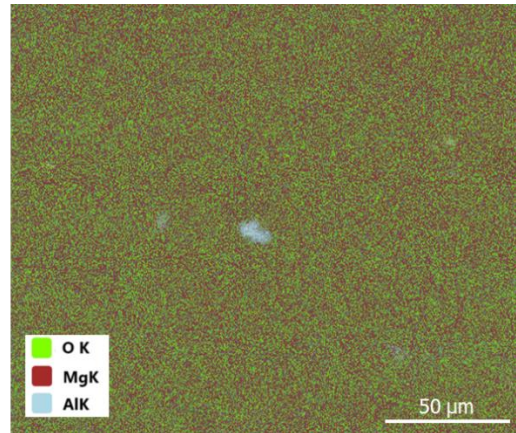
(a)



(b)



(c)



(d)

Figure 14 EDS maps of the SEM images displayed in Fig. 13, displaying the rich aluminum content of the pickup defects on the Al-Mg alloy surfaces rolled against the (a) uncoated, (b) Cr-coated, (c) TiN-coated and (d) TiCN-coated work rolls after 20 hot rolling passes.

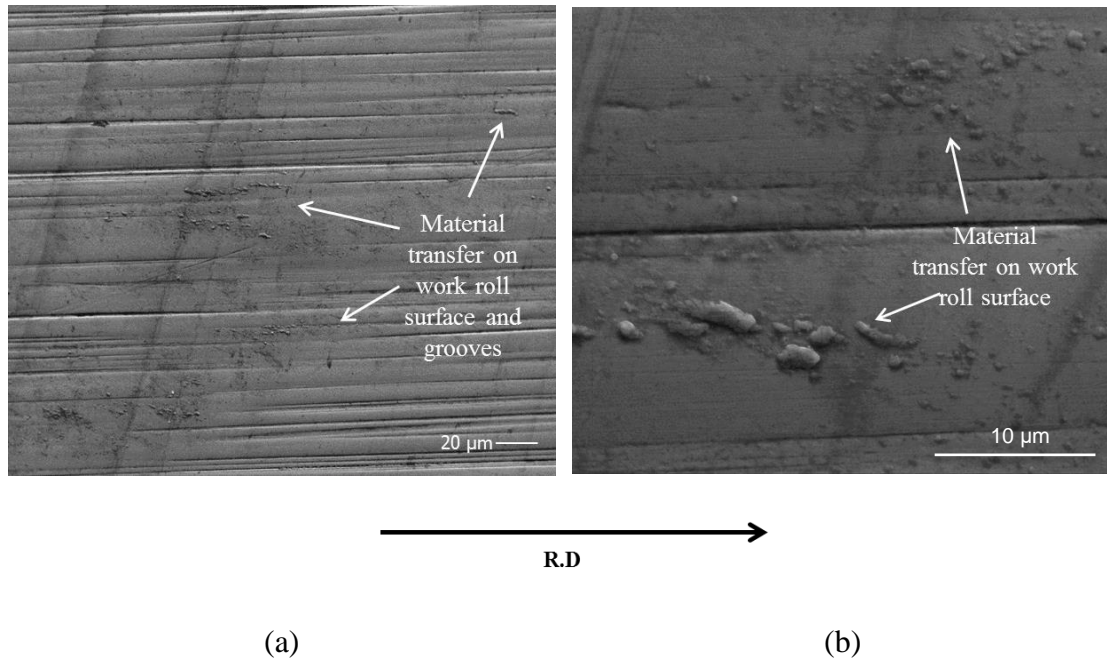


Figure 15 SEM images displaying material transfer to the (a) Cr-coated work roll at lower magnification (b) Cr-coated work roll at higher magnification after 1 hot rolling pass against an Al-Mg alloy under low lubrication flow rate.

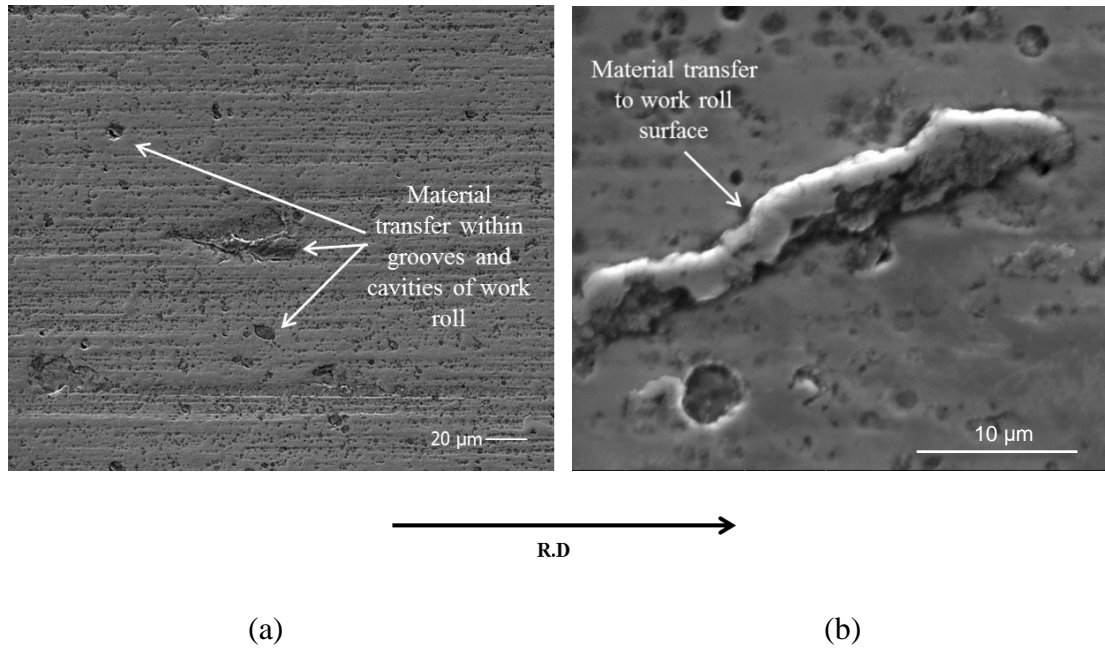
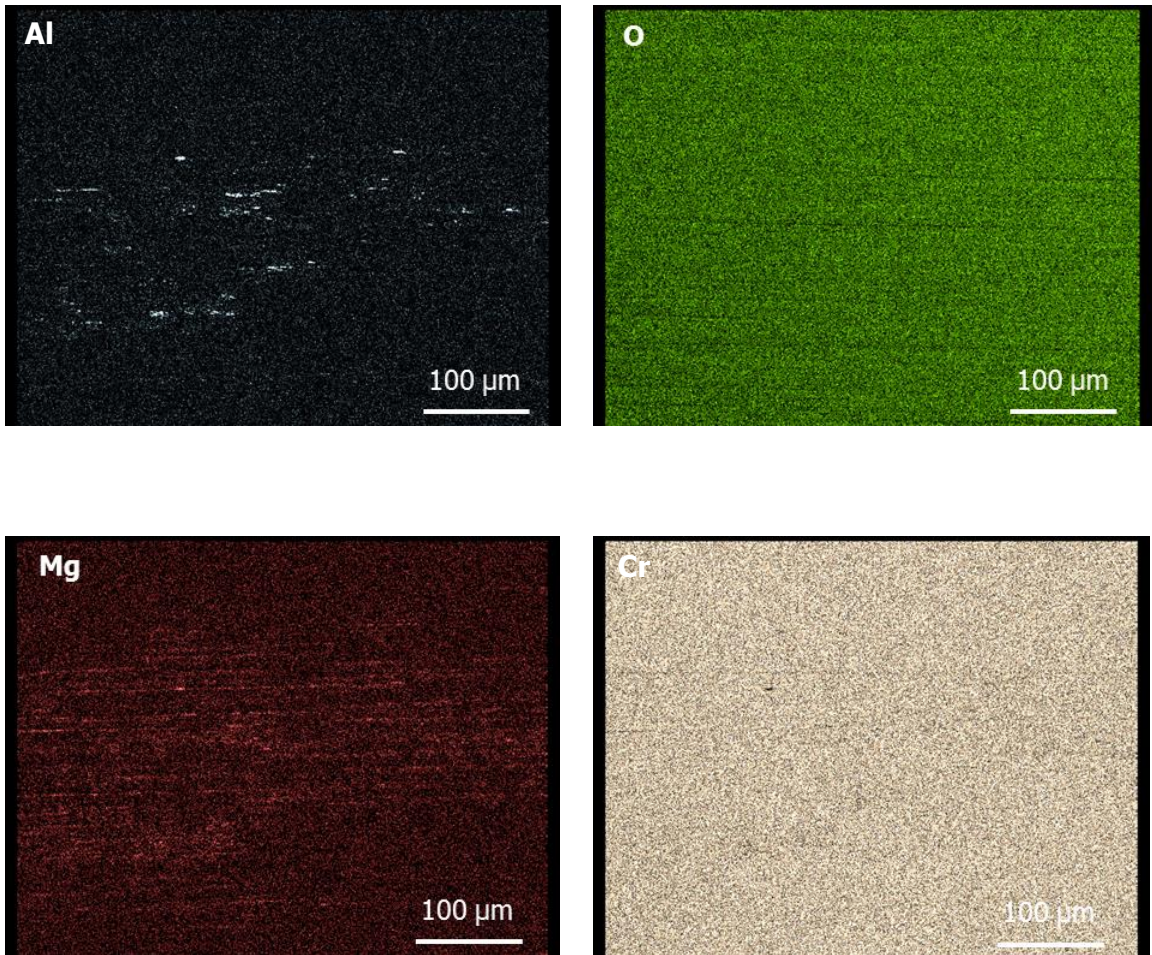
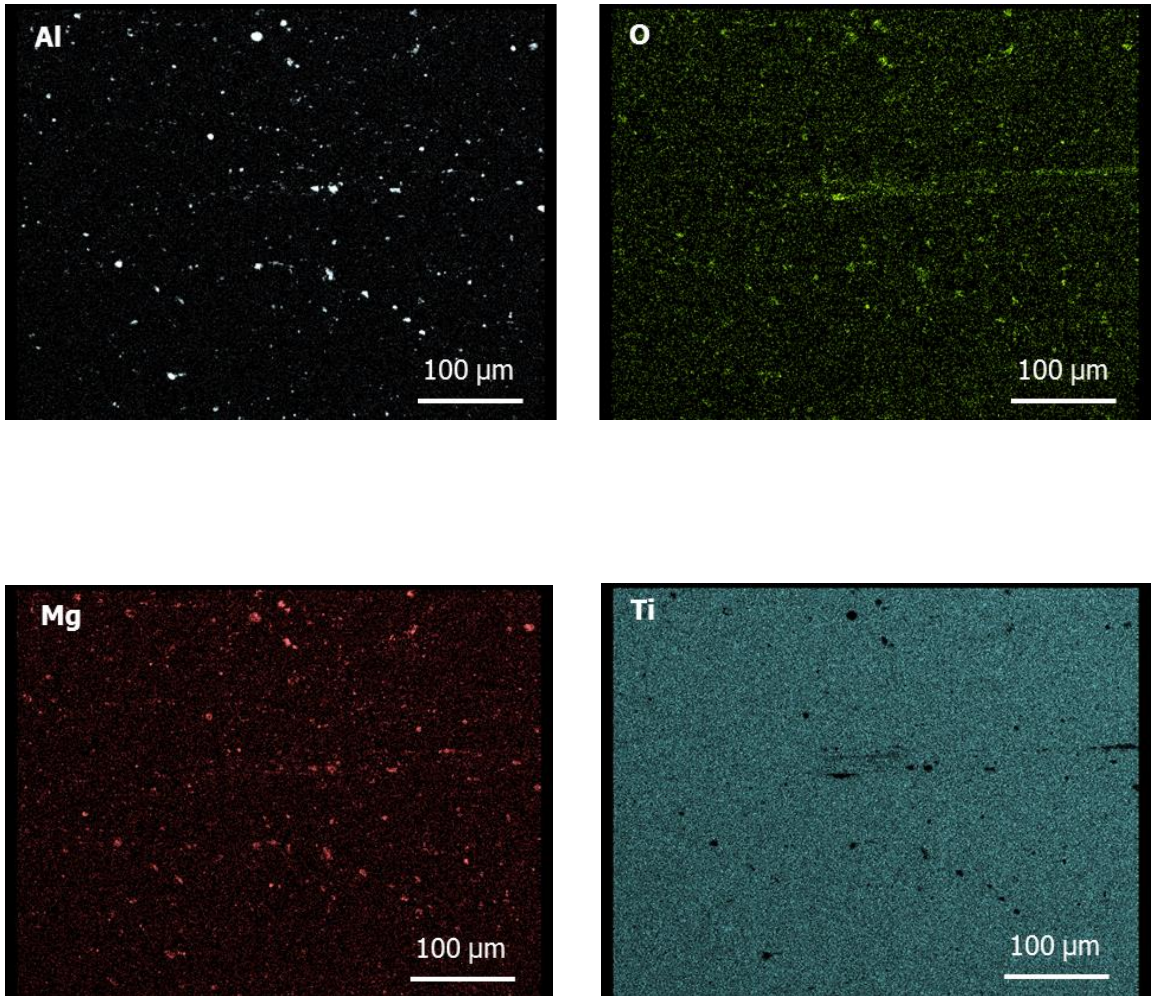


Figure 16 SEM images displaying material transfer to the (a) TiCN-coated work roll at lower magnification (b) TiCN-coated work roll at higher magnification after 1 hot rolling pass against an Al-Mg alloy under low lubrication flow rate.



(a)

Figure 17 EDS maps displaying Al, Mg, oxygen and the main elements of the coatings on the (a) Cr-coated work roll after 1 pass against an Al-Mg alloy under low lubrication flow rate.



(b)

Figure 17 EDS maps displaying Al, Mg, oxygen and the main elements of the coatings on the (b) TiCN-coated work roll after 1 pass against an Al-Mg alloy under low lubrication flow rate.

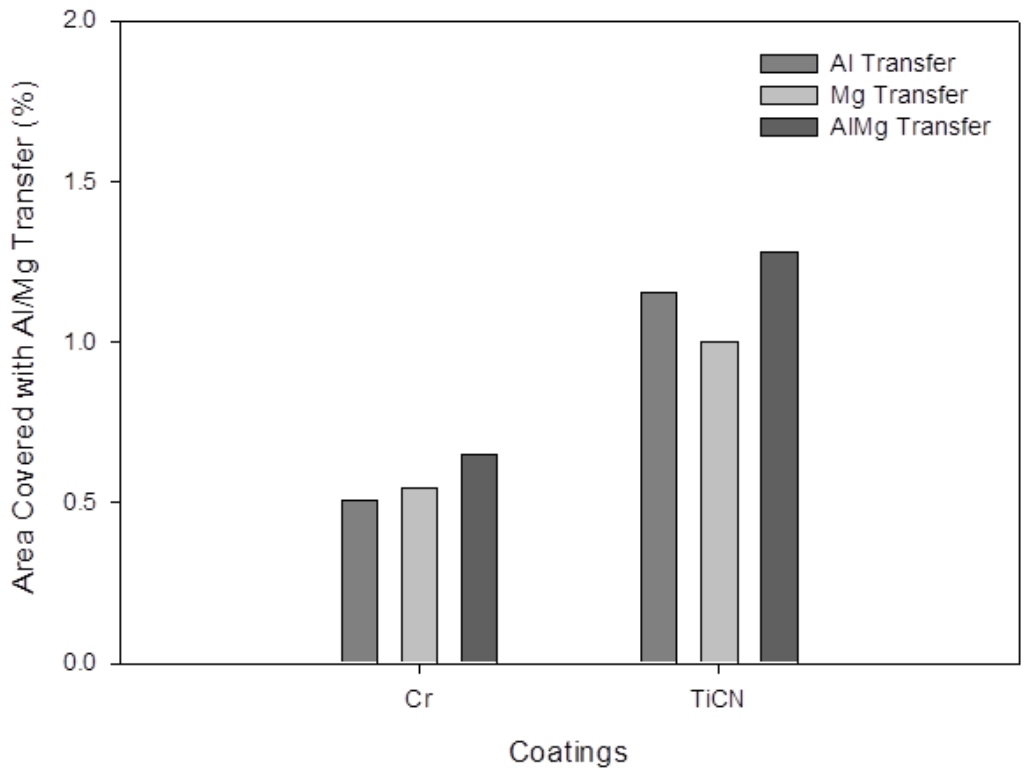
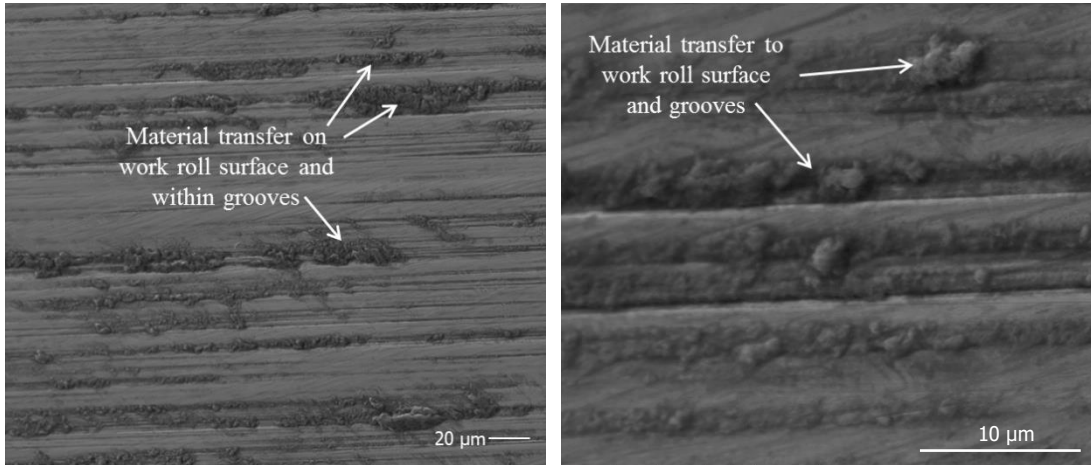


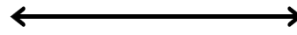
Figure 18 Material transfer area fractions on the work roll surfaces plotted for Cr and TiCN-coated work roll after 1 rolling pass under low lubrication flow rate.





(a)

(b)



**R. D.**

Figure 19 SEM images displaying material transfer to the (a) Cr-coated work roll at lower magnification (b) Cr-coated work roll at higher magnification after 10 hot rolling passes against an Al-Mg alloy under low lubrication flow rate.

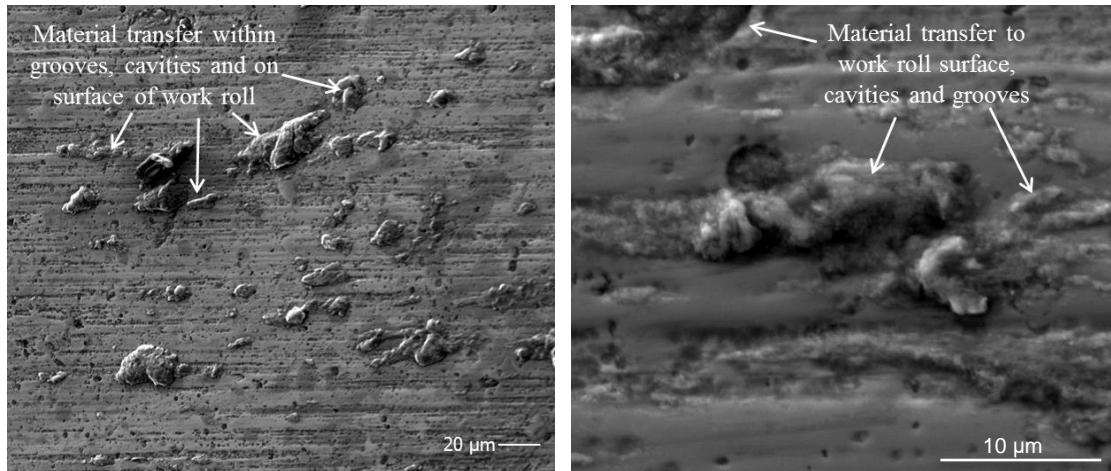
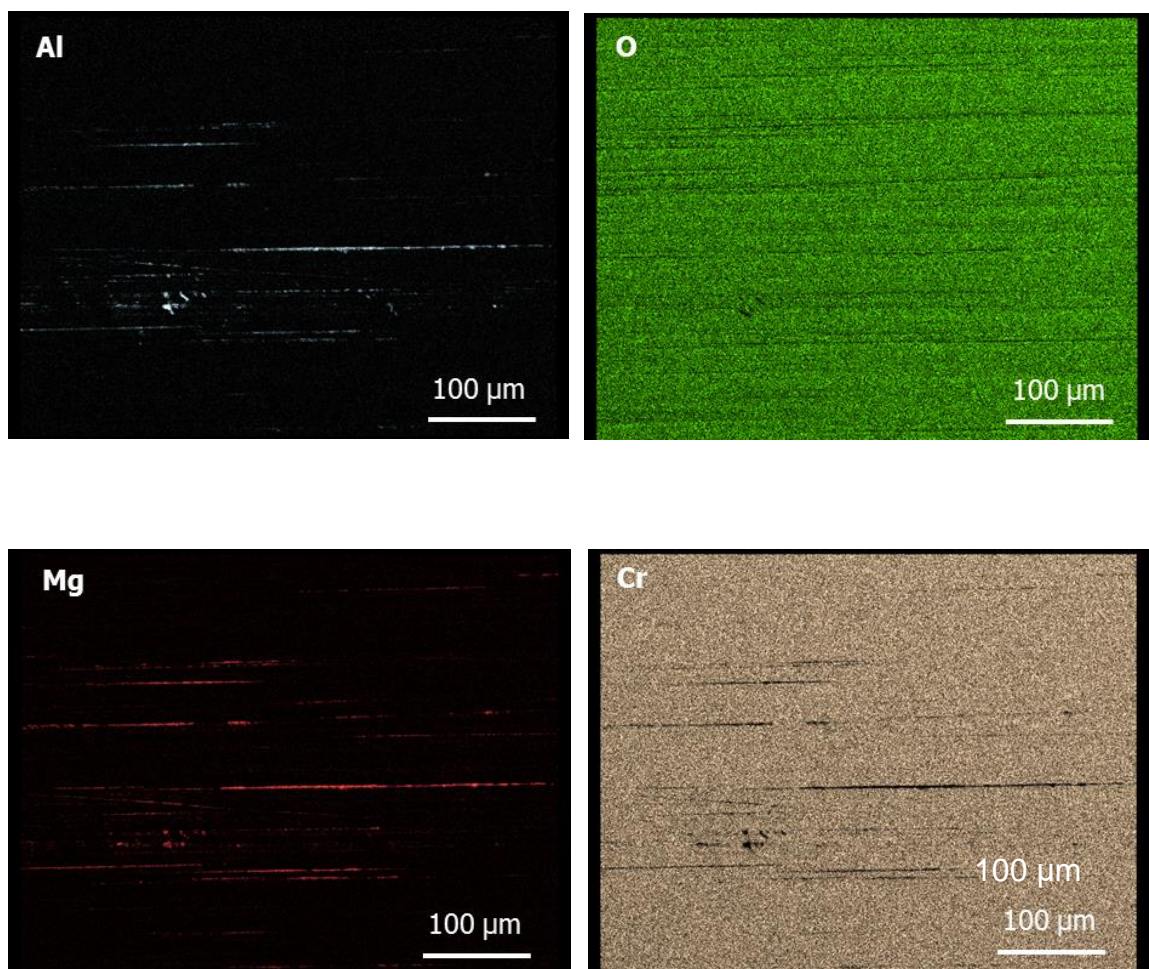
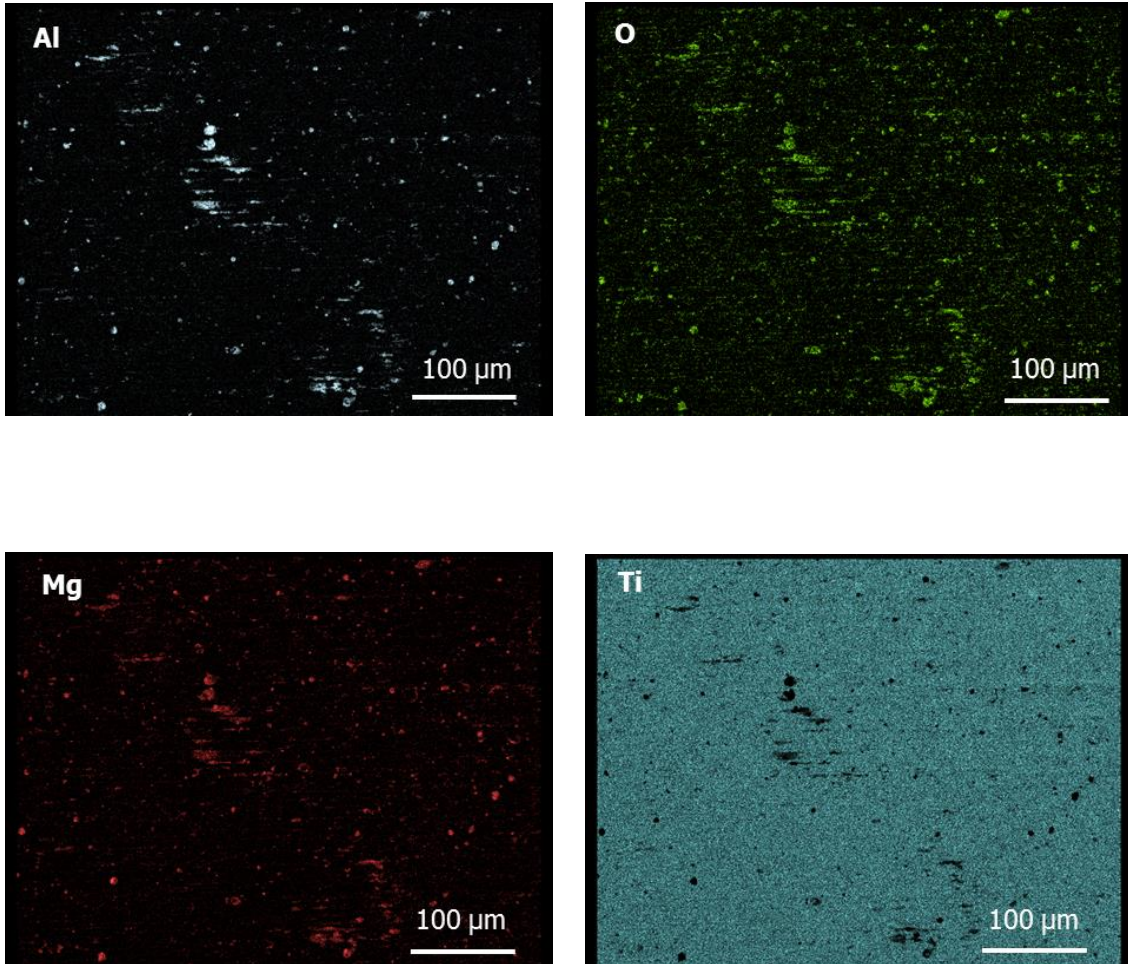


Figure 20 SEM images displaying material transfer to the (a) TiCN-coated work roll at lower magnification (b) TiCN-coated work roll at higher magnification after 10 hot rolling passes against an Al-Mg alloy under low lubrication flow rate.



(a)

Figure 21 EDS maps displaying Al, Mg, oxygen and the main elements of the coatings on the (a) Cr-coated work roll after 10 passes against an Al-Mg alloy under low lubrication flow rate.



(b)

Figure 21 EDS maps displaying Al, Mg, oxygen and the main elements of the coatings on the (b) TiCN-coated work roll after 10 passes against an Al-Mg alloy under low lubrication flow rate.

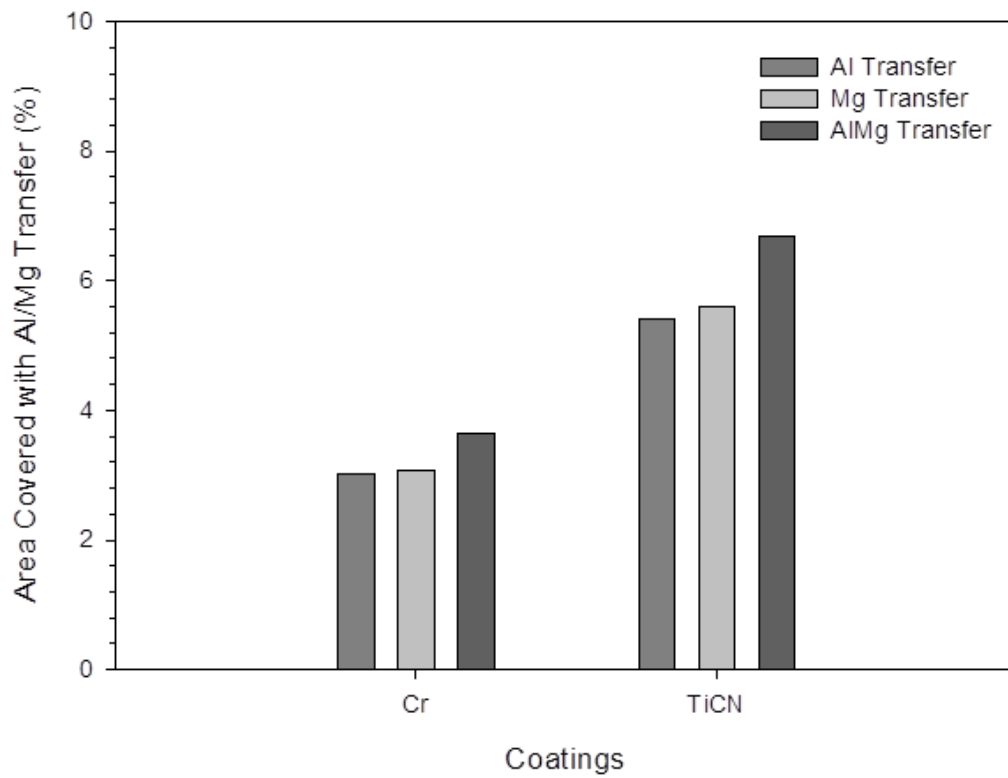
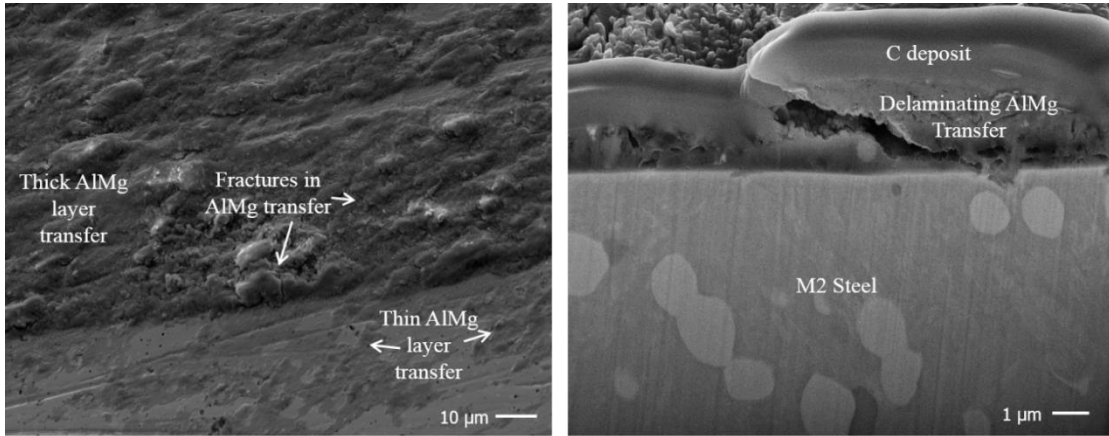


Figure 22 Material transfer area fractions on the work roll surfaces plotted for Cr and TiCN-coated work roll after 10 rolling passes under low lubrication flow rate.



(a)

(b)

Figure 23 (a) SEM image displaying cracks in Al/Mg transfer layer to the uncoated work roll surface and (b) cross-sectional SEM image displaying delamination of a fractured Al/Mg transfer layer on the uncoated work roll surface.

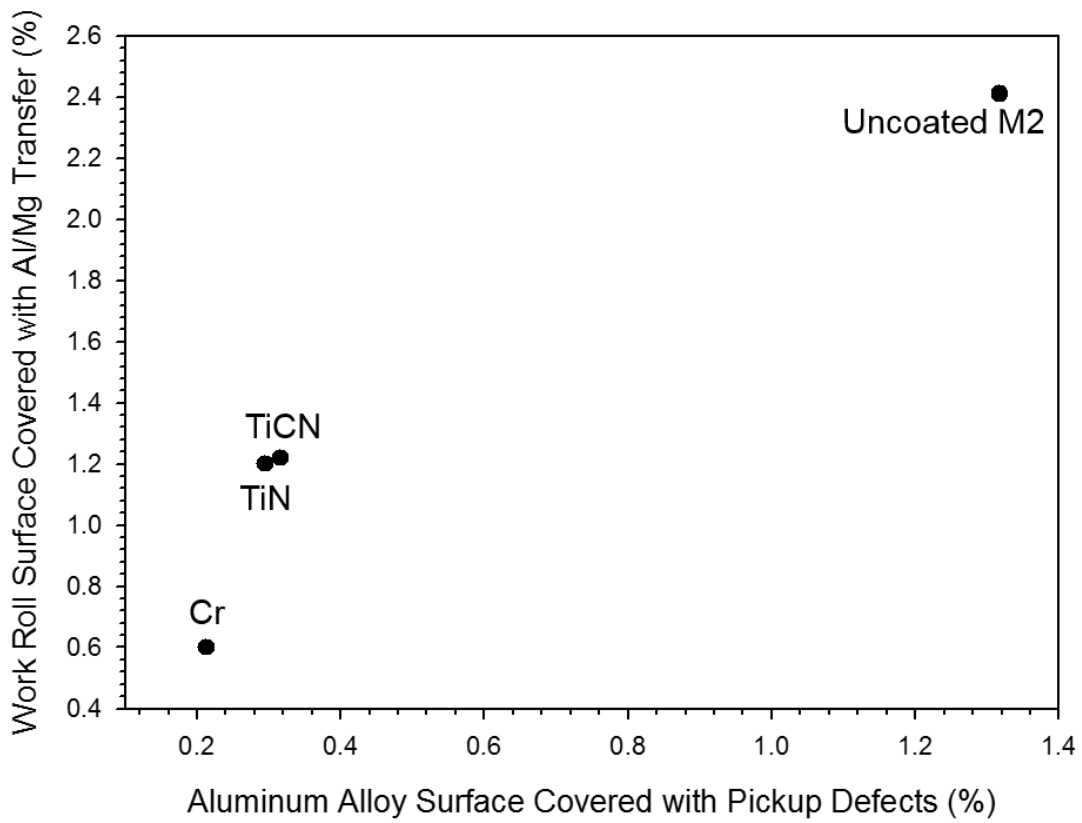


Figure 24 Al/Mg transfer area fraction on the work roll surfaces plotted against area fraction of the rolled aluminum alloy surface covered with pickup defects for the uncoated and coated work rolls after the 20 pass hot rolling schedule.

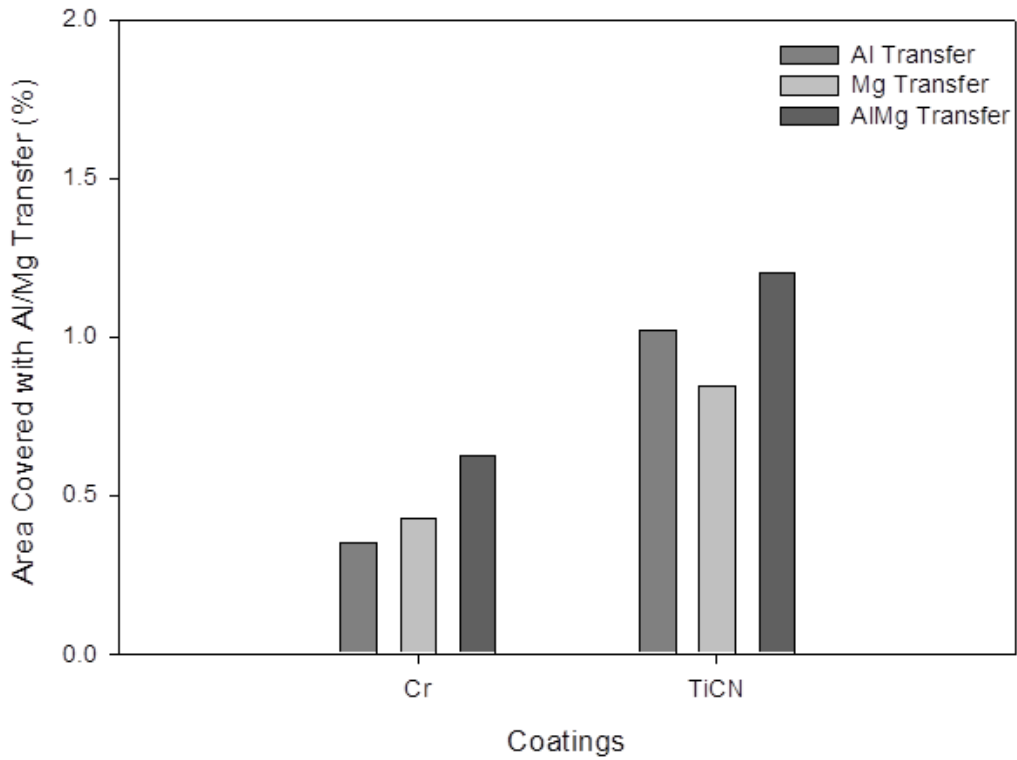


Figure 25 Material transfer area fractions on the work roll surfaces plotted for Cr and TiCN-coated work roll after 1 rolling pass under high lubrication flow rate.



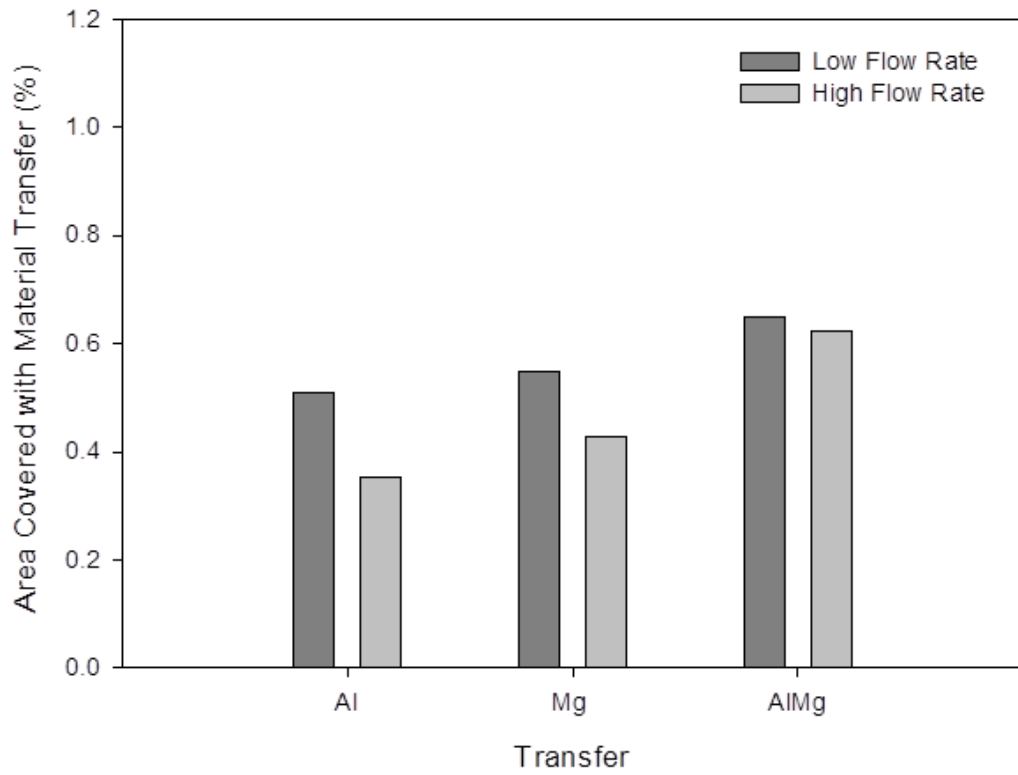


Figure 26 Material transfer area fractions on Cr-coated work roll after 1 pass under low and high lubrication flow rate.

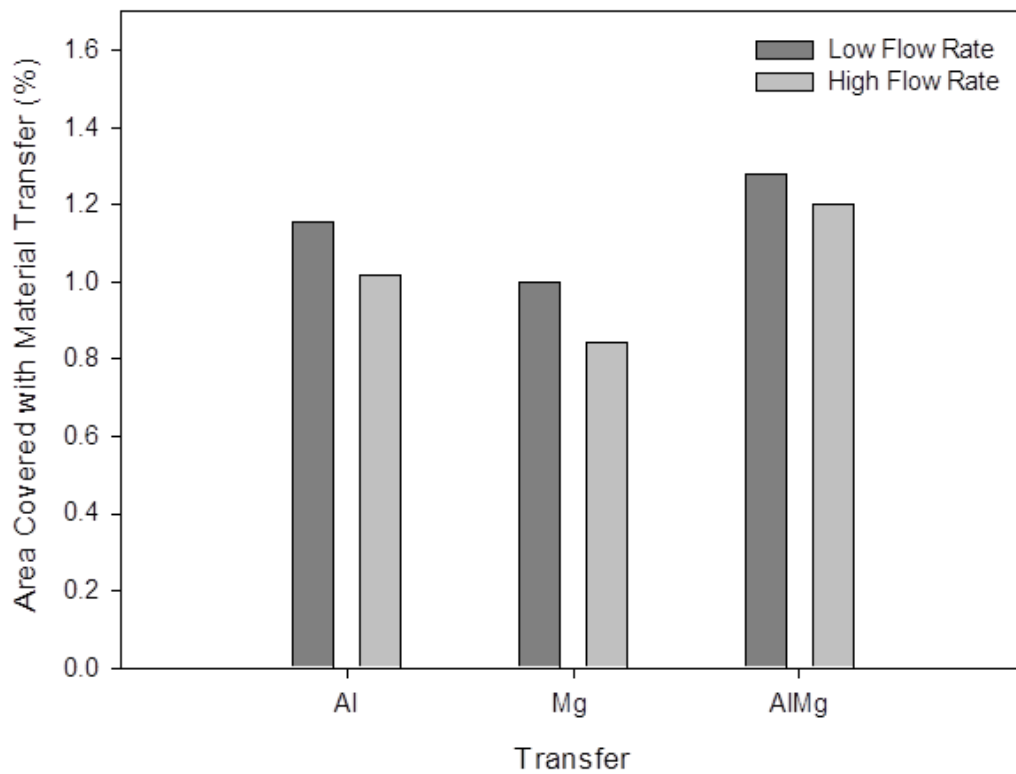


Figure 27 Material transfer area fractions on TiCN-coated work roll after 1 pass under low and high lubrication flow rate.

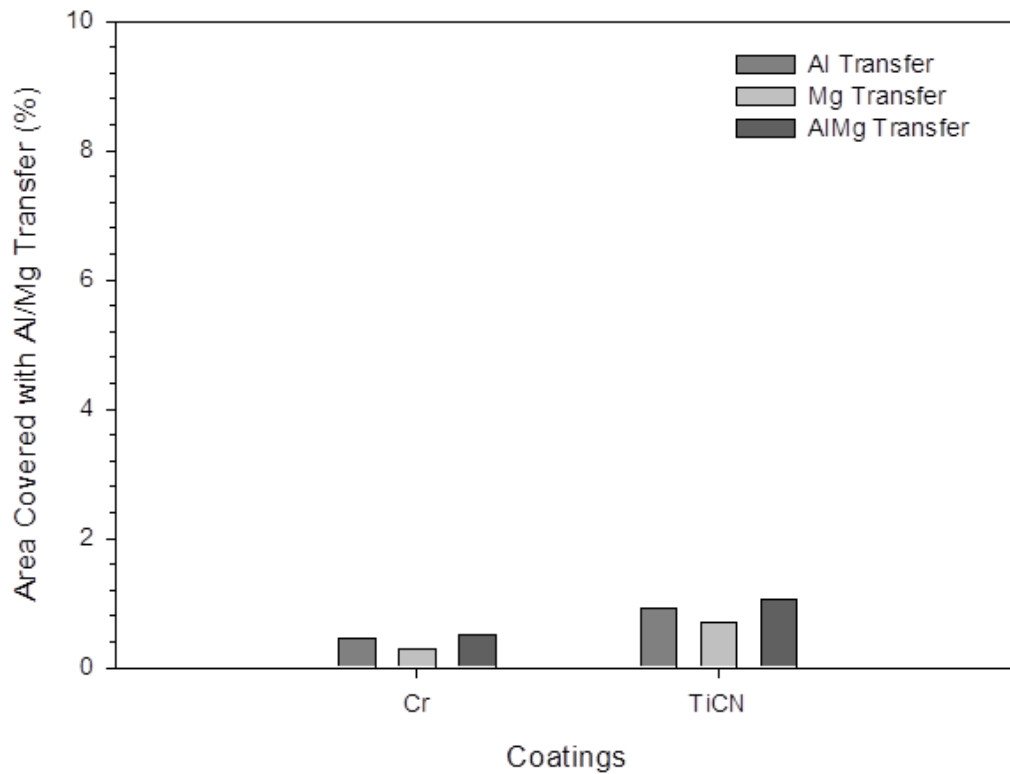


Figure 28 Material transfer area fractions on the work roll surfaces plotted for Cr and TiCN-coated work roll after 10 rolling passes under high lubrication flow rate.

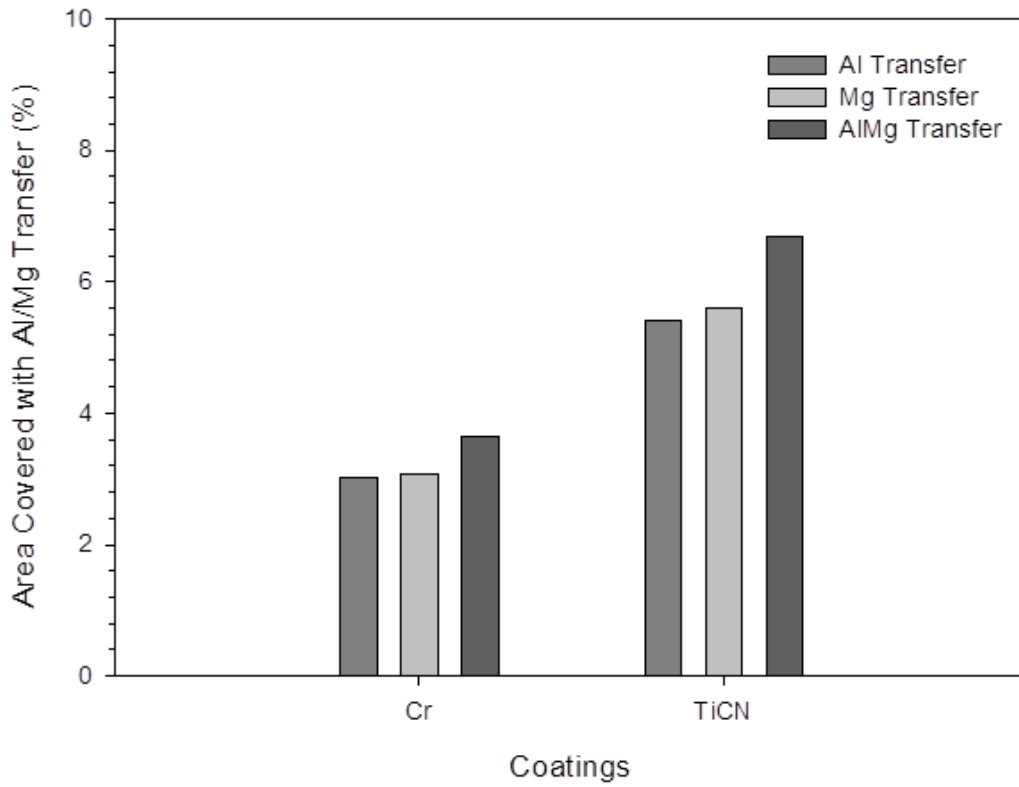


Figure 29 Material transfer area fractions on the work roll surfaces plotted for Cr and TiCN-coated work roll after 10 rolling passes under low lubrication flow rate.

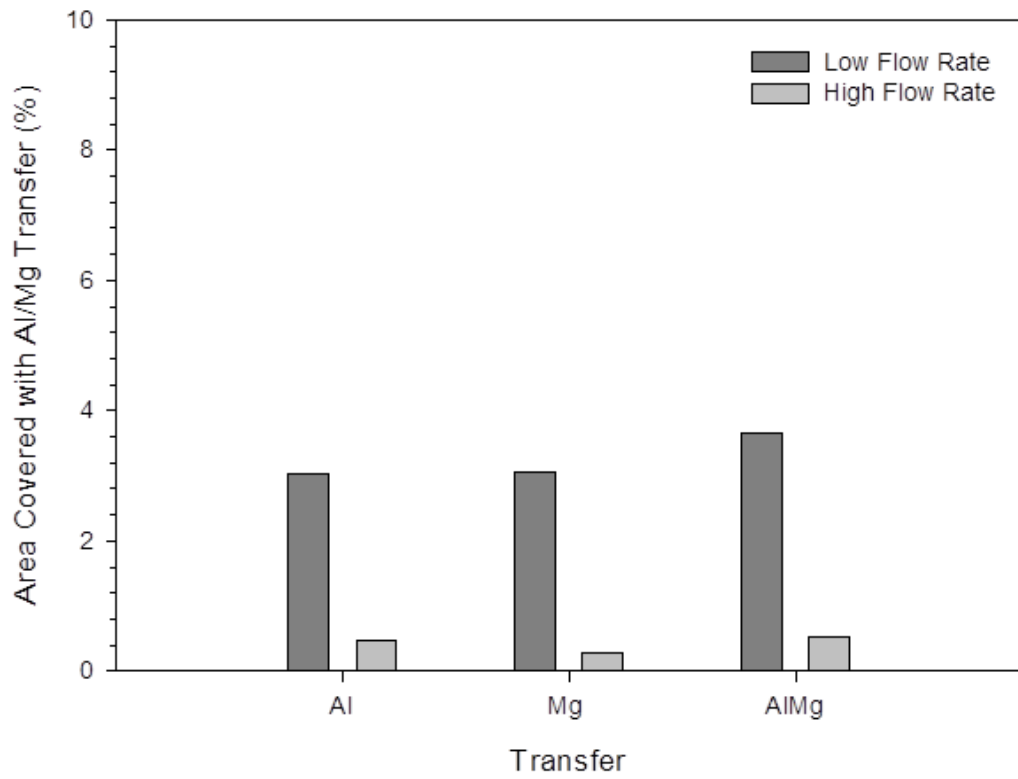


Figure 30 Material transfer area fractions on Cr-coated work roll after 10 passes under low and high lubrication flow rate.

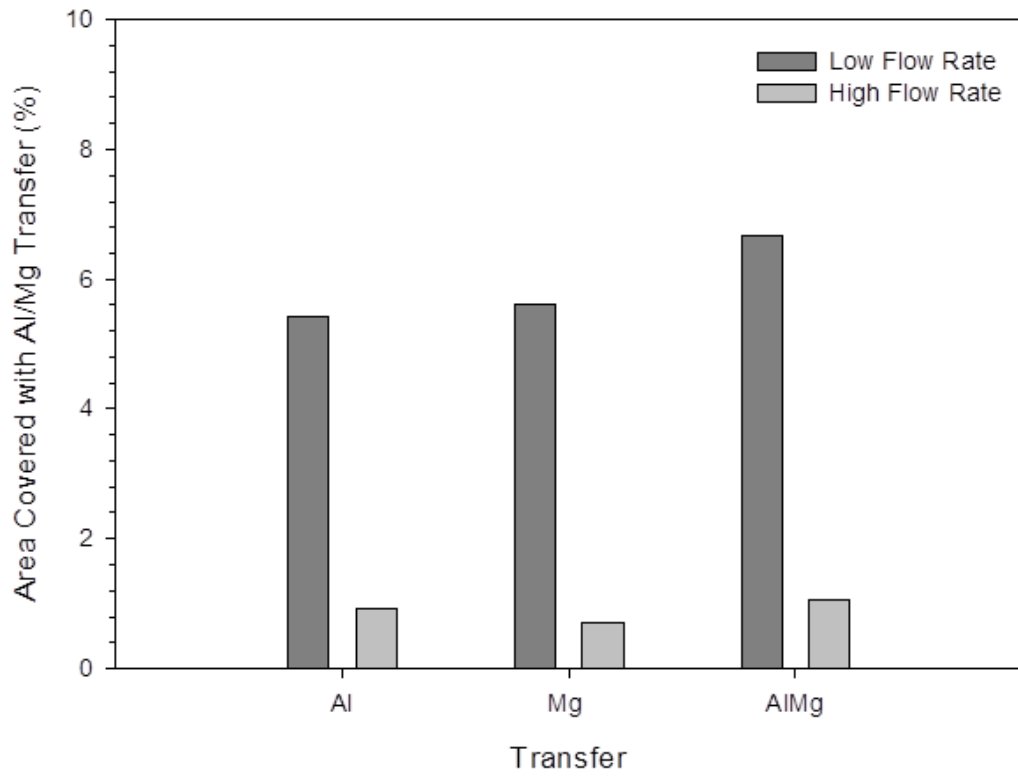


Figure 31 Material transfer area fractions on TiCN-coated work roll after 10 passes under low and high lubrication flow rate.

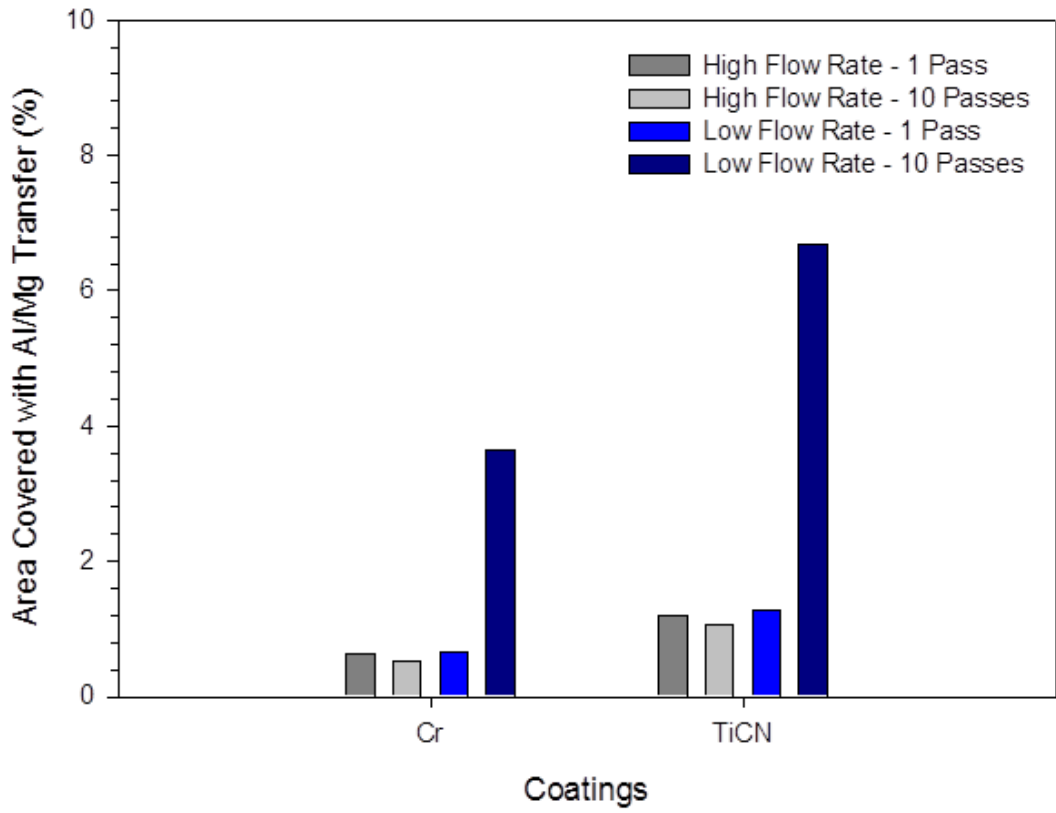


Figure 32 Material transfer area fractions on the work roll surfaces plotted for Cr and TiCN-coated work roll after 1 and 10 passes under high and low lubrication flow rate.

## REFERENCES

- [1] Hurley, Neil, Microstructural evolution during flash annealing of hot rolled 6061 aluminum alloys (2006). Theses and Dissertations. Paper 915.
- [2] Aluminium and Aluminium Alloys – Designations, <http://www.azom.com/article.aspx?ArticleID=310>, DOA: Apr 24 2001.
- [3] Aluminum 5182 Alloy (UNS A95182), <http://www.azom.com/article.aspx?ArticleID=8652>, DOA: Apr 29 2013.
- [4] Ramona Prillhofer, Gunther Rank, Josef Berneder, Helmut Antrekowitsch, Peter J. Uggowitzer and Stefan Pogatscher, Property Criteria for Automotive Al-Mg-Si Sheet Alloys, *Materials* (2014), 7, 5047-5068.
- [5] Saral Dutta. B. Tech. (Hons.), I.I.T, HOT ROLLING PRACTICE – An Attempted Recollection.
- [6] Roy Woodward, *The Rolling of Aluminium: the Process and the Product*, Aluminium Federation, Birmingham.
- [7] Luigi De Pari Jr., Wojciech Z. Misiolek, Theoretical predictions and experimental verification of surface grain structure evolution for AA6061 during hot rolling, *Acta Materialia* 56 (2008) 6174–6185.
- [8] H.E. Hu, L. Zhen, B.Y. Zhang, L. Yang, J.Z. Chen, Microstructure characterization of 7050 aluminum alloy during dynamic recrystallization and dynamic recovery, *MATERIALS CHARACTERIZATION* 59 (2008) 1185-1189.
- [9] H.J. McQueen, W. Blum, Dynamic recovery: sufficient mechanism in the hot deformation of Al (B99.99), *Materials Science and Engineering A290* (2000) 95–107.
- [10] M.M. Myshlyaev, H.J. McQueen, A. Mwembela, E. Konopleva, Twinning, dynamic recovery and recrystallization in hot worked Mg-Al-Zn alloy, *Materials Science and Engineering A337* (2002) 121/133.
- [11] Akpan, Emmanuel Isaac and Haruna, Idoko Andrew, Structural Evolution and Properties of Hot Rolled Steel Alloys, *Journal of Minerals & Materials Characterization & Engineering*, Vol. 11, No.4, pp.417-426, (2012).
- [12] M.S. Mirza, C.M. Sellars, K. Karhausen & P. Evans (2001) Multipass rolling of aluminium alloys: finite element simulations and microstructural evolution, *Materials Science and Technology*, 17:7, 874-879.
- [13] M.F. Frolich, M. Krzyzanowski, W.M. Rainforth, J.H. Beynon, Oxide scale behaviour on aluminium and steel under hot working conditions, *Journal of Materials Processing Technology* 177 (2006) 36–40.



- [14] Serkan Toros, Fahrettin Ozturk, Ilyas Kacar, Review of warm forming of aluminum–magnesium alloys, *Journal of materials processing technology* 207 (2008) 1-12.
- [15] Ken TAKATA, Warm Forming of Aluminum Alloys, NIPPON STEEL TECHNICAL REPORT No. 103 MAY (2013).
- [16] František Ďurovský, Ladislav Zboray, Želmíra Ferková, Computation of Rolling Stand Parameters by Genetic Algorithm, *Acta Polytechnica Hungarica* Vol. 5, No. 2, (2008) 59-70.
- [17] M.S. Chun, J.G. Lenard, Hot rolling of an aluminum alloy using oil:water emulsions, *Journal of Materials Processing Technology* 72 (1997) 283–292.
- [18] Rafael Colas, Jorge Ramirez, Ignacio Sandoval, Julio C. Morales, Luis A. Leduc, Damage in hot rolling work rolls, *Wear* 230 (1999) 56–60.
- [19] Osamu KATO, Hiroyasu YAMAMOTO, Matsuo ATAKA, Koe NAKAJIM, Mechanisms of Surface Deterioration of Roll for Hot Strip Rolling, *ISIJ International*, Vol. 32 (1992), No. 11, pp. 1216-1220.
- [20] M. Pellizzari, A. Molinari, G. Straffelini, Tribological behaviour of hot rolling rolls, *Wear* 259 (2005) 1281–1289.
- [21] M. David Hanna, Tribological evaluation of aluminum and magnesium sheet forming at high temperatures, *Wear* 267 (2009) 1046–1050.
- [22] Chaohui Zhang, Sisi Liu, Chenhui Zhang, Micro Crack of Aluminum Sheet During Cold Rolling, *World Journal of Mechanics*, (2011), 1, 169-175.
- [23] M2 Molybdenum High Speed Tool Steel (UNS T11302), <http://www.azom.com/article.aspx?ArticleID=6174>, Jul 17 2012.
- [24] L.Maria Irudaya Raj, Sathishkumar.J, B.Kumaragurubaran, P.Gopal, Analysis of Hard Chromium Coating Defects and its Prevention Methods, *International Journal of Engineering and Advanced Technology (IJEAT)* ISSN: 2249 – 8958, Volume-2, Issue-5, June (2013).
- [25] Xiaolu Pang, Kewei Gao, Huisheng Yang, Lijie Qiao, Yanbin Wang and A. A. Volinsky, Interfacial Microstructure of Chromium Oxide Coatings. *ADVANCED ENGINEERING MATERIALS* (2007), 9, No. 7.
- [26] Mümin ŞAHİN, PHYSICAL VAPOUR DECOMPOSITION METHOD, INTERNATIONAL SCIENTIFIC CONFERENCE 19 – 20 November 2010, GABROVO.
- [27] Zhiping Chen, P.F. Thomson, Friction against superplastic aluminium alloys, *Wear* 201 (1996) 22/-232.
- [28] W. Sun, K. Tieu, H. Li, Z. Jiang, G. Wang, X. Liu, Friction in the Roll Bite Under Various Hot Rolling Conditions, *The 3rd Symposium on Advanced Structural Steels and New Rolling Technologies*.

- [29] H.R. Le, M.P.F. Sutcliffe, J.A. Williams, Friction and material transfer in micro-scale sliding contact between aluminium alloy and steel, *Tribology Letters*, Vol. 18, No. 1, January (2005).
- [30] Akira Azushima, Yoshifumi Nakata, Takahiro Toriumi, Prediction of effect of rolling speed on coefficient of friction in hot sheet rolling of steel using sliding rolling tribo-simulator, *Journal of Materials Processing Technology* 210 (2010) 110–115.
- [31] H.R. Le, M.P.F. Sutcliffe, P.Z. Wang, G.T. Burstein, Surface oxide fracture in cold aluminium rolling, *Acta Materialia* 52 (2004) 911–920.
- [32] J.A. Picas, M.T. Baile, S. Menargues, E. Martin, A. Forn, DECORATIVE PVD COATINGS AS AN ENVIRONMENTALLY CLEAN ALTERNATIVE TO CHROME PLATING.
- [33] Xiaolu Pang, Kewei Gao, Fei Luo, Yusuf Emirov, Alexandr A. Levin, Alex A. Volinsky, Investigation of microstructure and mechanical properties of multi-layer Cr/Cr<sub>2</sub>O<sub>3</sub> coatings, *Thin Solid Films* 517 (2009) 1922–1927.
- [34] K. P. Lillerud and P. Kofstad, On High Temperature Oxidation of Chromium, *J. Electrochem. Soc.: SOLID-STATE SCIENCE AND TECHNOLOGY* November (1980), 2397-2410.
- [35] H.T. Ma, C.H. Zhou, L. Wang, High temperature corrosion of pure Fe, Cr and Fe–Cr binary alloys in O<sub>2</sub> containing trace KCl vapour at 750 °C, *Corrosion Science* 51 (2009) 1861–1867.
- [36] Y.L. Su and W.H. Kao, Tribological Behavior and Wear Mechanisms of TiN/TiCN/TiN Multilayer Coatings, *Journal of Materials Engineering and Performance* Volume 7(5) October (1998)--601.
- [37] Shanyong Zhang, TiN coating of tool steels: a review, *Journal of Materials Processing Technology*, 39 (1993) 165-177.
- [38] Zhengbing Qi, Peng Sun, Zhoucheng Wang, Microstructure and Mechanical Properties of TiCN Coatings Prepared by MTCVD, Technical Sessions—Proceedings of CIST 2008 & ITS-IFTToMM 2008 Beijing, China.
- [39] Rudolf Mišičko, Tibor Kvačkaj, Martin Vlado, Lucia Gulová Miloslav Lupták, Jana Bidulská DEFECTS SIMULATION OF ROLLING STRIP, *Materials Engineering*, Vol. 16, (2009), No. 3.
- [40] Nong Jin, Shiyu Zhou, Tzyy-Shuh Chang, IDENTIFICATION OF IMPACTING FACTORS OF SURFACE DEFECTS IN HOT ROLLING PROCESSES USING MULTI-LEVEL REGRESSION ANALYSIS.
- [41] G. Buytaert, B. Kernig, H.J. Brinkman, H. Terryn, Influence of surface pre-treatments on disturbed rolled-in subsurface layers of aluminium alloys, *Surface & Coatings Technology* 201 (2006) 2587–2598.
- [42] G. Buytaert, Premendra, J.H.W. de Wit, L. Katgerman, B. Kernig, H.J. Brinkman, H. Terryn, Electrochemical investigation of rolled-in subsurface layers in commercially pure aluminium

alloys with the micro-capillary cell technique, *Surface & Coatings Technology* 201 (2007) 4553–4560.

[43] Y. Liu, T. Hashimoto, X. Zhou, G. E. Thompson, G. M. Scamans, W. M. Rainforth and J. A. Hunter, Influence of near-surface deformed layers on filiform corrosion of AA3104 aluminium alloy, *Surf. Interface Anal.* (2013), 45, 1553–1557.

[44] X. ZHOU, Y. LIU, G.E. THOMPSON, G.M. SCAMANS, P. SKELDON, J.A. HUNTER, Near-Surface Deformed Layers on Rolled Aluminum Alloys, *METALLURGICAL AND MATERIALS TRANSACTIONS A VOLUME 42A, MAY* (2011)—1373.

[45] M. Fishkis U, J.C. Lin, Formation and evolution of a subsurface layer in a metalworking process, *Wear* 206 (1997) 156–170.

[46] S. Kuypers, G. Buytaert, H. Terryn, Depth profiling of rolled aluminium alloys by means of GDOES, *Surf. Interface Anal.* (2004); 36: 833–836.

[47] Premendra, J.H. Chen, F.D. Tichelaar, H. Terryn, J.H.W. deWit, L. Katgerman, Optical and transmission electron microscopical study of the evolution of surface layer on recycled aluminium along the rolling mills, *Surface & Coatings Technology* 201 (2007) 4561–4570.

[48] G. Buytaert, H. Terryn, S. Van Gils, B. Kernig, B. Grzemba, M. Mertens, Investigation of the (sub)surface of commercially pure rolled aluminium alloys by means of total reflectance, r.f. GDOES, SEM/EDX and FIB/TEM analysis, *Surf. Interface Anal.* (2006); 38: 272–276.

[49] G. Plassart, M. Aucouturier, R. Penelle, MICROSTRUCTURE AND CHEMISTRY OF AN Al-4.7 wt.%Mg ALLOY SUBSURFACE AFTER COLD-ROLLING, *Scripta Materialia*, Vol. 41, No. 10, pp. 1103–1108, (1999).

[50] G. Buytaert, H. Terryn, S. Van Gils, B. Kernig, B. Grzemba, M. Mertens, Study of the near-surface of hot- and cold-rolled AlMg0.5 aluminium alloy, *Surf. Interface Anal.* (2005); 37: 534–543.

[51] A.R. Riahi, A. Edrisy, A.T. Alpas, Effect of magnesium content on the high temperature adhesion of Al–Mg alloys to steel surfaces, *Surface & Coatings Technology* 203 (2009) 2030–2035.

[52] A.R. Riahi, A.T. Alpas, Adhesion of AA5182 aluminum sheet to DLC and TiN coatings at 25 °C and 420 °C, *Surface & Coatings Technology* 202 (2007) 1055–1061.

[53] A.R. Riahi, A.T. Morales, and A.T. Alpas, Evaluation of Vitreous and Devitrifying Enamels as Hot Forming Lubricants for Aluminum AA5083 Alloy, *Journal of Materials Engineering and Performance* Volume 17(3) June (2008)—387.

[54] Paul E. Krajewski and Arianna T. Morales, Tribological Issues During Quick Plastic Forming, *Journal of Materials Engineering and Performance* Volume 13(6) December (2004)—700.

- [55] J. Lee, N.V. Novikov, *Innovative Superhard Materials and Sustainable Coatings for Advanced Manufacturing*, Dordrecht, (2006).
- [56] A.M. Smith, M.P. Barlow, M.P. Amor, N.C. Davies, The Mechanism of Roll Coating Buildup During Hot Rolling of Aluminum, *ASLE Trans.* 21 (1977) 2296–230.
- [57] V.R. Howes, H.J. Lamb, The Effect of Strip Surface Finish on Formation of Roll Coatings During Hot Rolling of Aluminum, *Lubr. Eng.* 39 (1983) 158–161.
- [58] K.C. Tripathi, Mechanisms of Aluminum Pickup in Deformation, *Lubr. Eng.* 34 (1978) 364–371.
- [59] W.D. Münz, Titanium aluminum nitride films: a new alternative to TiN coatings, *J. Vac. Sci. Technol. A Vac. Surf. Film* 4 (1986) 2717.
- [60] J.H. Hsieh, A.L.K. Tan, X.T. Zeng, Oxidation and wear behaviors of Ti-based thin films, *Surf. Coat. Technol.* 201 (2006) 4094–4098.
- [61] T. Polcar, R. Novák, P. Široký, The tribological characteristics of TiCN coating at elevated temperatures, *Wear* 260 (2006) 40–49.
- [62] H. Mohrbacher, B. Blanpain, J.P. Celis, J.R. Roos, L. Stals, M. Van Stappen, Oxidational wear of TiN coatings on tool steel and nitrided tool steel in unlubricated fretting, *Wear* 188 (1995) 130–137.
- [63] M.L. McConnell, D.P. Dowling, N. Donnelly, K. Donnelly, R.V. Flood, The effect of thermal treatments on the tribological properties of PVD hard coatings, *Surf. Coat. Technol.* 116–119 (1999) 1133–1137.
- [64] E. Konca, Y.T. Cheng, A.M. Weiner, J.M. Dasch, A. Erdemir, A.T. Alpas, Transfer of 319 Al alloy to titanium diboride and titanium nitride based (TiAlN, TiCN, TiN) coatings: effects of sliding speed, temperature and environment, *Surf. Coat. Technol.* 200 (2005) 2260–2270.
- [65] K. Holmberg, A. Matthews, *Coatings Tribology: Properties, Mechanisms, Techniques and Applications in Surface Engineering*, Elsevier Science, (2009).
- [66] O.A. Gali, M. Shafiei, J.A. Hunter, A.R. Riahi, The Tribological Behavior of PVD Coated Work Roll Surfaces during Rolling of Aluminum, *Surf. Coatings Technol.* 260 (2014) 230–238.
- [67] V.R. Howes, M.P. Amor, Roll Coatings Formed during the Hot Rolling of Aluminium with Rolls of Different Materials, *Wear.* 79 (1982) 375–384.
- [68] V.R. Howes, M.P. Amor, The Interfacial Transfer of Aluminum to Steels and Ceramic Materials Under Loaded Contact at High Temperatures II: Both Surfaces at High Temperatures, *Wear.* 72 (1981).

## VITA AUCTORIS

NAME: Boya Li

PLACE OF BIRTH: Lanzhou, China

EDUCATION: Lanzhou No.1 Senior High School, Lanzhou, China, 2009

Xi'an Jiaotong University, Xi'an, China, 2014

University of Windsor, M.A.Sc., Windsor, ON, 2016